COMENIUS UNIVERSITY IN BRATISLAVA
FACULTY OF MATHEMATICS, PHYSICS AND INFORMATICS

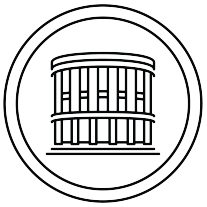

MODELS OF INFECTIOUS DISEASE AND THEIR NUMERICAL SOLUTION

DISSERTATION THESIS

2024 Mgr. Ján GAŠPER, DiS. art.

COMENIUS UNIVERSITY IN BRATISLAVA
FACULTY OF MATHEMATICS, PHYSICS AND INFORMATICS

MODELS OF INFECTIOUS DISEASE AND THEIR NUMERICAL SOLUTION

DISSERTATION THESIS

Study program:	Applied Mathematics
Study field:	1114 Applied Mathematics
Department:	Department of Applied Mathematics and Statistics
Supervisor:	prof. RNDr. Daniel Ševčovič, DrSc.

Bratislava 2024 **Mgr. Ján GAŠPER, DiS. art.**

Comenius University Bratislava
Faculty of Mathematics, Physics and Informatics

THESIS ASSIGNMENT

Name and Surname:	Mgr. Ján Gašper, DiS.art.
Study programme:	Applied Mathematics (Single degree study, Ph.D. III. deg., full time form)
Field of Study:	Mathematics
Type of Thesis:	Dissertation thesis
Language of Thesis:	English
Secondary language:	Slovak

Title: Models of infectious disease and their numerical solution

Annotation: Epidemiological models are used to describe the spread of an infectious disease in the population. In them, the population is often divided into sub-populations, on the one hand in relation to the disease, on the other hand, from the point of view of spatial, age or other composition of the population. Dynamical systems based on differential equations describe the temporal interaction between individual sub-populations and aim to qualitatively or quantitatively characterize the course of the disease in the population. These dynamical systems, whether discrete or continuous, deterministic or stochastic, contain a number of parameters whose appropriate calibration is necessary for the correct evaluation of models. The current trend of research activity in the field of epidemiological models is diseases preventable by vaccination, in which immunity is acquired through vaccination, but also a gradual loss of immunity and subsequent re-susceptibility to the disease. Similarly, a possible increase in immunity by means other than re-vaccination can also be included in the models. When dividing the population, the difficulty of parameter estimation increases enormously. More realistic results can be provided by appropriately selected stochastic dynamic models. For the practical solution of these systems, knowledge of effective numerical methods is required, as well as researching the possibilities of their optimization using specific features of the model.

Tutor:	prof. RNDr. Daniel Ševčovič, DrSc.
Consultant:	doc. Mgr. Soňa Kilianová, PhD.
Department:	FMFI.KAMŠ - Department of Applied Mathematics and Statistics
Head of department:	doc. Mgr. Igor Melicherčík, PhD.
Assigned:	09.01.2020
Approved:	09.01.2020 prof. RNDr. Daniel Ševčovič, DrSc. Guarantor of Study Programme

....

Student Tutor

Univerzita Komenského v Bratislave
Fakulta matematiky, fyziky a informatiky

ZADANIE ZÁVEREČNEJ PRÁCE

Meno a priezvisko študenta: Mgr. Ján Gašper, DiS.art.
Študijný program: aplikovaná matematika (Jednoodborové štúdium, doktorandské III. st., denná forma)
Študijný odbor: matematika
Typ záverečnej práce: dizertačná
Jazyk záverečnej práce: anglický
Sekundárny jazyk: slovenský

Názov: Models of infectious disease and their numerical solution
Modely šírenia infekčných ochorení a ich numerické riešenie

Anotácia: Epidemiologické modely slúžia na opis šírenia infekněho ochorenia v populácii. Populácia sa v nich často delí na subpopulácie jednak vo vzťahu k ochoreniu, jednak z pohľadu priestorového, vekového alebo iného zloženia populácie. Dynamicé systémy založené na diferenciálnych rovniciach opisujú časovú interakciu medzi jednotlivými subpopuláciami a majú za cieľ kvalitatívne alebo kvantitatívne charakterizovať priebeh ochorenia v populácii. Tieto dynamicé systémy, či už diskrétne alebo spojité, deterministické alebo stochastické, obsahujú množstvo parametrov, ktorých vhodná kalibrácia je potrebná na správne vyhodnocovanie modelov. Súčasným trendom výskmnej činnosti v oblasti epidemiologických modelov sú ochorenia preventabilné očkovaním, pri ktorých dochádza k získavaniu imunity prostredníctvom očkovania, ale taktiež k postupnej strate imunuty a následnej opätovnej náchylnosti na ochorenie. Podobne možno do modelov zahrnúť aj možné zvýšenie imunuty iným spôsobom než opätovným očkovaním. Pri delení populácie sa enormne zvyšuje náročnosť odhadu parametrov. Realistickejšie výsledky môžu priniesť vhodné zvolené stochastické dynamické modely. Na praktické riešenie týchto systémov je potrebná znalosť efektívnych numerických metód ako i skúmať možnosti ich zefektívňovania s využitím špecifických vlastností modelu.

Školiteľ: prof. RNDr. Daniel Ševčovič, DrSc.
Konzultant: doc. Mgr. Soňa Kilianová, PhD.
Katedra: FMFI.KAMŠ - Katedra aplikovanej matematiky a štatistiky
Vedúci katedry: doc. Mgr. Igor Melicherčík, PhD.

Dátum zadania: 09.01.2020

Dátum schválenia: 09.01.2020 prof. RNDr. Daniel Ševčovič, DrSc.
garant študijného programu

.....
študent

.....
školiteľ

I express my gratitude to my supervisor, prof. Daniel Ševčovič for his guidance. Thanks also belongs to my schoolmate and colleague, Jakub Hrdina, for his fellowship during my studies since the first year on the university. Many thanks to my wife, Kika, for her tolerant and encouraging attitude.

Abstract

GAŠPER Ján: Models of infectious disease and their numerical solution [Dissertation thesis] Comenius University in Bratislava, Faculty of Mathematics, Physics and Informatics, Department of Applied Mathematics and Statistics; Supervisor: prof. RNDr. Daniel Ševčovič, DrSc., Bratislava, 2024, 107 pages.

In this thesis, known compartmental epidemiological models and approaches to their numerical solutions will be analyzed. The first result of this thesis will be a new epidemiological model that includes immunity boosting of a recovered individual encountering an infectious individual. The new model will be generalized for an arbitrary immunity loss curve. The second result of this thesis will be spatially heterogeneous model with population diffusion modeled by a fractional Laplacian. The numerical solutions of new models will be implemented and the results will be visually presented.

Keywords: epidemiological models, SIR model, SIRS model, immunity boosting, heterogeneous SIR model, fractional Laplacian

Abstrakt

GAŠPER, Ján: Modely šírenia infekčných ochorení a ich numerické riešenie [Dizeratčná práca], Univerzita Komenského v Bratislave, Fakulta matematiky, fyziky a informatiky, Katedra aplikovanej matematiky a štatistiky; vedúci práce: prof. RNDr. Daniel Ševčovič, DrSc., Bratislava 2024, 107 strán.

V tejto práci analyzujeme známe kompartmentové epidemiologické modely a prístupy k ich numerickému riešeniu. Prvým výsledkom práce je nový epidemiologický model, ktorý zahŕňa posilňovanie imunity pri kontakte imúnneho jednotlivca s infekčným. Nový model zovšeobecníme pre ľubovoľnú krivku ubúdania imunity. Druhým výsledkom práce je priestorovo heterogénny model s difúziou populácie, ktorú budeme modelovať pomocou zlomkového Laplaciánu. Implementujeme numerické riešenia nových modelov a výsledky graficky znázorníme.

Kľúčové slová: epidemiologické modely, SIR model, SIRS model, posilnenie imunity, heterogénny SIR model, zlomkový Laplacián

Table of Contents

Chapter 1

Introduction

Mathematical epidemiology is a discipline of applied mathematics that has the goal of predicting and understanding the spread of infectious diseases. There are multiple approaches to this topic. In this thesis, an approach utilizing dynamical systems will be employed.

In this thesis, *compartmental models* will be utilized. They are built on top of the idea of dividing the population of individuals according to their disease status [84]. The compartments are *susceptible* (individuals who could become ill), *infectious* (individuals that were ill and were spreading the disease) and *recovered* (individuals that overcame the disease and cannot become ill). However, Keeling's original idea faded and was brought back several years later in 1979, when an improved version of the original model was presented in a textbook [5], as [84] refers.

In chapter 2 an overview of epidemiological models is presented. There are many approaches to modeling such a system: one can consider continuous or discrete time, continuous or discrete set of possible system states, stochastic or deterministic system etc. These approaches are discussed in section 2.1. In section 2.2, the standard SIR model is presented and in section 2.3 its extensions are presented.

The dynamical models are usually formulated as a system of differential equations. Several numerical methods used to solve the equations are presented in chapter 3. Methods for solving systems of ordinary differential equations are presented in section 3.1. Methods for solving parabolic partial differential equations in section 3.2. Special set of methods for solving stochastic models with discrete state space is presented in

section 3.3. Finally, methods for solving stochastic differential equations are presented in section 3.4.

In this thesis, a new epidemiological model is derived, that elaborates the idea of boosting immunity on recovered-infectious contact and is discussed in chapter 4. We start by analyzing the standard SIRS model and suggesting changes to incorporate the immunity boosting effect in section 4.1. Then we apply the idea of boosting to a model with a custom waning profile in section 4.2 and show four different formulations of the model: two for discrete time and two for continuous time. Finally, we provide numerical results of the models in section 4.3.

In chapter 5 a novel epidemiological model with fractional Laplace operator to model diffusion is derived. We summarize the idea of fractional Laplacian in section 5.1. We discuss the behavior of the model at the boundary of the studied spatial domain in section 5.2. Numerical methods are discussed in section 5.3 and numerical results of the model are provided in section 5.4.

Finally, chapter 6 contains selected parts of the code used in this thesis. The code is in languages Python and Julia.

Chapter 2

Overview of epidemiological models

In this chapter, we present the discussion of several types of dynamical epidemiological models.

2.1 Types of models

2.1.1 Continuous and discrete time

Modeling of spread of infectious diseases is usually done in either discrete time or in continuous time (apart from special time-free models such as graph-based described in chapter 16.3. of [69]). Discrete-time modeling leads to recursive sequences and time series models, meanwhile modeling with continuous time often leads to (deterministic or stochastic) differential equations. Both approaches have their place in modeling the spread of infectious diseases.

Recursive sequence is a good tool when the infection period is almost constant. Structure of the model can be simplified a lot, if the time step coincides with the infection period. Next case, in which a recursive sequence is appropriate, is a case of seasonal disease with a time step of the same length as the season period. This approach was used e.g. for modeling child diseases, with the seasonality present due to periodicity of the school year [10, 34, 55].

On the other hand one can consider modeling dynamical systems in continuous time. This approach often leads to differential equations of various kinds, such as ordinary differential equations, integral-differential equations, delayed differential equations, partial

differential equations, or stochastic differential equations. The problem of this approach is that the model usually cannot be solved analytically, so we are left with numerical solutions only [16]. Models using ordinary differential equations often assume Markov property, which may not be satisfied in practice. Artificially raising the dimension of the model is a workaround which was proven useful in [36]. There are many tools to analyze models with differential equations, such as perturbation theory, Poincaré maps, phase portrait analysis, Lyapunov functional or LaSalle's invariance principle. Another option to model non-markovian processes is to use integral-differential equations or partial differential equations such as in [31, 68], but analytical tools for these are much more exacting. These methods will be used also in this thesis in chapter 4.

2.1.2 Continuous and discrete state space

When the number of individuals in each compartment is high enough, treating the number of individuals as continuous quantities yields only a small relative error. Continuous state space allows us to use differential equations, which were discussed above. However, when a number of individuals is relatively small to the population, a continuous simplification might not be a good approximation, and can lead to infamous *atto-fox problem*. [1] This can be avoided by allowing only non-negative integers to represent the number of individuals in each compartment.

2.1.3 Deterministic and stochastic models

The spread of a disease is a random process, with randomness present in many steps: random daily contacts, pathogen transmission, immunity system response of individuals, etc. Therefore a stochastic model might be better, especially when one is interested in quantifying uncertainty. However stochastic models have their drawbacks, mainly, higher computational complexity. Stochastic models in continuous time with discrete state use the same tools as chemical kinetics, such as Gillespie algorithm, τ-leaping

[1] The atto-fox problem is a known disadvantage of biological models with continuous state space. The name comes from *atto-*, a SI prefix for 10^{-18}. The name comes from predator-prey model, which predicted that the population of foxes will be as small as 10^{-18}. The biological interpretation of this number is that foxes will go extinct, however the model showed different behavior. This problem was addressed in [76]

method, master equation etc. These methods are further discussed in section 2.3.7. When modeling in discrete time, τ-leaping method is still viable, along with models based on binomial distribution, such as the Greenwood model and Reed-Frost model [1, 43]. For overview of stochastic models and its applications, we refer the reader to [80].

On the other hand, deterministic models are usually much easier to analyze and solve numerically. Furthermore, in the limit case of large populations, the stochastic model approaches deterministic behavior [40]. Deterministic models can be transformed into stochastic by perturbing the model with a white noise in multiple ways [55]. We will discuss one type of such perturbation in section 2.3.8.

2.2 The basic SIR model

The SIR model is the best-known epidemiological model, using continuous time and continuous population. One of its first applications is in the article [66], in which the model was employed to predict the number of infected households. A year later, the first SIR model was published in [56] and its properties were analyzed.

In the model, the population is separated into three groups, or so-called *compartments*, due to infection status: *Susceptible* (further denoted S, can catch infection), *Infectious* (I, spreading the infection to S) and *Recovered* (R, overcame the disease and are immune). Further we refer to the number of susceptible, infectious and recovered at time t as $S(t), I(t), R(t)$, respectively. It is important to note that epidemiological status of infectious individuals may not be identical to medical status of diseased.

To build the model, we will use the following assumptions [1]:

- The infection is spread directly from infected individuals to others by a certain kind of contact (adequate contact) and in no other way
- Any non-immune individual in the group, after such contact with an infectious person in a given period, will develop the infection and will be infectious to others only within the following time period, after which he is wholly immune.
- Each individual has a fixed probability of coming into adequate contact with

any other specified individual in the group within one time interval, and this probability is the same for every member of the group.

- These conditions remain constant during the epidemic.

The only two things that can happen to an individual (further called *transitions*) are that susceptible individual meets infectious individual with the susceptible becoming infectious (which can be symbolically written as $S + I \to 2I$) or the infectious individual spontaneously becomes recovered (symbolically $I \to R$).[2] Epidemiological models can be better understood in *flow diagrams*, which visually depict compartments and transitions between them. For this model, the corresponding flow diagram (with rates that will be discussed below) can be found in Fig. 2.1.[3]

One approach is to formulate the model first with a discrete time step Δt and then take the limit $\Delta t \to 0^+$ to obtain differential equations governing the model. Let us consider a homogeneous, closed population, so that individuals have equal contact rate with each other and no migration takes place; let us denote the total number of individuals N, which we will assume is constant.

First, we will consider the $S + I \to 2I$ transition. Let m be the contact rate, so an individual meets $m\ \Delta t$ other people during a small time interval of duration Δt. Let p be the probability that pathogen is transmitted from infectious to susceptible during the contact and causes an infection. Out of $m\ \Delta t$ contacts during the time step, only $m\Delta t\ I(t)/N$ are with an infectious person. The probability of still being susceptible after the time step is $(1-p)^{m\Delta t\ I(t)/N}$. This process, however, needs to be considered for each of $S(t)$ individuals. If the population is so large that the law of large numbers holds, then during the time step $S(t)\left(1-(1-p)^{m\Delta t\ I(t)/N}\right)$ new infections will occur.

Next, the recovery transitions $I \to R$. The number of recoveries during the time step should be proportional to the number of infectious and length of the time step: $\gamma I\ \Delta t$.

Therefore we can write down the dynamics as:

$$S(t+\Delta t) = S(t) - S(t)\left(1-(1-p)^{m\Delta t\ I(t)/N}\right)$$

[2]Sometimes, the rate of the transition is written on top of the arrow, such as $S + I \xrightarrow{\beta\frac{SI}{N}} 2I$ or $I \xrightarrow{\gamma I} R$. Sometimes, for the sake of brevity, only the rate parameter is written: $S + I \xrightarrow{\beta} 2I$, $I \xrightarrow{\gamma} R$.

[3]Some authors add a dotted arrow from S compartment to β arrow, representing the fact that the rate of the new infection is dependent also on the number of individuals in I.

$$I(t+\Delta t) = I(t) + (1-p)^{m\Delta t\ I(t)/N} - \gamma I(t)\ \Delta t$$
$$R(t+\Delta t) = \gamma I(t)\ \Delta t,$$

which can be rearranged into:

$$\begin{aligned}
\frac{S(t+\Delta t) - S(t)}{\Delta t} &= S(t)\frac{1-(1-p)^{m\Delta t\ I(t)/N}}{\Delta t} \\
\frac{I(t+\Delta t) - I(t)}{\Delta t} &= S(t)\frac{1-(1-p)^{m\Delta t\ I(t)/N}}{\Delta t} - \gamma I(t) \\
\frac{R(t+\Delta t) - R(t)}{\Delta t} &= \gamma I(t).
\end{aligned}$$

Finally, taking the limit $\Delta t \to 0^+$ yields:

$$\begin{aligned}
\frac{dS(t)}{dt} &= -\beta\frac{S(t)I(t)}{N} \\
\frac{dI(t)}{dt} &= \beta\frac{S(t)I(t)}{N} - \gamma I(t) \\
\frac{dR(t)}{dt} &= \gamma I(t),
\end{aligned} \tag{2.1}$$

where $\beta = -m\ln(1-p)$ is *force of infection*. The model above represents the standard SIR model. This model is sometimes stated in terms of normalized variables $s(t) = S(t)/N$, $i(t) = I(t)/N$, $r(t) = R(t)/N$ as:

$$\begin{aligned}
\frac{ds(t)}{dt} &= -\beta s(t)i(t) \\
\frac{di(t)}{dt} &= \beta s(t)i(t) - \gamma i(t) \\
\frac{dr(t)}{dt} &= \gamma i(t).
\end{aligned} \tag{2.2}$$

These models, in both forms, can be reduced to a system of two ordinary differential equations, because the number of recovered individuals can be inferred from the number of people in other compartments. Instead of a differential equation for recovered

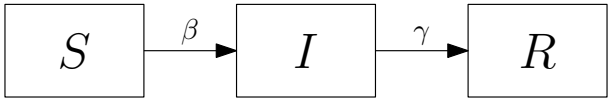

Fig. 2.1: Flow diagram of basic SIR model

individuals, we may write an algebraic equation $R(t) = N - S(t) - I(t)$, or $r(t) = 1 - s(t) - i(t)$.

The *basic reproduction number* – $\mathcal{R}_0$ – is an important number that determines qualitative behavior of the model. It represents the average secondary number of infectious cases from one infectious individual in a fully susceptible population. If $\mathcal{R}_0 < 1$, the number of infectious people will fade; if $\mathcal{R}_0 > 1$, the number of infectious people will grow. In the standard SIR model, the basic reproduction number has value of β/γ. [54, 55]

2.3 Extensions of SIR model

The basic SIR model may lack important aspects of the disease: incubation period, births and deaths, immunity waning, heterogeneity of the population etc. Therefore a number of extensions of the model was made. Some more advanced models combine these extensions, especially models with the intention of being predictive. An excellent overview of different models and underlying biological rationale can be found in the article [78]. More detailed summary is presented in the textbook [55].

2.3.1 Incubation period: SEIR model

One of the most common extensions of the standard SIR model is the incorporation of incubation period. This is usually done by adding a compartment of *exposed* (E) into the model. These are individuals that are infected by the pathogen, but not spreading it yet. The model can be described in terms of transitions as: $S + I \to E$, $E \xrightarrow{\sigma} I$, $I \to R$, see Fig. 2.2. In terms of differential equations the model reads:

$$\begin{aligned}
\frac{dS(t)}{dt} &= -\beta \frac{S(t)I(t)}{N} \\
\frac{dE(t)}{dt} &= \beta \frac{S(t)I(t)}{N} - \sigma E(t) \\
\frac{dI(t)}{dt} &= \sigma E(t) - \gamma I(t) \\
\frac{dR(t)}{dt} &= \gamma I(t).
\end{aligned}$$

Due to the delay in the infection period, this model shows slower spread of infection through the population [55]. The SEIR model with further extensions is often used in models of disease prediction and public policy control, for example in articles [11, 12, 52, 25, 49].

2.3.2 Population dynamics

One of the popular extensions of the basic SIR model is to include population dynamics: births, migration and deaths. In this case, N, the total number of people may not be constant. The basic SIR model is extended by transitions $\emptyset \overset{\nu N}{\to} S$, $S \overset{\mu}{\to} \emptyset$, $I \overset{\mu}{\to} \emptyset$, $R \overset{\mu}{\to} \emptyset$, where $\emptyset$ represents people to be born or dead people and people to migrate in and out of considered population. The first of transitions above represents births of new individuals. Since newborns did not overcome the disease, they belong to the susceptible compartment.[4] The latter three transitions represent natural deaths, independent of the epidemiological status.[5]

The flow diagram for the model is in Fig. 2.3. The entire model in form of differential equations is:

$$\begin{aligned}
\frac{dS(t)}{dt} &= -\beta\frac{S(t)I(t)}{N(t)} - \mu S(t) + \nu N(t) \\
\frac{dI(t)}{dt} &= \beta\frac{S(t)I(t)}{N(t)} - \gamma I(t) - \mu I(t) \\
\frac{dR(t)}{dt} &= \gamma I(t) - \mu R(t). \\
N(t) &= S(t) + I(t) + R(t).
\end{aligned}$$

The parameters ν, μ can be chosen such that the total population is constant. When

[4] Some models suited for children diseases add another compartment M for newborns protected by maternal immunity. The model is then called $MSIR$ model.

[5] There are also models that include disease-induced deaths. For more detailed explanation see ch. 2.2. of [55].

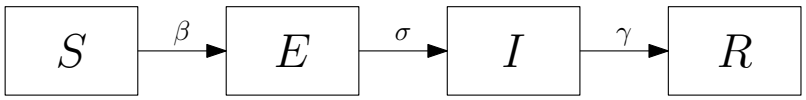

Fig. 2.2: Flow diagram of SEIR model.

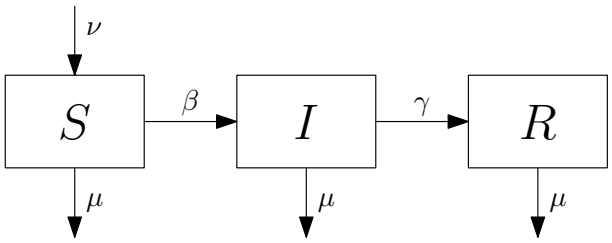

Fig. 2.3: Flow diagram for SIR model with population dynamics

this happens, the derivative of total population is zero:

$$\begin{aligned} 0 = \frac{dN(t)}{dt} &= \frac{d}{dt}\left(S(t) + I(t) + R(t)\right) \\ &= \frac{dS(t)}{dt} + \frac{dI(t)}{dt} + \frac{dR(t)}{dt} \\ &= \nu N(t) - \mu S(t) - \mu I(t) - \mu R(t) = N(t)(\nu - \mu) \end{aligned}$$

which is zero when $\nu = \mu$.

The model with constant population can be seen as using transitions $S \xrightarrow{\mu} S$, $I \xrightarrow{\mu} S$ and $R \xrightarrow{\mu} S$ instead of those introduced above. These transitions can be interpreted so that a new individual is born at the exact time when another individual from compartment either S, I or R dies.

2.3.3 Vaccination: SIRV model

For some diseases, a vaccination shortly after birth is common. This is modeled via separate transitions for vaccinated and not vaccinated newborns: $\emptyset \xrightarrow{N\nu(1-x)} S$ and $\emptyset \xrightarrow{\nu x} R$, where x is the proportion of successfully vaccinated newborns. Symbols $\emptyset$ represents individuals that are not yet considered in the model.

The flow diagram is depicted in fig. 2.4 and the model in the form of differential equations is:

$$\begin{aligned} \frac{dS(t)}{dt} &= -\beta\frac{S(t)I(t)}{N(t)} - \mu S(t) + \nu(1-x)N(t) \\ \frac{dI(t)}{dt} &= \beta\frac{S(t)I(t)}{N(t)} - \gamma I(t) - \mu I(t) \\ \frac{dR(t)}{dt} &= \gamma I(t) - \mu R(t) + \nu x N(t). \\ N(t) &= S(t) + I(t) + R(t). \end{aligned}$$

Again, by choice $\nu = \mu$ the total population remains constant.

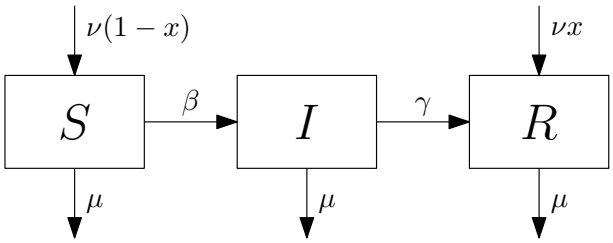

Fig. 2.4: Flow diagram for SIR model with population dynamics

2.3.4 Immunity waning: SIRS model

Recovery from many diseases does not grant lifelong immunity – recovered individuals can become susceptible again. In order to reflect this, a new transition $R \xrightarrow{\omega} S$ is added. The model dynamics can be seen in Fig. 2.5 and the model reads:

$$\begin{aligned} \frac{dS(t)}{dt} &= -\beta\frac{S(t)I(t)}{N} + \omega R(t) \\ \frac{dI(t)}{dt} &= \beta\frac{S(t)I(t)}{N} - \gamma I(t) \\ \frac{dR(t)}{dt} &= \gamma I(t) - \omega R(t) \end{aligned} \tag{2.3}$$

For time-dependent rates of immunity loss we refer the reader to our previous work [31], in which such a model is described in great detail. For biological details of waning immunity we refer the reader to [85].

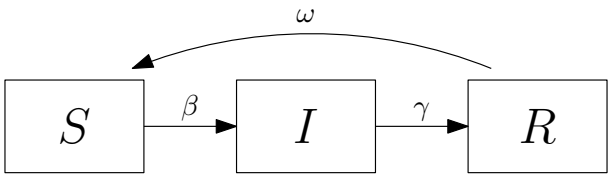

Fig. 2.5: Flow diagram for SIRS model

2.3.5 Discrete heterogeneous models

One of the assumptions of the basic SIR model was homogeneity of the population. However, any larger population does not meet this assumption, which can weaken both the predictive and analytic value of the model. The heterogeneity in the model is usually either spatial, age, or related to risk behavior. The heterogeneous model assumes n internally homogeneous groups. However, these groups interact with each other in a heterogeneous manner.

In mathematical model, each of the S, I, R compartments is subdivided into n compartments: $S_1 \dots S_n, I_1 \dots I_n, R_1 \dots R_n$. The contact patterns are encoded into the *WAIFW* [6] matrix B (capital beta). However, this matrix has n^2 parameters, which can be – especially in large-scale models – very hard to infer from data, so expert estimations are often used. For some models, matrix B is assumed to be in a certain form. A nice example of this technique is the article [30], in which the spread of sexually transmitted diseases is discussed. The population is divided by the number of sexual partners and matrix B has form: $B_{i,j} = \beta \frac{ij}{\sum_k k n_k}$, where n_k is the proportion of individuals with exactly k partners and β is a scaling parameter.

In terms of differential equations the heterogeneous model has form:

$$\begin{aligned}
\frac{dS_i(t)}{dt} &= -\sum_{j=1}^{n} B_{i,j} \frac{S_i(t) I_j(t)}{N_j(t)} \\
\frac{dI_i(t)}{dt} &= \sum_{j=1}^{n} B_{i,j} \frac{S_i(t) I_j(t)}{N_j(t)} - \gamma I_i(t) \\
\frac{dR_i(t)}{dt} &= \gamma I_i(t),
\end{aligned}$$

where $B_{i,j}$ is an element of matrix B in i-th row, j-th column. More details can be added into the model by including change of the group by an individual, such as in the case of work commuting (for spatial models) or aging (for age models).

A recent example of usage of heterogeneous SEIR model for understanding contact patterns is article [65], in which the population was split into multiple age groups and effects of different protection measures were estimated.

One may be also interested in limiting behavior of the model for $n \to \infty$. This is, in general, possible, granted that WAIFW matrix approach some limit. The model then leads to partial differential equations, with one variable representing time and the other representing heterogeneous parameters. Methods of finding reproduction number in this kind of heterogeneous model are discussed in [27]. In [63], an immunological structure of population is modeled, instead of spatial heterogeneity.

[6] Abbreviated *Who Acquires Infection From Whom*.

2.3.6 Spatial models with diffusion

The spatial dimension may be treated as a continuous quantity. Instead of incorporating WAIFW in the form of a convolution kernel, a diffusion of population is used to spread the infection. This approach is called *reaction-diffusion system*.[7] For a more detailed discussion on spatial models, we refer the reader to chapter 7.4 of [55], chapter 11 of [67] and review [26].

Let us consider a population living on an interval $[0, L]$. Let $S(t,x), I(t,x), R(t,x)$ denote the *density* of the individual in respective compartments at time t at position x.[8] Individuals may interact only with other individuals at the same location. Furthermore, the population will migrate along the interval $[0, L]$ according to the diffusion term. For diffusion term, the Laplacian is usually used.

The SIR model with diffusion can be expressed as:

$$\frac{dS(t,x)}{dt} - \kappa\,\Delta S(t,x) = -\beta\frac{S(t,x)I(t,x)}{N(t,x)} \tag{2.4}$$

$$\frac{dI(t,x)}{dt} - \kappa\,\Delta I(t,x) = \beta\frac{S(t,x)I(t,x)}{N(t,x)} - \gamma I(t,x) \tag{2.5}$$

$$\frac{dR(t,x)}{dt} - \kappa\,\Delta R(t,x) = \gamma I(t,x), \tag{2.6}$$

$$N(t,x) = S(t,x) + I(t,x) + R(t,x) \tag{2.7}$$

where κ is diffusion rate and Δ is a Laplace operator. The model can be naturally extended into two (or possibly more) dimensions.

The model must include boundary condition. The Neumann boundary condition is a usual choice, which will be discussed later in section 5.2. An extension of this model will be introduced and analyzed in section 5.

2.3.7 Stochastic models with discrete state space

In this section, stochastic models will be discussed. In this section, we will focus on models in continuous time and discrete state space. For a great introduction into the topic, see [32] and [59].

[7] The term *reaction-diffusion system* comes from chemistry models, in which the substances can react to form new products, and are subject to diffusion, as in a stationary liquid container.

[8] Density of population means that the total number of i.e. susceptible individuals at time t on interval $[a,b] \subseteq [0,L]$ is $\int_a^b S(t,x)dx$.

We will consider a model with n compartments and m transitions. The number of individuals in the i-th compartment will be called *copy number* of that compartment. The vector of non-negative integers containing copy numbers at time t of all compartments will be called *state vector at time* t and will be denoted $x(t)$. Change in state vector after j-th transition will be denoted ν_j, $\nu_j \in \mathbb{N}_+^m$. The matrix with columns $\nu_1 \dots \nu_m$ will be called *stoichiometric matrix* and denoted A:[9]

$$A = \begin{bmatrix} | & | & & | \\ \nu_1 & \nu_2 & \cdots & \nu_m \\ | & | & & | \end{bmatrix}.$$

Each transition is associated with its *transition rate function*, which takes the state vector and outputs the rate of the transition. Grouping together outputs of all rate functions into a vector, we get one *rate function*, denoted $a(x)$. [10] The sum of rates will be denoted $a_0(x)$:

$$a_0(x) = a_1(x) + a_2(x) + \ldots + a_m(x) = \mathbf{1}^T a(x),$$

where $\mathbf{1}$ is a column vector of ones.

The rate of transition in context of stochastic models should be understood in terms of limit probability:

$$a_j(x) = \lim_{\Delta t \to 0^+} \frac{\Pr(j\text{-th transition will occur in next } \Delta t \mid \text{state vector is } x)}{\Delta t}$$

In other words, the rate multiplied by sufficiently small Δt is the probability that the corresponding transition will occur during the next time step of size Δt. [11]

Let us further assume that two transitions cannot happen simultaneously and transitions are independent. Assuming independence, the probability of two transitions happening at the same time is of order $(\Delta t)^2$, so the rate of such an event is zero.

[9] A significant proportion of stochastic models was derived from chemistry and molecular biology models, hence the nomenclature follows this terminology.

[10] When the context is clear, the argument of rate function is omitted. The outputs of the function are called *rates* or *propensities* of transitions.

[11] Another interpretation of the rate is $d/dt(\ln(1 - F_j(t)))$, where $F_j(t)$ is the distribution function of time to the next j-th transition. This interpretation comes handy for simulation of non-markovian stochastic systems, in which the rate function does not depend on the current state vector only, but also its history.

For the case of the SIR model, $n = 3$, $m = 2$. The compartments are ordered: S, I, R and transitions are ordered: $S + I \to 2I, I \to R$. The stoichiometry matrix has form:

$$A = \begin{bmatrix} -1 & 0 \\ 1 & -1 \\ 0 & 1 \end{bmatrix}.$$

The first column says that after the $S + I \to 2I$ transition, there is one individual less in the S compartment and one individual more in I compartment. Analogically, after $I \to R$ transition there is one individual less in the I compartment and one more in R compartment.

To get the rate function we will analyze the SIR framework once more, without averaging random events. Let us consider events during the small time step Δt. First, let us consider transition $S + I \to 2I$. Probability that a susceptible person meets some other person during the time step is $m\ \Delta t$, probability that the other person is infectious is $I(t)/N(t)$ and probability of successful pathogen transmission is p. Then, the probability that single susceptible person becomes infected during the next time step is:

$$(1 - p)^{m\ \Delta t I(t)/N}.$$

Considering this event for all $S(t)$ individuals that may become infectious, we get the rate:

$$a_1\left([S(t), I(t), R(t)]^T\right) = \lim_{\Delta t \to 0^+} \frac{S(t)(1-p)^{m\ \Delta t I(t)/N}}{\Delta t} = \beta \frac{S(t)I(t)}{N},$$

where, again, $\beta = mp$.

Regarding the transition representing recovery, we assume that every infectious individual has probability of recovering during the next time step $\gamma\ \Delta t$. Considering that there are $I(t)$ individuals, the rate is:

$$a_2([S(t), I(t), R(t)]^T) = \lim_{\Delta t \to 0^+} \frac{I(t)\gamma\ \Delta t}{\Delta t} = \gamma I(t).$$

With defined stoichiometry matrix and rate function, the model is now complete. Stochastic model can be, similarly to the deterministic model, reduced down to two compartments with unchanged rate functions and a stoichiometry matrix

$$S = \begin{bmatrix} -1 & 0 \\ 1 & -1 \end{bmatrix}.$$

2.3.8 Stochastic models with continuous state space

In this section, one type of stochasticity will be presented, which models the uncertainty in parameters. [12] Assume that β and γ, slightly fluctuate, so that $\beta(dt + dW_t^{(1)})$ and $\gamma(dt + dW_t^{(2)})$ are used instead of $\beta\ dt$ and $\gamma\ dt$. The dW_t terms are called *stochastic differential* and represent infinitesimal change of Wiener process. [13] The model then turns into a set of *stochastic differential equations*:

$$\begin{aligned} dS(t) &= -\beta \frac{S(t)I(t)}{N} \left(dt + dW_t^{(1)} \right) \\ dI(t) &= \beta \frac{S(t)I(t)}{N} \left(dt + dW_t^{(1)} \right) - \gamma I(t) \left(dt + dW_t^{(2)} \right) \\ dR(t) &= \gamma I(t) \left(dt + dW_t^{(2)} \right). \end{aligned} \tag{2.8}$$

where stochastic differentials $dW_t^{(1)}$ and $dW_t^{(2)}$ are uncorrelated, i.e. $\mathbb{E}[dW_t^{(1)} dW_t^{(2)}] = 0$.

For more detailed discussion on various types of stochasticity, we refer the reader to chapter 6 of [55].

[12] This particular type of randomness is connected to models presented above in section 2.3.7. This connection will be discussed later in section 3.4.2.

[13] An intuitive explanation of stochastic differential is a normally-distributed random variable with zero mean and variance dt.

Chapter 3

Overview of numerical methods

In this chapter, we present numerous types of numerical methods for solving models. We focus on models formulated in terms of ordinary differential equations, partial differential equations, Gillespie framework and stochastic differential equations.

3.1 Ordinary differential equations

In this section an overview of methods for solving differential equations is presented. We present methods for solving *initial problem* here, in which a set of differential equations together with initial condition. [1] Under certain conditions such as Lipschitz continuity, existence and uniqueness of the solution is guaranteed [16]. For a great introduction into numerical methods see textbooks [17] and [8] or overviews [18] and [46].

3.1.1 Euler method

One of the easiest methods to implement is to discretize continuous time into time steps of (usually) equal length Δt. The system of differential equations is then approximated by the first-order Taylor polynomial, usually by using approximation

$$\frac{d}{dt}f(t) \approx \frac{f(t+\Delta t) - f(t)}{\Delta t}.$$

The system of equations for the basic SIR model (2.1) then becomes:

$$\frac{S(t+\Delta t) - S(t)}{\Delta t} = -\beta \frac{S(t)I(t)}{N}$$

[1] There are other types of problems, such as boundary value problems.

$$\frac{I(t+\Delta t)-I(t)}{\Delta t} = \beta\frac{S(t)I(t)}{N} - \gamma I(t)$$
$$\frac{R(t+\Delta t)-R(t)}{\Delta t} = \gamma I(t),$$

or equivalently:

$$S(t+\Delta t) = S(t) - \Delta t\,\beta\frac{S(t)I(t)}{N}$$
$$I(t+\Delta t) = I(t) + \Delta t\left(\beta\frac{S(t)I(t)}{N} - \gamma I(t)\right)$$
$$R(t+\Delta t) = R(t) + \Delta t\,\gamma I(t),$$

Some readers may recognize these equations as *explicit Euler method* for numerically solving a system of ordinary differential equations. Along with the initial condition $S(0), I(0), R(0)$ this set of equations has a unique solution.

The step length Δt must be short enough so that the solution of these difference equations is *stable*, i.e. does not "blow" to infinity, nor become negative.

When approximation of derivative

$$\frac{d}{dt}f(t) \approx \frac{f(t)-f(t-\Delta t)}{\Delta t}$$

is used, we get to a set of equations that have to be solved in each time step:

$$S(t) = S(t-\Delta t) - \Delta t\,\beta\frac{S(t)I(t)}{N}$$
$$I(t) = I(t-\Delta t) + \Delta t\left(\beta\frac{S(t)I(t)}{N} - \gamma I(t)\right)$$
$$R(t) = R(t-\Delta t) + \Delta t\,\gamma I(t).$$

This method is known as *implicit Euler method* for numerically solving differential equations. The name *implicit* comes from the fact that the unknown function appears on both sides of the equation. So a set of algebraic equations must be solved in every time step. This method is always stable [17].

Another popular finite difference method is *Crank-Nicholson method*, which is an "average" of the two above:

$$S(t) = S(t-\Delta t) - \frac{\Delta t}{2}\left(\beta\frac{S(t)I(t)}{N} + \beta\frac{S(t-\Delta t)I(t-\Delta t)}{N}\right)$$
$$I(t) = I(t-\Delta t) + \frac{\Delta t}{2}\left(\beta\frac{S(t)I(t)}{N} + \beta\frac{S(t-\Delta t)I(t-\Delta t)}{N} - \gamma I(t) - \gamma I(t-\Delta t)\right)$$

$$R(t) = R(t - \Delta t) + \frac{\Delta t}{2} \left(\gamma I(t) + \gamma I(t - \Delta t)\right).$$

This method is always stable and yields a better approximation of a solution of the differential equation system: the error term of Crank-Nicholson method is of order $\mathcal{O}(\Delta t^2)$ instead of $\mathcal{O}(\Delta t)$ with Euler method [17]. The method is implicit.

3.1.2 Linear multistep method

Another idea of solving differential equations numerically came from the identity:

$$\int_0^{\Delta t} f'(t + s)ds = f(t + \Delta t) - f(t).$$

But since f' was evaluated only at $t, t - \Delta t, t - 2\Delta t, \ldots$, the integral on the left-hand side cannot be calculated exactly. However f' can be approximated by interpolation. For example in two-step method, the interpolation polynomial is constructed through $f'(t)$ and $f'(t - \Delta t)$:

$$f'(t + s) \approx f(t) + s\frac{f'(t) - f'(t - \Delta t)}{\Delta t}.$$

Which gives us formula:

$$\begin{aligned} f(t + \Delta t) &= f(t) + \int_0^{\Delta t} f'(t + s)ds \\ &\approx f(t) + \int_0^{\Delta t} f'(t) + s\frac{f'(t) - f'(t - \Delta t)}{\Delta t}ds \\ &= f(t) + \Delta t\, f'(t) + \frac{\Delta t}{2}\left(f'(t) - f'(t - \Delta t)\right) \\ &= f(t) + \Delta t \left(\frac{3}{2}f'(t) - \frac{1}{2}f'(t - \Delta t)\right). \end{aligned}$$

This method is known as *Adams-Bashforth method* of order 2. One can see that the name of this family of numerical methods, *linear multistep methods* comes from the right-hand side, where we can find linear combinations of f' evaluated at different time steps. The basic SIR model in this schema can be expressed as:

$$S(t + \Delta t) = S(t) + \Delta t \left(-\frac{3}{2}\beta\frac{S(t)I(t)}{N} + \frac{1}{2}\beta\frac{S(t - \Delta t)I(t - \Delta t)}{N}\right)$$

$$I(t + \Delta t) = I(t) + \Delta t \left(\frac{3}{2}\beta\frac{S(t)I(t)}{N} - \frac{1}{2}\beta\frac{S(t - \Delta t)I(t - \Delta t)}{N} - \frac{3}{2}\gamma I(t) + \frac{1}{2}\gamma I(t - \Delta t)\right)$$

$$R(t+\Delta t) = R(t) + \Delta t \left(\frac{3}{2}\gamma I(t) - \frac{1}{2}\gamma I(t-\Delta t)\right).$$

Similar to Euler method, linear multistep method also comes in implicit flavor. The identity

$$\int_{-\Delta t}^{0} f'(t+s)ds = f(t) - f(t-\Delta t)$$

with the same interpolant (3.1.2) gives us:

$$\begin{aligned} f(t) &= f(t-\Delta t) + \int_{-\Delta t}^{0} f'(t+s)ds \\ &\approx f(t-\Delta t) + \int_{-\Delta t}^{0} f'(t) + s\frac{f'(t) - f'(t-\Delta t)}{\Delta t}ds \\ &= f(t-\Delta t) + \Delta t\, f'(t) - \frac{\Delta t^2}{2}\left(\frac{f'(t) - f'(t-\Delta t)}{\Delta t}\right) \\ &= f(t-\Delta t) + \frac{f'(t) + f'(t-\Delta t)}{2} \end{aligned}$$

This method is implicit, because in order to calculate $f'(t)$ on the right-hand side, one must (usually) know the value $f(t)$ on the left-hand side. This family of methods is known as *Adams-Moulton method*. This particular method is also known as *trapezoidal rule*.

This method applied to SIR model gives us numerical schema:

$$\begin{aligned} S(t) &= S(t-\Delta t) + \frac{\Delta t}{2}\left(-\beta\frac{S(t)I(t)}{N} - \beta\frac{S(t-\Delta t)I(t-\Delta t)}{N}\right) \\ I(t) &= I(t-\Delta t) + \frac{\Delta t}{2}\left(\beta\frac{S(t)I(t)}{N} + \beta\frac{S(t-\Delta t)I(t-\Delta t)}{N} - \gamma I(t) - \gamma I(t-\Delta t)\right) \\ R(t) &= R(t-\Delta t) + \frac{\Delta t}{2}\left(\gamma I(t) + \gamma I(t-\Delta t)\right) \end{aligned}$$

There is a very powerful combination of explicit and implicit linear multistep methods, called *predictor-corrector* method. It avoids solving a set of equations in each time step, while still preserving some good numerical properties. The idea is to use the explicit method to "predict" the value of $f(t+\Delta t)$ and calculate $f'(t+\Delta t)$ and then use this value in implicit method to calculate "correction":

$$f_p(t+\Delta t) = f_c(t) + \Delta t\left(\frac{3}{2}f'(t) - \frac{1}{2}f'(t-\Delta t)\right)$$

$$f_c(t+\Delta t) = f_c(t) + \frac{\Delta t}{2}\left(f'_c(t) + f'_p(t+\Delta t)\right)$$

where subscripts p, c stand for predicted and corrected value. f'_p is derivative evaluated from predicted value and f'_c is derivative evaluated from corrected value. There are many choices of predictor-corrector pairs, differing in order, for example the predictor of order 1 and corrector of order 2 is called *Heun's method* [16]. The correction step can be used multiple times, either a given number of times, or until some convergence criterion is satisfied.

The SIR model in this schema reads:

$$\begin{aligned}
S_p(t+\Delta t) &= S_c(t) + \Delta t\left(-\frac{3}{2}\beta\frac{S_c(t)I_c(t)}{N} + \frac{1}{2}\beta\frac{S_c(t-\Delta t)I_c(t-\Delta t)}{N}\right)\\
I_p(t+\Delta t) &= I_c(t) + \Delta t\left(\frac{3}{2}\beta\frac{S_c(t)I_c(t)}{N} - \frac{1}{2}\beta\frac{S_c(t-\Delta t)I_c(t-\Delta t)}{N}\right.\\
&\qquad\left. -\frac{3}{2}\gamma I_c(t) + \frac{1}{2}\gamma I_c(t-\Delta t)\right)\\
R_p(t+\Delta t) &= R_c(t) + \Delta t\left(\frac{3}{2}\gamma I_c(t) - \frac{1}{2}\gamma I_c(t-\Delta t)\right)
\end{aligned}$$

$$\begin{aligned}
S_c(t+\Delta t) &= S_c(t) + \frac{\Delta t}{2}\left(-\beta\frac{S_p(t+\Delta t)I_p(t+\Delta t)}{N} - \beta\frac{S_c(t)I_c(t)}{N}\right)\\
I_c(t+\Delta t) &= I_c(t) + \frac{\Delta t}{2}\left(\beta\frac{S_p(t+\Delta t)I_p(t+\Delta t)}{N}\right.\\
&\qquad\left. +\beta\frac{S_c(t)I_c(t)}{N} - \gamma I_p(t+\Delta t) - \gamma I_c(t)\right)\\
R_c(t+\Delta t) &= R_c(t) + \frac{\Delta t}{2}\left(\gamma I_p(t+\Delta t) + \gamma I_c(t)\right)
\end{aligned}$$

There are more methods from this family, with interpolating polynomials of higher degrees. However, with the higher degree of the method, the stability usually worsens. [2] For detailed discussion on these methods, we refer the curious reader to chapter 3 of [44].

[2] The problem of stability can be approached intuitively from the point of Runge phenomenon for high-degree interpolating polynomials.

3.1.3 Runge-Kutta methods

One of the most popular family of numerical methods for solving differential equations is the Runge-Kutta family. These methods are usually implemented in common numerical software such as R, Scipy or Julia [14, 82, 72]. For a brief introduction we refer the reader to the article [45] and for a more detailed explanation to [44].

The idea is to calculate the derivative multiple times during one step and estimate the solution by a suitable linear combination of these derivatives. The derivatives may depend on time as well as on the value of the function: $f' = f'(t, f(t))$. By choosing a good linear combination, one can eliminate the largest error terms. For example, "the Runge-Kutta" method of order 4 uses 4 evaluations of derivative in each time step:

$$\begin{aligned} k_1 &= f'\left(t, f(t)\right) \\ k_2 &= f'\left(t + \frac{\Delta t}{2}, f(t) + \frac{\Delta t}{2} k_1\right) \\ k_3 &= f'\left(t + \frac{\Delta t}{2}, f(t) + \frac{\Delta t}{2} k_2\right) \\ k_4 &= f'\left(t + \Delta t, f(t) + \Delta t\, k_3\right). \end{aligned}$$

Then, $f(t + \Delta t)$ can be approximated by $f(t) + \frac{\Delta t}{6}\left(k_1 + 2k_2 + 2k_3 + k_4\right)$ with error term of order $\mathcal{O}(\Delta t^5)$[44]. The schema is sometimes written in the form of tableau, which is called *Butcher tableau*[3]:

0				
1/2	1/2			
1/2		1/2		
1			1	
	1/6	1/3	1/3	1/6

Each row represents one of values $k_1, \ldots, k_4$. The left column represents the coefficients of Δt in the first argument of f'. Numbers in the bottom row are linear combination coefficients of the final approximation. Numbers in the middle array represent coefficients of ks in each calculation of new k. For the sake of brevity we do not expand the

[3]Some earlier authors put the coefficients of the linear combination as a last column of this table, for example [33].

entire numerical schema of this method for the SIR model.

A slight variation of the method has slightly different coefficients and requires more operations during one time step, but the error coefficient is smaller:

$$
\begin{aligned}
k_1 &= f'\left(t, f(t)\right) \\
k_2 &= f'\left(t + \frac{\Delta t}{3}, f(t) + \frac{\Delta t}{3} k_1\right) \\
k_3 &= f'\left(t + \frac{2\Delta t}{3}, f(t) - \frac{\Delta t}{3} k_1 + \Delta t\ k_2\right) \\
k_4 &= f'\left(t + \Delta t, f(t) + \Delta t\ k_1 - \Delta t\ k_2 + \Delta t\ k_3\right)
\end{aligned}
$$

and $f(t + \Delta t)$ is approximated by $f(t) + \frac{\Delta t}{8}\left(k_1 + 3k_2 + 3k_3 + k_4\right)$. The Butcher tableau for this method is:

0				
1/3	1/3			
2/3	-1/3	1		
1	1	-1	1	
	1/6	1/3	1/3	1/6

3.1.4 Runge-Kutta methods with adaptive stepsize

What made the Runge-Kutta family of methods so successful was the possibility to control the step length: in difficult-to-integrate regions, the step size would shorten. The idea is to calculate two approximations of different order and use their difference to estimate the error. The step length is then chosen so that error is within some desired tolerance. Much of the computational power can be saved, if the one approximation "recycles" coefficients from the other, in which case we say that the two methods are *embedded*. Some of these methods are listed in [33, 29].

The most common method is *Runge-Kutta-Fehlberg method*, which uses methods of order 4 and 5. The difference between these approximations, denoted TE (truncation error) is of order $\mathcal{O}(\Delta t^4)$. If the desired tolerance is ε, the step length must be less than $\Delta t \cdot \left(\frac{\varepsilon}{TE}\right)^{1/5}$. In practice, this value is multiplied by 0.9 [45]. The exact coefficients might differ between implementations. Even Fehlberg himself provides two sets of coefficients

in pages 12 and 13 of [33]. Later authors found different sets of coefficients that might be either computationally less expensive, provide better stability or smaller truncation error.

Another popular method from this family is *Bogacki-Shampine method*, introduced in [13], which uses approximations of order 3 and 2 and is usually implemented in numerical packages [82, 72].

There are also *implicit* Runge-Kutta methods, which require solving a set of algebraic equations in each time step. These equations are solved by some numerical method. Providing the Jacobian of the right-hand side of the differential equation system is generally recommended for speedup and accuracy [82].

3.1.5 Differential transformation method (DTM)

When an algebraic expression for the differential equations is provided, one can usually construct (truncated) a polynomial expression that (approximately) solves the system. The problem of solving differential equations is transformed into solving algebraic equations for polynomial coefficients. Because this method combines analytical and numerical methods, it belongs to the family of *semi-analytical methods*. This method was used for solving epidemiological models in e.g. [2, 3, 9].

For the sake of simplicity, only expansion of f at $t = 0$ will be discussed. The solution of differential equation is written in form:

$$f(t) = \sum_{k=0}^{\infty} \frac{t^k}{k!} \left. \frac{d^k f(t)}{dt} \right|_{t=0}$$

Let us denote the coefficients of t^k as $F(k)$:

$$f(t) = \sum_{k=0}^{\infty} t^k F(k)$$

$F(k)$ is called *transformed function* corresponding to $f(t)$. Similarly, let $u(t)$ and $v(t)$ be some functions with their transformed functions $U(k)$ and $V(k)$ respectively and let $\alpha \in \mathbb{R}$ be a scalar. Then transformed functions have following properties [48]:

1. If $f(t) = u(t) \pm v(t)$, then $F(k) = U(k) \pm V(k)$.

2. If $f(t) = u(t)v(t)$, then $F(k) = \sum_{i=0}^{k} U(k-i)V(i)$.

3. If $f(t) = \alpha u(t)$, then $F(k) = \alpha U(k)$.

4. If $t(f) = \frac{d}{dt}u(t)$, then $F(k) = (k+1)U(k+1)$.

5. If $t(f) = \frac{d^n}{dt^n}u(t)$, then $F(k) = \frac{(k+1)!}{k!}U(k+n)$.

6. If $f(t) = t^n$, then $F(k) = \delta_{n-k} = \begin{cases} 1 & \text{if } k = n \\ 0 & \text{otherwise.} \end{cases}$

7. If $f(t) = \exp(\alpha t)$, then $F(k) = \frac{\alpha^k}{k!}$

Let us now express the standard SIR model with the initial condition $S(0) = S_0, I(0) = I_0, R(0) = R_0$ via this method. Let $s(k), i(k), r(k)$ be transformed functions $S(t), I(t), R(t)$, respectively. Then:

$$s(0) = S_0, \quad i(0) = I_0, \quad r(0) = R_0,$$

$$\begin{aligned}
(k+1)s(k+1) &= -\frac{\beta}{N}\sum_{i=0}^{k} s(i)i(k-i) \\
(k+1)i(k+1) &= \frac{\beta}{N}\sum_{i=0}^{k} s(i)i(k-i) - \gamma i(k) \\
(k+1)r(k+1) &= \gamma i(k)
\end{aligned}$$

where the first three equations represent the initial condition and the last three equations represent dynamics. This particular system is already eliminated and can be solved iteratively:

$$\begin{aligned}
s(1) &= -\beta\frac{I_0 S_0}{N} \\
i(1) &= \beta\frac{I_0 S_0}{N} - \gamma I_0 \\
r(1) &= \gamma I_0 \\
s(2) &= \frac{I_0 S_0 \beta\left(I_0\beta + N\gamma - S_0\beta\right)}{2N^2} \\
i(2) &= \frac{I_0\left(N\gamma\left(N\gamma - S_0\beta\right) - S_0\beta\left(I_0\beta + N\gamma - S_0\beta\right)\right)}{2N^2} \\
r(2) &= \frac{I_0\gamma\left(-N\gamma + S_0\beta\right)}{2N} \\
&\vdots
\end{aligned}$$

This expansion can be also done numerically, if values S_0, I_0, R_0 are given. The infinite system is truncated and solved for some maximum value $k \leq k_{max}$. The functions $S(t), I(t), R(t)$ are then reconstructed as

$$S(t) = \sum_{k=0}^{k_{max}} s(k)t^k$$
$$I(t) = \sum_{k=0}^{k_{max}} i(k)t^k$$
$$R(t) = \sum_{k=0}^{k_{max}} r(k)t^k.$$

In practice, multi-step differential transform method is used, in which the solution is found on small consecutive time intervals, with solution at the right side of one time interval becomes initial condition of the next.[4] This method was employed in mathematical epidemiology in [9] or even chaotic dynamical systems as in [70]. The time interval length can be estimated from the transformed functions $s(k), i(k), r(k)$ so that the truncation error is within desired tolerance.

3.2 Parabolic partial differential equations

Let us consider the parabolic partial differential equation

$$\frac{\partial u(t,x)}{\partial t} - \kappa \frac{\partial^2 u(t,x)}{\partial x^2} = 0$$

on a finite domain $x \in [0, L]$. The function is given some boundary conditions, for convenience $u(t,x)|_{x=0} = 0 = u(t,x)|_{x=L}$ and an initial condition $u(t,x)|_{t=0} = u_0(x)$. [5] In this section, we present two methods for solving this equation. [6]

3.2.1 Method of lines

The method of lines transforms the partial differential equation into a system of coupled ordinary differential equations. Several points in the spatial domain $[0, L]$ are

[4] Multistep DTM with time intervals $[0, dt], [dt, 2\ dt], [2\ dt, 3\ dt]$ with $k_{max} = 1$ is equivalent to explicit Euler method.

[5] Boundary conditions will be further discussed later in section 5.2.

[6] The presented methods also apply to hyperbolic partial differential equation $\frac{\partial^2 u(t,x)}{\partial t^2} - \kappa \frac{\partial^2 u(t,x)}{\partial x^2} = 0$.

selected, for example $0, \frac{L}{k}, \frac{2L}{k}, \ldots, \frac{(k+1)L}{k}, L$ and a set of ordinary differential equations is constructed:

$$\begin{aligned}
\frac{d}{dt}u(t,0) &= 0 \\
\frac{d}{dt}u(t,\tfrac{L}{k}) &= \kappa\frac{\partial^2}{\partial x^2}u(t,x)|_{x=\frac{L}{k}} \\
\frac{d}{dt}u(t,\tfrac{2L}{k}) &= \kappa\frac{\partial^2}{\partial x^2}u(t,x)|_{x=\frac{2L}{k}} \\
&\vdots \\
\frac{d}{dt}u(t,\tfrac{(k-1)L}{k}) &= \kappa\frac{\partial^2}{\partial x^2}u(t,x)|_{x=\frac{(k-1)L}{k}} \\
\frac{d}{dt}u(t,L) &= 0
\end{aligned}$$

with initial conditions

$$\begin{aligned}
u\left(0,\frac{nL}{k}\right) = 0 = u_0\left(\frac{nL}{k}\right), \\
u(0,\frac{iL}{k}) = u_0\left(\frac{iL}{k}\right).
\end{aligned}$$

The second-order derivatives on the right-hand side of the system can be approximated by second-order finite differences:

$$\left.\frac{\partial^2}{\partial x^2}u(t,x)\right|_{x=\frac{nL}{k}} \approx \frac{k^2}{L^2}\left[u\left(t,\frac{(n-1)L}{k}\right) - 2u\left(t,\frac{nL}{k}\right) + u\left(t,\frac{(n+1)L}{k}\right)\right],$$

which leads to a system of linear ordinary differential equations that can be written in a compact vector-matrix form:[7]

$$\frac{d}{dt}\begin{bmatrix} u(t,0) \\ u(t,L/k) \\ u(t,2L/k) \\ \vdots \\ u(t,(k-1)L/k) \\ u(t,L) \end{bmatrix} = \kappa\frac{k^2}{L^2}\begin{bmatrix} 0 & & & & & \\ -1 & 2 & 1 & & & \\ & -1 & 2 & 1 & & \\ & & \ddots & \ddots & \ddots & \\ & & & -1 & 2 & 1 \\ & & & & & 0 \end{bmatrix}\begin{bmatrix} u(t,0) \\ u(t,L/k) \\ u(t,2L/k) \\ \vdots \\ u(t,(k-1)L/k) \\ u(t,L) \end{bmatrix}.$$

This equation can be solved explicitly via matrix exponentiation, or numerically via one of numerical methods for solving ordinary differential equations.

[7] Zero elements of the matrix were omitted.

3.2.2 Fourier series

The function $u(t,x)$ can be written in terms of its Fourier series with variable coefficients:

$$u(t,x) = \sum_{n=1}^{\infty} y_n(t) \sin\left(\frac{n\pi x}{L}\right),$$

where $y_n(0)$ are Fourier coefficients of initial condition u_0. [8] Plugging this ansatz into the equation and changing the order of sum and differentiation gives us:

$$\frac{\partial}{\partial t}\sum_{n=1}^{\infty} y_n(t) \sin\left(\frac{n\pi x}{L}\right) = \kappa \frac{\partial^2}{\partial x^2}\sum_{n=1}^{\infty} y_n(t) \sin\left(\frac{n\pi x}{L}\right)$$

$$\sum_{n=1}^{\infty} \frac{\partial}{\partial t} y_n(t) \sin\left(\frac{n\pi x}{L}\right) = \kappa \sum_{n=1}^{\infty} y_n(t) \frac{\partial^2}{\partial x^2} \sin\left(\frac{n\pi x}{L}\right)$$

$$\sum_{n=1}^{\infty} y_n'(t) \sin\left(\frac{n\pi x}{L}\right) = \kappa \sum_{n=1}^{\infty} -y_n(t) \frac{n^2\pi^2}{L^2} \sin\left(\frac{n\pi x}{L}\right).$$

Now, by comparing the coefficients of $sin(n\pi x/L)$ on both sides yields a set of ordinary differential equations:

$$y_n'(t) = -\kappa \frac{n^2\pi^2}{L^2} y_n(t),$$

which can be solved analytically or numerically via one of the methods listed above.

3.3 Stochastic models with discrete state space

3.3.1 Master equation

One may be interested in probability distribution of state vectors after some time T. This might be done for the purpose of simulation, calculating likelihood or statistics such as mean, variance and correlation between copy numbers. If one is interested in

[8] This is the main contribution of Fourier in his *Analytic theory of heat* [35]. As soon as in paragraph 19 of his 433-paragraph-long book, he states: *[...] in order to express this property the analytical formulæ contain terms composed of exponentials and of quantities analogous to trigonometric functions.* And in the next paragraph: *If we could observe the changes of temperature for every in at every point of a solid homogeneous mass we should discover in these series of observations the properties of recurring series as of sines and logarithms..*

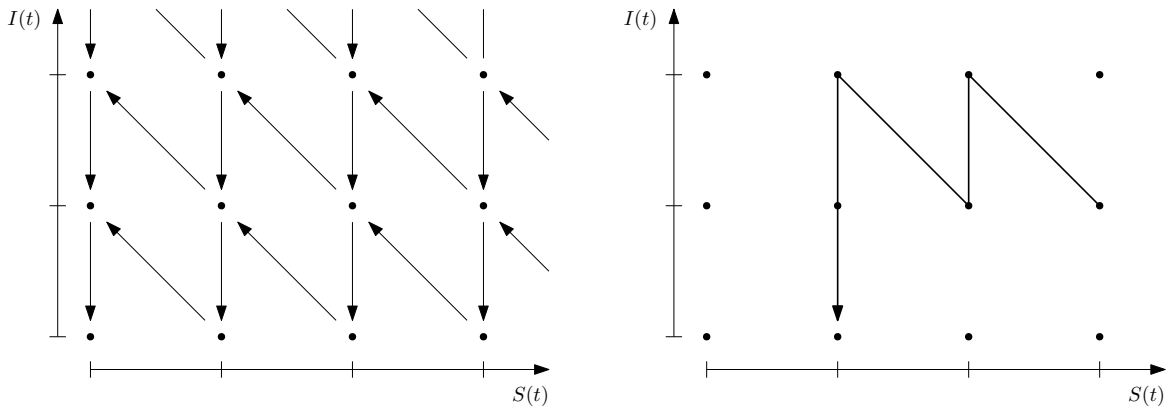

Fig. 3.1: Left: Graph of reduced SIR model. Edges pointing top left represent new infection transitions, edges pointing down represent recovery. Right: example of one simulation. The state vector begins at $[S, I]^T = [3, 1]^T$, continuing through $[2, 2]^T$, $[2, 1]^T$, $[1, 2]^T$, $[1, 1]^T$ and ending at $[1, 0]^T$.

estimates of these numbers, repeated simulations might be a good option. However, the probability distribution may be calculated rigorously using so-called *master equation*, which is an (usually infinite) system of linear ODEs. [9]

The state space can be viewed as a graph with nodes representing states and oriented edges representing possible transitions between them. Example of such a graph for the basic SIR model (reduced to two compartments) is depicted in Fig. 3.1 left. Notice that edges of this graph represent columns of stoichiometry matrix. The stochastic simulation then can be viewed as a random walk on this graph and the master equation represents this walk. Examples of such a walk can be seen on the right-hand side of the same figure.

The probability that after a short time step Δt the system is in state x is equal to probability that the system was already at the state and nothing happened added to the sum of probabilities that the system was at state $x - \nu_j$ and j-th transition occurred.

Let $p_x(t)$ denote the probability that at time t the system is in state x. The equation for $p_x(t)$ is:

$$p_x(t + \Delta t) = p_x(t)(1 - a_0(x)\Delta t) + \sum_{j=0}^{n} p_{x-\nu_j}(t) a_j(x - \nu_j)\, \Delta t,$$

[9] Only special cases of an infinite system of ODEs can be solved [15]. In the general case, one can truncate the state space in some reasonable way and solve the system numerically.

which in the limit $\Delta t \to 0^+$ can be rearranged into ordinary differential equation

$$\frac{dp_x(t)}{dt} = -a_0(x) + \sum_{j=0}^{n} p_{x-\nu_j}(t) a_j(x-\nu_j).$$

This coupled system of ordinary differential equations is known as the master equation.

For stochastic SIR model the master equation is:

$$\frac{dp_{[S,I,R]}}{dt} = -\beta\frac{SI}{N} - \gamma I + \beta\frac{(S+1)(I-1)}{N} + \gamma(I+1),$$

where $p_{[S,I,R]}(t)$ is a probability that at time t there will be S susceptible, I infectious and R recovered individuals. Together with initial condition

$$p_{[S,I,R]} = \begin{cases} 1 & \text{if} [S,I,R] = [S(0), I(0), R(0)] \\ 0 & \text{otherwise,} \end{cases}$$

where $S(0), I(0), R(0)$ is the initial number of susceptible, infectious and recovered individuals at time 0, one can solve the truncated system by some numerical method.

3.3.2 Gillespie algorithm

The best-known technique to solve the continuous-time, discrete-state setup is *gillespie algorithm*, published in papers [38, 39]. There are multiple extensions of this algorithm, such as saving computing power by reusing random numbers [37], or extension of the algorithm for non-markovian processes [64].

We will sketch the main idea of the algorithm, referring to [38, 32] for a more rigorous approach. First step of the algorithm is to find the time of the next transition. The probability that the j-th transition occurs during the next time step of small length Δt is $a_j\ \Delta t$. The probability that any transition occurs is $a_0\ \Delta t$, the sum of the propensities of individual transitions. During a bigger time interval of length T, no transition happen with probability $(1 - a_0\ \Delta t)^{\frac{T}{\Delta t}}$, as there are $T/\Delta t$ independent time intervals. Now, taking the limit $\Delta t \to 0^+$, we find that no transition will happen with probability $\exp(-a_0 T)$, which is the survival function of exponential distribution with parameter a_0. Therefore, time to the next reaction is exponentially distributed with parameter a_0.

The second step is to find the reaction that occurred at the time. It can be proven that probability that j-th reaction occurred is a_j/a_0.[10]

Now we may write down gillespie algorithm:

1. Initialize starting vector $x(0)$ and final time T for simulation. Initialize time variable $t = 0$.
2. Calculate propensities $a_1, \dots a_n$ and their sum a_0 for current state vector. If $a_0 = 0$, set t to T and terminate.
3. Generate τ from $Exp(a_0)$.[11]
4. If $t + \tau > T$, set t to T and terminate.
5. Generate u from $\mathcal{U}(0, a_0)$. Select the reaction j, the smallest integer for which $u < \sum_{k=1}^{j} a_k$.
6. Set x to $x + \nu_j$, set t to $t + \tau$ and go to 2.

The Gillespie algorithm can be applied to the standard SIR model with the state vector $x(t) = [S(t), I(t), R(t)]^T$, propensities $a_1(S, I, R) = \beta\frac{SI}{N}$, $a_2(S, I, R) = \gamma I$ and transition vectors $\nu_1 = [-1, 1, 0]^T$ and $\nu_2 = [0, -1, 1]^T$.

3.3.3 Tau-leaping algorithm

The Gillespie algorithm might become inefficient if reactions tend to occur at high rates, because each transition requires two random numbers generations and at most $n - 1$ comparisons. For these cases, the *τ-leap* algorithm was proposed [41]. Instead of recalculating propensities after each reaction, they are recalculated periodically after each time step τ. The parameter τ should satisfy *leap condition*:

> Require τ to be small enough that the change in state during $[t, t + \tau]$ will be so slight that no propensity function will suffer appreciable (i.e. macroscopically non-infinitesimal) change in value[41].

[10] This is probability that minimum from n exponentially distributed random variables $r_1, \dots, r_n$ with parameters $a_1, \dots, a_n$ is r_j.

[11] The original implementation used $\mathcal{U}(0, 1)$ distribution only, from which the exponentially distributed value was obtained via inverse transform method $\tau = -\ln(1 - u)/a_0$, where $u \sim \mathcal{U}(0, 1)$.

In fact, Gillespie suggests more strict conditions for selecting τ and falling back to Gillespie algorithm if τ would be too small.

If the rates can be considered constant during the interval $[t, t+\tau]$ and transitions occur independently, then the number of j-th transitions during the interval has Poisson distribution with mean τ/a_j.[12] After the τ is chosen, the number of occurrences of each transition is generated and the state vector is updated.

The tau-leaping algorithm states:

1. Initialize starting vector $x(0)$ and final time T for simulation. Initialize time variable $t = 0$.

2. Calculate propensities $a_1, \dots a_n$ and their sum a_0 for current state vector. If $a_0 = 0$, set t to T and terminate.

3. Choose τ that satisfies the leap condition. If $t + \tau > T$, set τ to $T - t$.

4. For each $j = 1, \dots, n$, generate z_j from $\mathcal{P}oiss(\tau \cdot a_j)$.

5. Update x to $x + \sum_{k=1}^{n} z_j \nu_j$. If any $x_i < 0$, take back this update and go to 4.

6. Set t to $t + \tau$. If $\tau = T$, terminate, else go to 2.

This algorithm also has some downsides: Because the change of the state vector may yield negative integers in the state vector, a check in step 5 is needed. If there is an insignificant probability that some element of the state vector x will be negative after the leap, some authors propose more strict conditions on τ selection [21]. For even improved speed of τ selection see [20]. On the other hand, being too specific on τ may introduce some bias which needs to be corrected and post-leap check needs to be performed [6].

[12] It follows from the property that the number of occurrences of independent events with exponentially distributed waiting time, during a unit of time follows Poisson distribution. In fact, this procedure is the used as a way of generating random numbers from Poisson distribution [57, 7].

3.4 Stochastic models with continuous state space

3.4.1 Fokker-Planck equation

The Fokker-Planck equation is the continuous counterpart of the discrete Master equation, presented in section 3.3.1. Instead of the probability of a given state, the *probability density function* is modeled. Let us denote the probability density function of state x at time t as $p(x,t)$. The equation for p is called *Fokker-Planck equation*. In the case of one-dimensional stochastic process described by stochastic differential equation

$$dX_t = \mu(X_t,t)\,dt + \sigma(X_t,t)\,dW_t,$$

the Fokker-Planck equation reads [73, 75]:

$$\frac{\partial p(x,t)}{\partial t} = -\frac{\partial}{\partial x}[\mu(x,t)\,p(x,t)] + \frac{1}{2}\frac{\partial^2}{\partial x^2}[\sigma^2(x,t)\,p(x,t)].$$

In many cases, this equation does not have a solution in explicit form and numerical method has to be employed. For more details on the equation, its solution and generalization to multivariate distributions, we refer the reader to chapters 4 – 6 of textbook [73].

This equation can be used to solve the probability distribution of the number of infectious individuals after a certain time. Also metrics such as expected value, variance and possibly covariance can be inferred from the solution of the equation.

3.4.2 Euler-Maruyama method

Consider the tau-leaping algorithm, presented in section 3.3.3. Under certain conditions, [13] one can approximate Poisson-distributed random variables z_j with parameter τa_j from step 4 of tau-leaping algorithm with normally-distributed random variables with both the mean and variance τa_j [41, 42]. This step effectively treats the copy numbers

[13] Gillespie in his paper [42] says about these conditions: "If there exists a time interval during which none of the system's propensity functions will suffer a noticeable change of value, yet every reaction channel will be expected to fire many more times than once. It is true that satisfying these conditions will nearly always require *large* molecular populations; however, the practical question of *how large* can be answered only by appealing directly to those dynamic conditions."

as continuous quantities. By denoting time step as Δt, instead of τ, we can write a numerical schema for the standard SIR model as:

$$\begin{aligned} S(t+\Delta t) &= S(t) - \beta \frac{S(t)I(t)}{N}\left(\Delta t + \Delta W_t^{(1)}\right) \\ I(t+\Delta t) &= \beta \frac{S(t)I(t)}{N}\left(\Delta t + \Delta W_t^{(1)}\right) - \gamma I(t)\left(\Delta t + \Delta W_t^{(2)}\right) \\ R(t+\Delta t) &= \gamma I(t)\left(\Delta t + \Delta W_t^{(2)}\right), \end{aligned}$$

where $\Delta W_t^{(1)}, \Delta W_t^{(2)}$ are independent random numbers generated from normal distribution with zero mean and Δt variance.

This numerical schema can be also derived from a stochastic differential equation (2.8) from section 2.3.8, where differentials dS, dI, dR are replaced with finite differences $S(t+\Delta t) - S(t)$, $I(t+\Delta t) - I(t)$ and $R(t+\Delta t) - R(t)$, respectively and differential terms dt and dW_t are replaced with ΔW_t. This method of generating trajectories from a given stochastic differential equation is known as *Euler-Maruyama* method.

3.4.3 Leimkuhler–Matthews method

The Leimkuhler–Matthews method is a modification of the Euler-Maruyama method. It is best suited for generating long-term trajectories [60]. Besides the state vector X_t, this method uses a momentum vector P_t. The schema for generating trajectories described by stochastic differential equation with constant diffusion term $\sigma \equiv const.$

$$dX_t = \mu(X_t, t)\, dt + \sigma\, dW_t,$$

the schema reads:

$$\begin{aligned} X'_{t+\Delta t} &= X_t + \mu(X_t, t) + \frac{1}{2}\sigma P_t \\ \text{generate } P_{t+\Delta t} &\sim N(\vec{0}, \Delta t I) \\ X_{t+\Delta t} &= X'_{t+\Delta t} + \frac{1}{2}\sigma P_{t+\Delta t}, \end{aligned}$$

where $X'_{t+\Delta t}$ is a "candidate" value for $X_{t+\Delta t}$, which is refined in the next step.

3.4.4 Runge-Kutta methods for stochastic differential equations

Runge-Kutta methods can be generalized for generating trajectories of stochastic differential equations. A great introduction into the topic of stochastic Runge-Kutta methods

can be found in chapter 6 of lecture notes [75].

Consider a general Itô stochastic differential equation in the form:

$$dX_t = \mu(X_t, t)\, dt + \sigma(X_t, t)\, dW_t$$

where μ and σ are sufficiently smooth drift and volatility functions. Then the trajectory of the process can be generated by formula [74]:

$$\begin{aligned} k_1 &= \mu(t, X_t)\Delta t + (\Delta W_t - S_k)\sigma(t, X_t) \\ k_2 &= \mu(t + \Delta t, S_t + k_1) + (\Delta W_t + S_k)\sigma(t + \Delta t, X_t + k_1) \\ X_{t+\Delta t} &= X_t + \frac{1}{2}(k_1 + k_2) \end{aligned}$$

where ΔW_k is a random number generated from a normal distribution with zero mean and variance Δt and S_k is $\pm\sqrt{\Delta t}$, each with probability $1/2$. The method has strong convergence of order 1.

Formulae of higher order are available, for example in [28].

Chapter 4

Immunity boosting

SIRS is an epidemiological model that takes immunity waning into account. Its name is derived from the added transition from *recovered* compartment back to the *susceptible* compartment: The typical state of an individual in case of an epidemiological event is $S \to I \to R \to S$. For further details we refer the reader to the textbook [55], chapter 2.4. A detailed stability analysis of models with waning immunity was done by [68]: it was shown that such models can become unstable because of the circulating nature of an individual's epidemiological status. In the article [31] a custom waning profile was discussed and an efficient numerical schema was presented.

However, it can be observed that immunity can be also boosted, when a recovered individual meets an infectious one. A model with immunity boosting was recently studied in [22], in which the S compartment was subdivided into $S_1, \ldots, S_5$ by different immunity status. However, we utilize a different approach here: instead of slowly increasing the risk of infection, we assume that an individual is fully immune for a certain period of time, after which is completely susceptible.

We take two approaches here: the first will be modeling by the means of ordinary differential equations while the second will be by the means of integral-differential equations. While the first approach is simpler in terms of both implementation and numerical routines, it works on assumption of Erlang distributions of the immune period, which may not always be met. Therefore we will also consider a more general case such as in [31].

4.1 Immunity boosting via ordinary differential equations

4.1.1 Standard SIRS model

Let us consider a standard SIRS model with population dynamics, given by system of ordinary differential equations:

$$\begin{aligned}\frac{dS(t)}{dt} &= -\beta\frac{I(t)S(t)}{N} + \omega R(t) - \mu S(t) + \mu N\\ \frac{dI(t)}{dt} &= \beta\frac{I(t)S(t)}{N} - \gamma I(t) - \mu I(t)\\ \frac{dR(t)}{dt} &= \gamma I(t) - \omega R(t) - \mu R(t),\end{aligned}$$

with β being the force of infection, γ the inverse of mean infectious period and ω the inverse of mean immune period and $N := S(t) + I(t) + R(t) = const.$ is the total population. To analyze this model and incorporate immunity boosting we apply Euler forward method to the system of equations:

$$R(t + \Delta t) = R(t) + \gamma I(t)\ \Delta t - \omega R(t)\ \Delta t - \mu R(t)\ \Delta t.$$

The term $\gamma I\ \Delta t$ represent the number of people that recover from the disease during the small time step of length Δt and the term $\omega R(t)\ \Delta t$ represent the number of recovered people that lose immunity during the time step. Note that the number of people that are about to lose immunity in the next time step is not dependent on the time of immunization. If we consider immunity boosting as a means of immunization, we do not expect to see any changes of the model as we will show in the following paragraph.

Out of the $\omega R(t)\ \Delta t$ people that are about to lose immunity in the next time step, the immunity is not lost for those individuals that meet infectious person and have contact with the pathogen, that is:

$$\beta\frac{I(t)\,(\omega R(t)\Delta t)}{N(t)}\Delta t.$$

So the discretized equation for recovered in SIRS model with immunity boosting is:

$$R(t + \Delta t) = R(t) + \gamma I(t)\ \Delta t - \left(\omega R(t)\ \Delta t - \beta\frac{I(t)\,(\omega R(t)\Delta t)}{N(t)}\Delta t\right) - \mu R(t)\ \Delta t,$$

which can be transformed back into a differential equation by rearranging the terms:

$$R(t + \Delta t) - R(t) = \gamma I(t)\ \Delta t - \left(\omega R(t)\ \Delta t - \beta\frac{I(t)\,(\omega R(t)\Delta t)}{N(t)}\Delta t\right) - \mu R(t)\ \Delta t$$

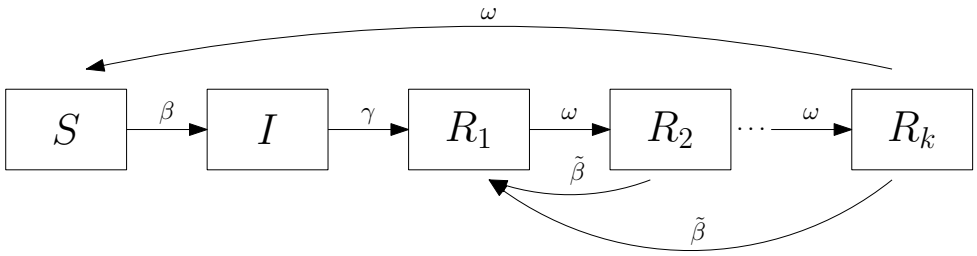

Fig. 4.1: Flow diagram of SIRRS model.

$$\frac{R(t+\Delta t)-R(t)}{\Delta t} = \gamma I(t) \ - \left(\omega R(t) - \beta \frac{I(t)\,(\omega R(t)\Delta t)}{N(t)}\right) - \mu R(t).$$

Now, taking limit $\Delta t \to 0$ gives us the differential equation for recovered:

$$\frac{dR(t)}{dt} = \gamma I(t) - (\omega R(t) - 0) - \mu R(t),$$

which is the exact same equation for recovered as in the standard SIRS model. This should not surprise us, because the SIRS model is *markovian*, i.e. the transitions are independent of the time spent as recovered.

4.1.2 SIRRS model

As we saw in the previous section, the standard SIRS model is not suitable for incorporating immunity boosting. However, there are still models only using ODEs that are capable of capturing it. We will use the so-called "linear chain trick", which was successfully used for modeling different distributions of latent and infectious periods, such as in [36]. In our case, we use the same method to model the immunity period. The idea is to split immunity loss process into k stages, so immunity loss process becomes: $I \xrightarrow{\gamma} R_1 \xrightarrow{\omega} R_2 \xrightarrow{\omega} \ldots \xrightarrow{\omega} R_k \xrightarrow{\omega} S$. This is schematically presented in figure 4.1.

Using this multi-stage process, we can model the immunity waning process in terms of ODEs, while implementing immunity boosting and assert some properties of the immunity waning process. We assert that the time of protective immunity has Erlang

distribution with mean $k\omega$ and variance $\frac{k}{\omega^2}$.[1] [2]

For the sake of generality, we assume that active contact with infectious people may be different for a susceptible individual than for a recovered individual. The contact rate of an infectious and recovered individual and the probability of pathogen transmission are included in parameter $\tilde{\beta}$ with similar meaning than β. [3] If the immune individual receives the pathogen, he is considered to be immunized again. Therefore we also add transitions (with fictional transition $R_1 \to R_1$, so the model formulation will be valid for $k = 1$ as well):

$$R_1 \xrightarrow{\tilde{\beta}\frac{IR_2}{N}} R_1, \quad R_2 \xrightarrow{\tilde{\beta}\frac{IR_2}{N}} R_1, \quad R_3 \xrightarrow{\tilde{\beta}\frac{IR_3}{N}} R_1, \qquad \ldots, \quad R_k \xrightarrow{\tilde{\beta}\frac{IR_k}{N}} R_1,$$

The entire model then stands:

$$\begin{aligned}
\frac{dS(t)}{dt} &= -\beta\frac{I(t)S(t)}{N} + \omega R_k(t) - \mu S(t) + \mu N \\
\frac{dI(t)}{dt} &= \beta\frac{I(t)S(t)}{N} - \gamma I(t) - \mu I(t) \\
\frac{dR_1(t)}{dt} &= \gamma I(t) - \omega R_1(t) + \sum_{i=2}^{k} \tilde{\beta}\frac{I(t)R_i(t)}{N} - \mu R_1(t) \\
\frac{dR_2(t)}{dt} &= \omega R_1(t) - \omega R_2(t) - \tilde{\beta}\frac{I(t)R_2(t)}{N} - \mu R_2(t) \\
&\vdots \\
\frac{dR_k(t)}{dt} &= \omega R_{k-1}(t) - \omega R_k(t) - \tilde{\beta}\frac{I(t)R_k(t)}{N} - \mu R_k(t)
\end{aligned}$$

We will refer to this model as the SIRRS model.

By more complicated dynamics in sub-compartments R_j we could obtain mixed Erlang, by which a wide variety of distributions can be approximated. One such method

[1] If we knew the mean M and standard deviation SD, we could estimate k as $\left[\frac{M^2}{SD^2}\right]$ and ω as $\frac{M}{k}$, with $[\cdot]$ denoting rounding to the nearest integer. Note that due to the discrete nature of parameter k, the variance is only approximately correct. For an illustrative depiction of Erlang distribution, please refer to https://www.geogebra.org/m/k8cxjjsx.

[2] There is an interesting limit behavior for limit $k \to \infty$, while $\frac{k}{\omega} = const$. The mean duration of protective immunity is held constant, but the variance vanishes to zero. As we approach the limit, the model behaves as a delayed-differential model with lag $k\omega$.

[3] That is, contact rate, multiplied by probability of successful pathogen transmission. While "successful" transmission for S–I contact is such that pathogen causes change of epidemiological status from susceptible to infected, for R–I contact it is such that it causes an immunization response.

based on matching moments of distributions can be found in [23]. The shape of waning profiles was studied in e.g. [61, 85, 86].

4.2 Immunity boosting with custom waning profile

This section of the thesis is based on our previous work [31], which has been published in 2019 in the Journal of Computational Science. In the paper, the SIRS-type model with general waning profile was introduced and numerical results were presented.

In this thesis, we enhance the model with a general immunity waning profile by considering immunity boosting. In this setup, we have compartments S, I, R corresponding to susceptible, infectious, recovered individuals, respectively.

We denote the number of individuals in these compartments by $S(t), I(t), R(t)$. Furthermore, let us consider the function $\tilde{R}(t, \tau)$ representing density of individuals, who are recovered at time t whose time of last immunization event happened at $t - \tau$. The immunization event is either recovery, or immunity boosting of recovered via encountering an infectious individual. The total number of recovered individuals at time t is:

$$R(t) = \int_0^\infty \tilde{R}(t, \tau)\, d\tau$$

for model with continuous time, or

$$R(t) = \sum_{i=0}^{\infty} \tilde{R}(t, i \cdot \Delta t)\, \Delta t$$

for model with discrete time.

The equation for infectious is the same as before:

$$\frac{dI(t)}{dt} = \beta \frac{S(t)I(t)}{N(t)} - \gamma I(t).$$

The equation for susceptible can be calculated as the remaining population that is not susceptible nor infectious, once the number of recovered is known:

$$S(t) = N - I(t) + R(t).$$

It is, however possible to express the equation for susceptible in terms of differential equation, as we did in [31], but there is no advantage in doing so.

4.2.1 Discrete formulation of the model

Let $P(\tau)$ be the probability that a person infected at time t did not lose the immunity until time $t+\tau$. We expect the function P to be non-increasing with range $[0,1]$. An important concept will be conditional probability of individuals retaining immunity up to time $\tau+\Delta t$, given that immunity was still present at time τ. This can be expressed using conditional probability as:

$$\frac{\Pr(\text{immunity at } \tau) \cap \Pr(\text{immunity at } \tau+\Delta t)}{\Pr(\text{immunity at } \tau)} = \frac{\Pr(\text{immunity at } \tau+\Delta t)}{\Pr(\text{immunity at } \tau)} = \frac{P(\tau+\Delta t)}{P(\tau)}.$$

The first equality is satisfied, because in order to have immunity at $\tau+\Delta t$, one must have not lost immunity at τ.

Now let us write down dynamics for $\tilde{R}(t,\tau)$. We will again use the Euler method to proceed with the analysis of the model. After a small time step Δt, recovered individuals may lose immunity, maintain immunity, boost immunity or decease. The number of people who maintain immunity during the time step is the same as the number of people who had immunity at the beginning of the time step and did not boost immunity nor lose immunity and did not die. If these three events are independent, then:

$$\overbrace{\tilde{R}(t+\Delta t,\tau+\Delta t)}^{\text{maintain immunity}} = \overbrace{\left(\tilde{R}(t,\tau)-\tilde{\beta}\frac{I(t)\tilde{R}(t,\tau)}{N}\Delta t\right)}^{\text{not boost immunity}} \overbrace{\frac{P(\tau+\Delta t)}{P(\tau)}}^{\text{not lose immunity}} \overbrace{(1-\mu\Delta t)}^{\text{not die}}, \tag{4.1}$$

which is an explicit equation for recovered.

We also need to provide a boundary condition for $\tilde{R}(t,0)$. We again proceed by considering the discrete-time formulation and then taking the limit of step size.

The $\tilde{R}(t,0)$ is the density of individuals, who became fully immune in the time interval $[t-\Delta t,t]$; either by contact with an infectious individual, or recovery. The number of recovered individuals whose immunity boosted is

$$\sum_{i=0}^{\infty}\tilde{\beta}\frac{I(t-\Delta t)\tilde{R}(t-\Delta t,i\,\Delta t)}{N} = \tilde{\beta}\frac{I(t-\Delta t)R(t-\Delta t)}{N}$$

and the density of individuals who recovered and gained immunity is:

$$\gamma I(t-\Delta t)P(0).$$

Note the factor $P(0)$, that represents the proportion of

The boundary condition of $\tilde{R}(t,0)$ has form:

$$\tilde{R}(t,0) = \tilde{\beta}\frac{I(t-\Delta t)R(t-\Delta t)}{N} + \gamma I(t-\Delta t)P(0).$$

The finite difference model has form:

$$\begin{aligned}
S(t+\Delta t) &= N - I(t+\Delta t) - R(t+\Delta t) \\
I(t+\Delta t) &= I(t) + \beta\frac{S(t)I(t)}{N}\Delta t - \gamma I(t)\Delta t - \mu I(t)\ \Delta t \\
\tilde{R}(t+\Delta t, \tau+\Delta t) &= \tilde{R}(t,\tau)\left(1-\tilde{\beta}\frac{I(t)}{N}\Delta t\right)\frac{P(\tau+\Delta t)}{P(\tau)}(1-\mu\Delta t) \\
R(t) &= \sum_{i=0}^{\infty}\tilde{R}(t, i\cdot\Delta t)\ \Delta t
\end{aligned}$$

with an initial condition:

$$\begin{aligned}
S(t)|_{t=0} &= S_0 \\
I(t)|_{t=0} &= I_0 \\
\tilde{R}(t,\tau)|_{t=0} &= \tilde{R}_I(\tau).
\end{aligned}$$

4.2.2 Simplified discrete model

We will repeatedly apply equation (4.1) to some initial condition $\tilde{R}(t,0)$ and get:

$$\tilde{R}(t+n\ \Delta t, n\ \Delta t) = \tilde{R}(t,0)\frac{P(n\ \Delta t)}{P(0)}(1-\mu\ \Delta t)^n\prod_{i=0}^{n-1}\left(1-\tilde{\beta}\frac{I(t+i\ \Delta t)}{N}\Delta t\right),$$

which we can rephrase as:

$$\tilde{R}(t, n\ \Delta t) = \tilde{R}(t-n\ \Delta t, 0)\frac{P(n\ \Delta t)}{P(0)}(1-\mu\ \Delta t)^n\prod_{i=1}^{n}\left(1-\tilde{\beta}\frac{I(t-i\ \Delta t)}{N}\Delta t\right)$$

by mapping $t \mapsto t - n\ \Delta t$ and $i \mapsto n - i$.

From this we get total number of recovered individuals as:

$$\begin{aligned}
R(t) &= \sum_{n=0}^{\infty}\tilde{R}(t, n\ \Delta t)\Delta t \\
&= \Delta t\sum_{n=0}^{\infty}\tilde{R}(t-n\ \Delta t, 0)\frac{P(n\Delta t)}{P(0)}(1-\mu\ \Delta t)^n\prod_{i=1}^{n}\left(1-\tilde{\beta}\frac{I(t-i\Delta t)}{N}\Delta t\right)
\end{aligned}$$

To improve computing performance and numerical stability, we take a logarithm of the expression

$$\prod_{i=1}^{n}\left(1-\tilde{\beta}\frac{I(t-i\ \Delta t)}{N}\Delta t\right).$$

Let us create an auxiliary function $B_n(t)$ for this:[4] [5]

$$B_n(t)=\ln\prod_{i=1}^{n}\left(1-\tilde{\beta}\frac{I(t-i\ \Delta t)}{N}\Delta t\right)$$

$$=\sum_{i=1}^{n}\ln\left(1-\tilde{\beta}\frac{I(t-i\ \Delta t)}{N}\Delta t\right)$$

with $B_0(t)\equiv 0$ being the empty sum.

So that

$$R(t)=\Delta t\sum_{n=0}^{\infty}R_B(t-n\ \Delta t)\frac{P(n\Delta t)}{P(0)}(1-\mu\ \Delta t)^n e^{B_n(t)},$$

Where $R_B(t)=\tilde{\beta}\frac{I(t-\Delta t)R(t-\Delta t)}{N}+\gamma I(t-\Delta t)P(0)$ is original boundary condition for $\tilde{R}$. By this rearrangement, we no longer need a two-dimensional compartment $\tilde{R}$; we need just its boundary R_B and B_n, which makes the computation less demanding on memory.

The entire model reads:

$$\begin{aligned}
S(t+\Delta t)&=N-I(t+\Delta t)-R(t+\Delta t)\\
I(t+\Delta t)&=I(t)+\beta\frac{S(t)I(t)}{N}\Delta t-\gamma I(t)\ \Delta t-\mu I(t)\ \Delta t\\
R(t+\Delta t)&=\Delta t\sum_{n=0}^{\infty}R_B(t-(n-1)\Delta t)\frac{P(n\ \Delta t)}{P(0)}(1-\mu\ \Delta t)^n e^{B_n(t+\Delta t)}\\
R_B(t+\Delta t)&=\tilde{\beta}\frac{I(t)R(t)}{N}+\gamma I(t)P(0)\\
B_n(t+\Delta t)&=\sum_{i=1}^{n}\ln\left(1-\tilde{\beta}\frac{I(t+\Delta t-i\ \Delta t)}{N}\Delta t\right)
\end{aligned}$$

with initial conditions

$$S(t)|_{t=0}=S_0$$

[4] We chose the name B, because the meaning of the variable is propensity of immunity *boosting*.

[5] The function $f(x)=\ln(1+x)$ has its own implementation in languages such as `fortran`, `numpy` or `julia` that is more accurate where x is close to zero. This function is usually named `log1p`.

$$I(t)|_{t\leq 0} = I_I(t)$$
$$R(t)|_{t\leq 0} = R_I(t)$$
$$R_B(t)|_{t\leq 0} = R_{BI}(t)$$

4.2.3 Partial differential formulation of continuous model

Rearranging terms of equation (4.1), we get:

$$\tilde{R}(t+\Delta t,\tau+\Delta t) = \tilde{R}(t,\tau)\left(1-\tilde{\beta}\frac{I(t)}{N}\Delta t\right)\frac{P(\tau+\Delta t)}{P(\tau)}(1-\mu\Delta t) \tag{4.2}$$

$$\frac{\tilde{R}(t+\Delta t,\tau+\Delta t)}{\tilde{R}(t,\tau)} = \left(1-\tilde{\beta}\frac{I(t)}{N}\Delta t\right)\frac{P(\tau+\Delta t)}{P(\tau)}(1-\mu\Delta t)\Delta t)$$

For the last step to be correct, we will have to prove that $R(t,\tau) > 0$, which will be done later. Now, applying logarithm to both sides of the equation gives us:

$$\ln\tilde{R}(t+\Delta t,\tau+\Delta t) - \ln\tilde{R}(t,\tau) = \ln\left(1-\tilde{\beta}\frac{I(t)}{N}\Delta t\right) + \ln P(\tau+\Delta t) - \ln P(\tau) + \ln(1-\mu\Delta t)$$

We divide both sides by Δt and add special zero to the left-hand side of the equation:

$$\frac{1}{\Delta t}\Big(\ln\tilde{R}(t+\Delta t,\tau+\Delta t) - \ln\tilde{R}(t,\tau+\Delta t) + \ln\tilde{R}(t,\tau+\Delta t) - \ln\tilde{R}(t,\tau)\Big) =$$
$$= \frac{1}{\Delta t}\ln\left(1-\tilde{\beta}\frac{I(t)}{N}\Delta t\right) + \frac{\ln P(\tau+\Delta t) - \ln P(\tau)}{\Delta t} + \frac{\ln(1-\mu\Delta t)}{\Delta t}$$

Finally, by taking the limit $\Delta t \to 0^+$ we arrive to partial differential equation:

$$\frac{\partial\ln\tilde{R}(t,\tau)}{\partial t} + \frac{\partial\ln R(t,\tau)}{\partial\tau} = -\tilde{\beta}\frac{I(t)}{N} + \frac{d}{d\tau}\ln P(\tau) - \mu$$

$$\frac{1}{\tilde{R}(t,\tau)}\left(\frac{\partial\tilde{R}(t,\tau)}{\partial t} + \frac{\partial R(t,\tau)}{\partial\tau}\right) = -\tilde{\beta}\frac{I(t)}{N} + \frac{P'(\tau)}{P(\tau)} - \mu, \tag{4.3}$$

which is the equation for the compartment of recovered.

In the case of continuous model, the boundary condition has form:

$$\tilde{R}(t,0) = \tilde{\beta}\frac{I(t)R(t)}{N} + \gamma I(t)P(0).$$

The entire model can be written as:

$$S(t) = N - I(t) - R(t)$$

$$\frac{dI(t)}{dt} = \beta\frac{S(t)I(t)}{N} - \gamma I(t) - \mu I(t)$$

$$\frac{1}{\tilde{R}(t,\tau)}\left(\frac{\partial\tilde{R}(t,\tau)}{\partial t} + \frac{\partial R(t,\tau)}{\partial\tau}\right) = -\tilde{\beta}\frac{I(t)}{N} + \frac{P'(\tau)}{P(\tau)} - \mu$$

$$R(t) = \int_0^\infty \tilde{R}(t,\tau)\, d\tau$$

$$\tilde{R}(t,\tau)|_{\tau=0} = \tilde{\beta}\frac{I(t)R(t)}{N} + \gamma I(t)P(0)$$

with initial conditions:

$$S(t)|_{t=0} = S_0$$

$$I(t)|_{t=0} = I_0$$

$$\tilde{R}(t,\tau)|_{t=0} = \tilde{R}_I(\tau)$$

4.2.4 Integro-differential formulation of continuous model

It is possible to find an analytic solution of equation (4.3), which is:

$$\tilde{R}(t,\tau) = \tilde{R}(t-\tau,0)\frac{P(\tau)}{P(0)}\exp(-\mu\tau)\exp\left(-\frac{\tilde{\beta}}{N}\int_0^\tau I(t-s)ds\right).$$

The inner integral can be simplified, if we introduce an auxiliary function $C(t)$, that will represent cumulative cases of infectious individuals:

$$\int_0^\tau I(t-s)ds = \int_{t-\tau}^t I(s)ds = C(t) - C(t-\tau),$$

where $C(t)$ is the primitive function of $I(t)$, i.e. $\frac{dC(t)}{dt} = I(t)$.

The total number of recovered individuals is:

$$\begin{aligned} R(t) &= \int_0^\infty \tilde{R}(t,\tau)d\tau \\ &= \int_0^\infty \tilde{R}(t-\tau,0)\frac{P(\tau)}{P(0)}\exp(-\mu\tau)\exp\left(-\frac{\tilde{\beta}}{N}\int_0^\tau I(t-s)ds\right)\, d\tau \\ &= \int_0^\infty R_B(t-\tau)\frac{P(\tau)}{P(0)}\exp(-\mu\tau)\exp\left(-\frac{\tilde{\beta}}{N}(C(t)-C(t-\tau))\right)\, d\tau, \end{aligned}$$

where $R_B(t) = \tilde{R}(t-\tau, 0) = \tilde{\beta}\frac{I(t)R(t)}{N} + \gamma I(t)P(0)$ is the boundary condition for $\tilde{R}$.

The entire model then reads:

$$\begin{aligned}
S(t) &= N - I(t) - R(t) \\
\frac{dI(t)}{dt} &= \beta\frac{S(t)I(t)}{N} - \gamma I(t) - \mu I(t) \\
R(t) &= \int_0^\infty R_B(t-\tau)\frac{P(\tau)}{P(0)}\exp(-\mu\tau)\exp\left(-\frac{\tilde{\beta}}{N}(C(t) - C(t-\tau))\right)\, d\tau \\
R_B(t) &= \tilde{\beta}\frac{I(t)R(t)}{N} + \gamma I(t)P(0) \\
\frac{dC(t)}{dt} &= I(t)
\end{aligned}$$

with initial conditions:

$$\begin{aligned}
S(t)|_{t=0} &= S_0 \\
I(t)|_{t\leq 0} &= I_I(t) \\
R(t)|_{t\leq 0} &= R_I(t) \\
C(t)|_{t\leq 0} &= \int_0^t I_I(s)ds.
\end{aligned}$$

4.3 Numerical results

4.3.1 SIRS model

The model was implemented and numerically solved in Python 3.8.8 with packages `numpy` and `scipy` by Runge–Kutta–Fehlberg method (RK45) [47, 82]. Figures were plotted with `matplotlib` package [51]. The choice of parameters is academic and its goal is to illustrate properties of the model. The initial condition was chosen to be: $S(t)|_{t=0} = 9999, I(t)|_{t=0} = 1$ and $R_i(t)|_{t=0} = 0$ for $i = 1 \dots k$.

Parameters of the following numerical experiments are chosen to illustrate the model behavior, rather than to describe a real-life situation; however, they are chosen to be somewhat reasonable in the context of epidemiological modeling.

The standard SIRS model is a special case of the SIRRS model with $k = 1$. This is included, so it can serve as a benchmark for other models. The choice of parameters is presented in the tab. 4.1 and results are shown in fig. 4.2.

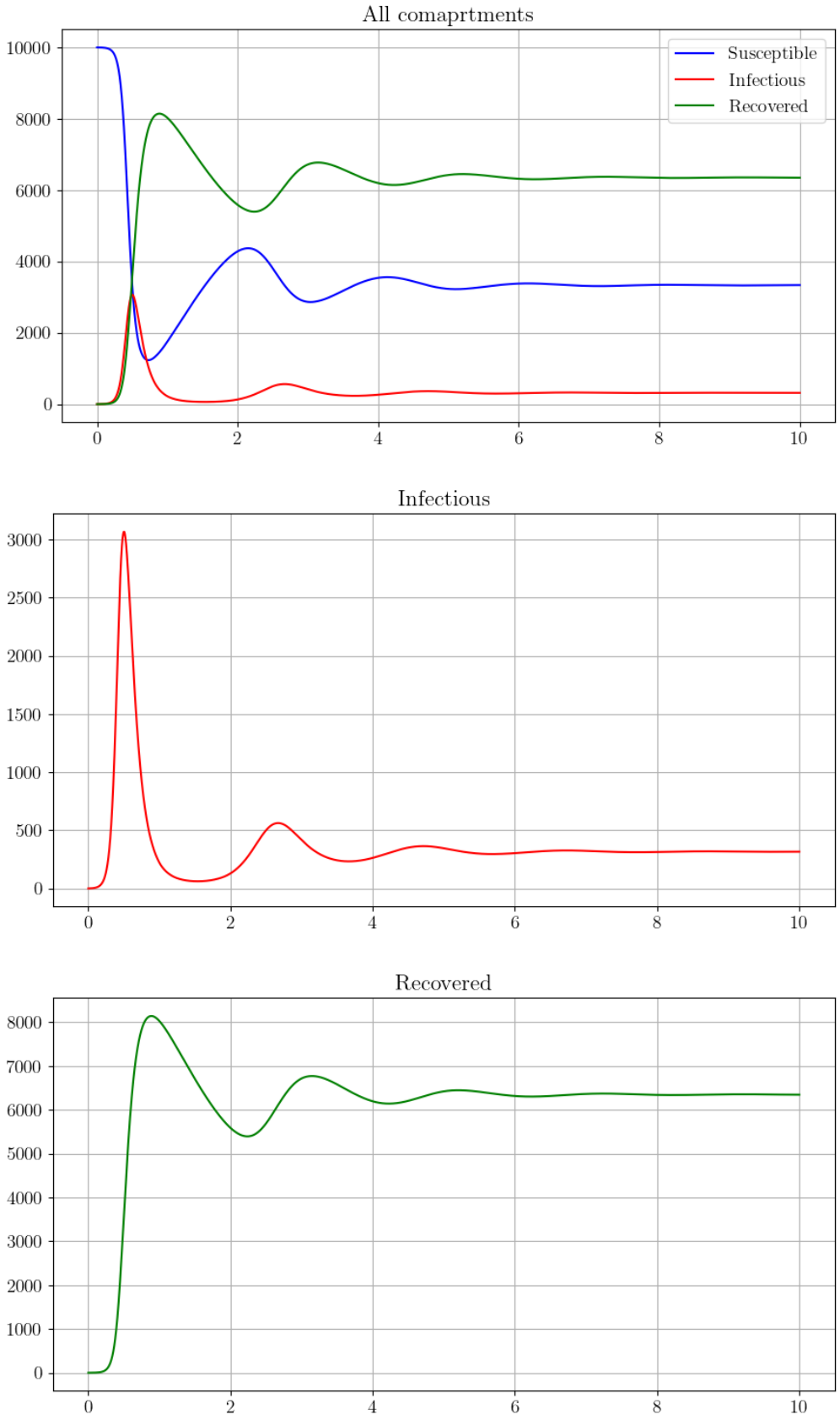

Fig. 4.2: Numerical results of standard SIRS model.

Parameter	β	γ	μ	ω	k	$\tilde{\beta}$
Value	30	10	0	0.5	1	–

Tab. 4.1: Parameter values for SIRS model

4.3.2 SIRRS model

The model was implemented and numerically solved in Julia 1.8.0 with packages `DifferentialEquations` and `StaticArrays` [72]. The Runge-Kutta-type of numerical schema of order 5(4) was employed [79]. The snippet of code used in this section is listed in section 6.1.

For SIRRS model we chose three scenarios: the first with $\tilde{\beta} = 0$, the second with $\tilde{\beta} = \beta$ and the third with $\tilde{\beta} = 10\beta$, to investigate the effect of $\tilde{\beta}$ to the infectious compartment. We observe that increasing $\tilde{\beta}$ elongates the relapse period. The precise connection between $\tilde{\beta}$ and frequency of peaks may be investigated via linearization of the system at endemic equilibrium. However, there is no general analytic solution to the linearization of the SIRRS model.

The parameter values can be found in tables 4.2 and solution to the model with these parameters is presented in figures 4.3, 4.4 and 4.5.

For a better picture of the internal structure of the R compartment, the solution for each intermediate stage $R_1, \ldots, R_k$ are plotted together with their sum in the bottom part of the figure.

Parameter	β	γ	μ	ω	k	$\tilde{\beta}$
Scenario 1	30	10	0	8	16	0
Scenario 2	30	10	0	8	16	30
Scenario 3	30	10	0	8	16	300

Tab. 4.2: Parameter values of SIRRS model for scenarios 1 – 3

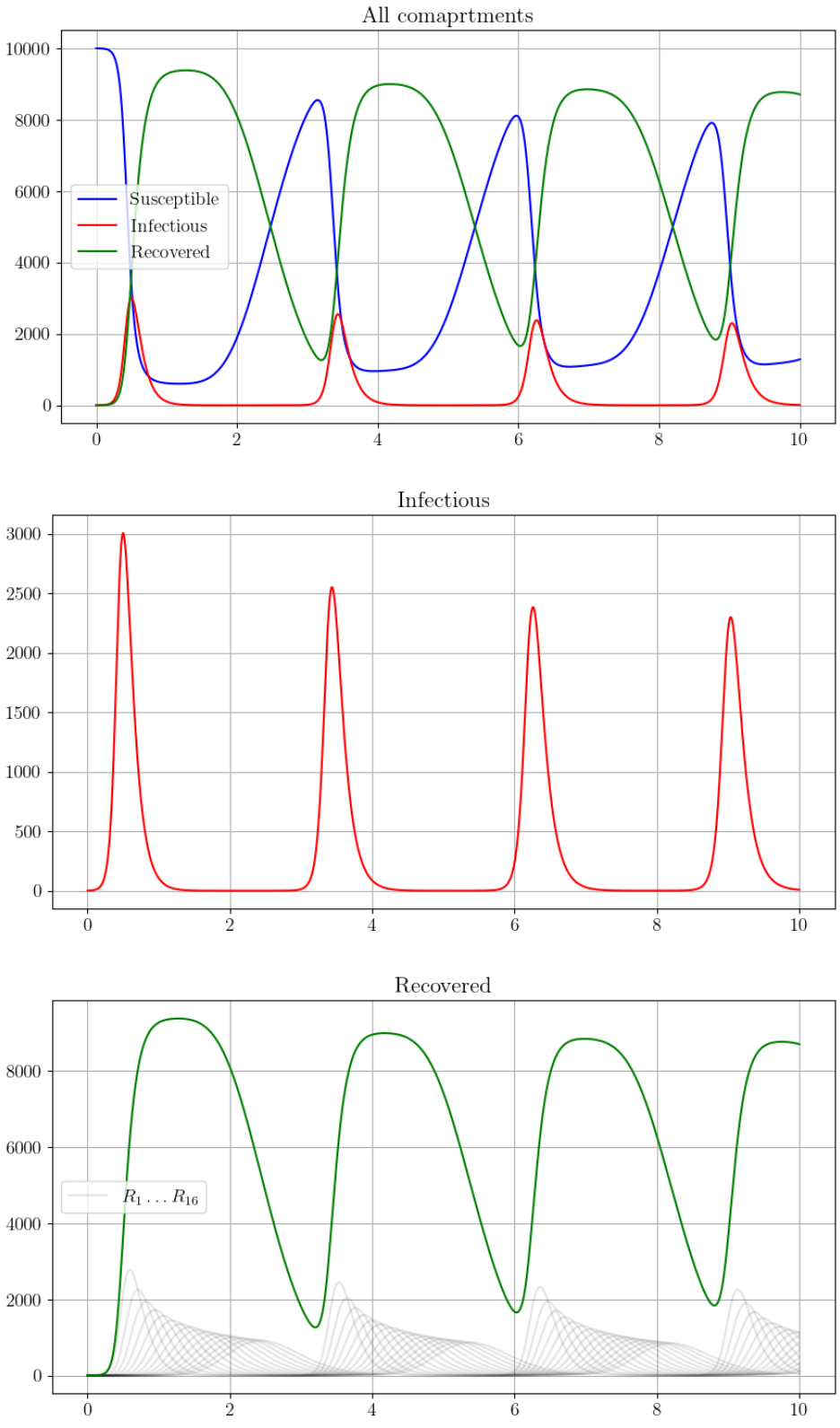

Fig. 4.3: Numerical results of SIRRS model, scenario 1.

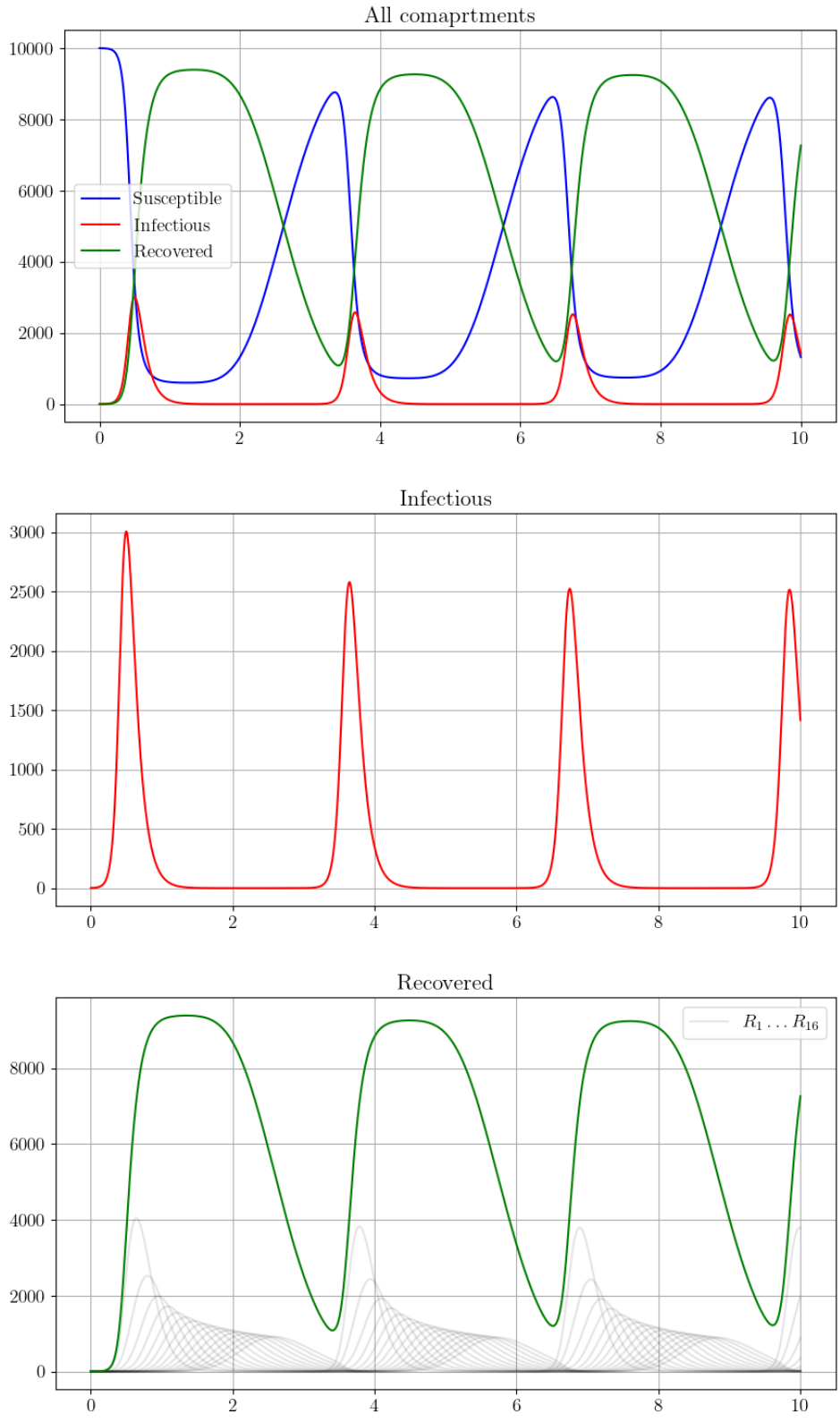

Fig. 4.4: Numerical results of SIRRS model, scenario 2.

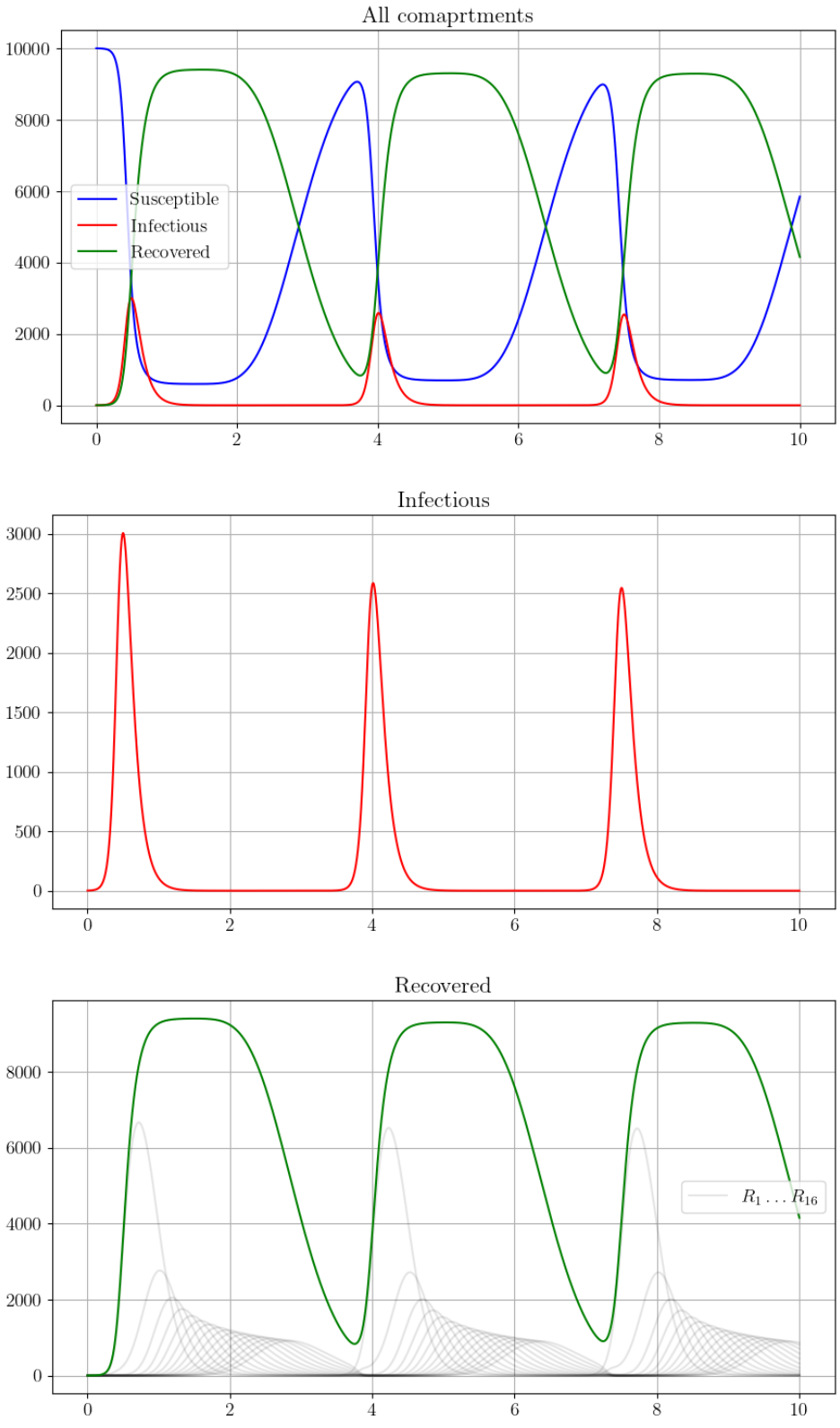

Fig. 4.5: Numerical results of SIRRS model, scenario 3.

4.3.3 Custom waning profiles

The model with custom waning profiles presented in section 4.2.2 was implemented in Julia 1.8.0, using packages `StaticArrays` for speedup and `OffsetArrays` for convenience. The figures were plotted by the `PyPlot` package. The infinite sum in the equation for $R(t)$ was truncated to $\sum_{n=0}^{\lceil \tau_{max}/\Delta t \rceil}$, where τ_{max} is time horizon in which we consider immunization effect and $\lceil \cdot \rceil$ mean rounding up to the next integer. [6] The most important lines of source code are presented in section 6.2.

The novelty of this model was custom waning profiles. To demonstrate the effect of different waning profiles, we explore four different functions P. They are all (truncated) distributions of random variables and represent their *survival function*. [7] All waning profiles are depicted in figure 4.6. All models were solved with a time step $\Delta t = 0.002$ and in immunization horizon $\tau_{max} = 5$.

The first comes from a random variable with Erlang distribution with parameters $k = 8, \lambda = 8$, so the mean is 2 and variance is $1/4$. The waning profile has form:

$$P_1(\tau) = \sum_{n=0}^{k-1} e^{-\lambda\tau} \frac{(\lambda\tau)^n}{n!},$$

The model with this waning profile should yield the same results as the SIRRS model, since both assume Erlang distribution of immune period.

The second function comes from the shifted Bernoulli random variable. The recovered retains immunity for 1 year with probability $1/5$, or for 2.25 years with probability $4/5$. The mean of this random variable is 2 and variance is $1/4$. The waning profile is:

$$P_2(\tau) = \begin{cases} 1 & \text{if } \tau < 1 \\ 4/5 & \text{if } 1 \leq \tau < 2.25 \\ 0 & \text{if } 2.25 \leq \tau. \end{cases}$$

The third function comes from truncated normal distribution with mean 2 and

[6] This is equivalent of truncating the function P into $P_{truncated}(\tau) = \begin{cases} P(\tau) & \text{if } \tau \leq \tau_{max} \\ 0 & \text{otherwise.} \end{cases}$

[7] The survival function $S(\tau)$ of a random variable with cumulative distribution function $F(\tau)$ is defined as $S(\tau) = 1 - F(\tau)$.

variance 1. The waning profile has form:

$$P_3(\tau) = \Phi(\tau - 2)$$

where Φ is cumulative distribution function of normal random variable with zero mean and unit variance, i.e. $\Phi(x) = \frac{1}{2}\left(1 + \text{erf}(x/\sqrt{2})\right)$. Note that $P_3(0) \doteq 0.977 < 1$. [8] This represents the fact that only 97.7% of freshly recovered individuals have antibody levels high enough to protect them from relapse. [9] This phenomenon is further discussed in our previous work [31].

The fourth and final waning profile comes from uniform distribution with parameters 0 and 4, i.e. with mean 2 and variance $4/3$. The waning profile is:

$$P_4(\tau) = \max\{1 - \tau/4, 0\}.$$

Despite all waning profiles coming from random variables with mean 2, we can observe that the profile has an effect on the epidemiological curve. In scenarios 1, 3 and 4 we can observe lower peaks of infection in each wave, whereas in scenario 2 the peak is stable. Scenarios 3 and 4 show broader and lower shape of infection peak than scenarios 1 and 2. Scenario 4 seems to quickly settle near endemic equilibrium.

Parameter	β	γ	μ	$\tilde{\beta}$	P
Scenario 1	30	10	0	30	P_1
Scenario 2	30	10	0	30	P_2
Scenario 3	30	10	0	30	P_3
Scenario 4	30	10	0	30	P_4

Tab. 4.3: Parameter values of SIRRS model with custom waning profiles for scenarios 1 – 4

[8] Because the function P is defined on a non-negative domain, the mean time of retaining immunity is slightly larger than 2.

[9] Similar effect can be observed after vaccination, which is referred to as *primary vaccination failure* [87].

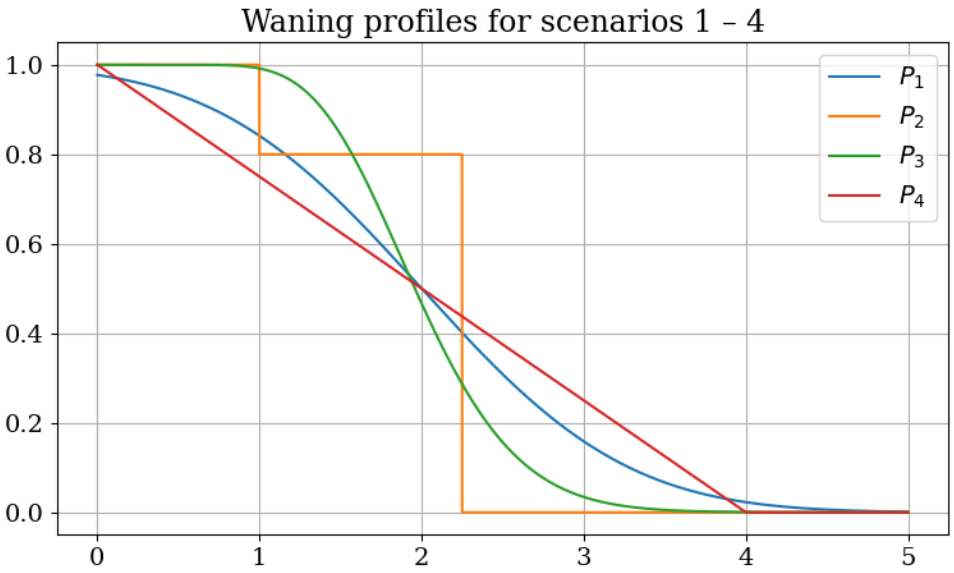

Fig. 4.6: Waning profiles for scenarios 1 – 4.

4.4 Conclusion

In this chapter, we discussed SIRS-type models with immunity boosting. We showed that in the standard SIRS model, the immunity boosting has no effect. We derived two novel models.

The first was formulated via the linear chain trick, in terms of ordinary differential equations and assumed Erlang distribution of immune period.

The second model was formulated as a set of algebraic equation, integral equation, ordinary differential equation and partial differential equation with a general waning profile. We provided re-formulation of the model in terms of two algebraic equations, ordinary two differential equations integro-differential and one integral equation. We also provided an efficient numerical schema for the model, based on finite differences.

Finally, the numerical results of both novel models were presented in the form of graphs. The results were focused on the novel features of the model. With the SIRRS model, the effect of $\tilde{\beta}$ was investigated. We could observe that the higher $\tilde{\beta}$, the longer the relapse time. With custom waning profiles, the effect of a particular waning profile P was demonstrated. The code snippets for these numerical results are provided in section 6.1.

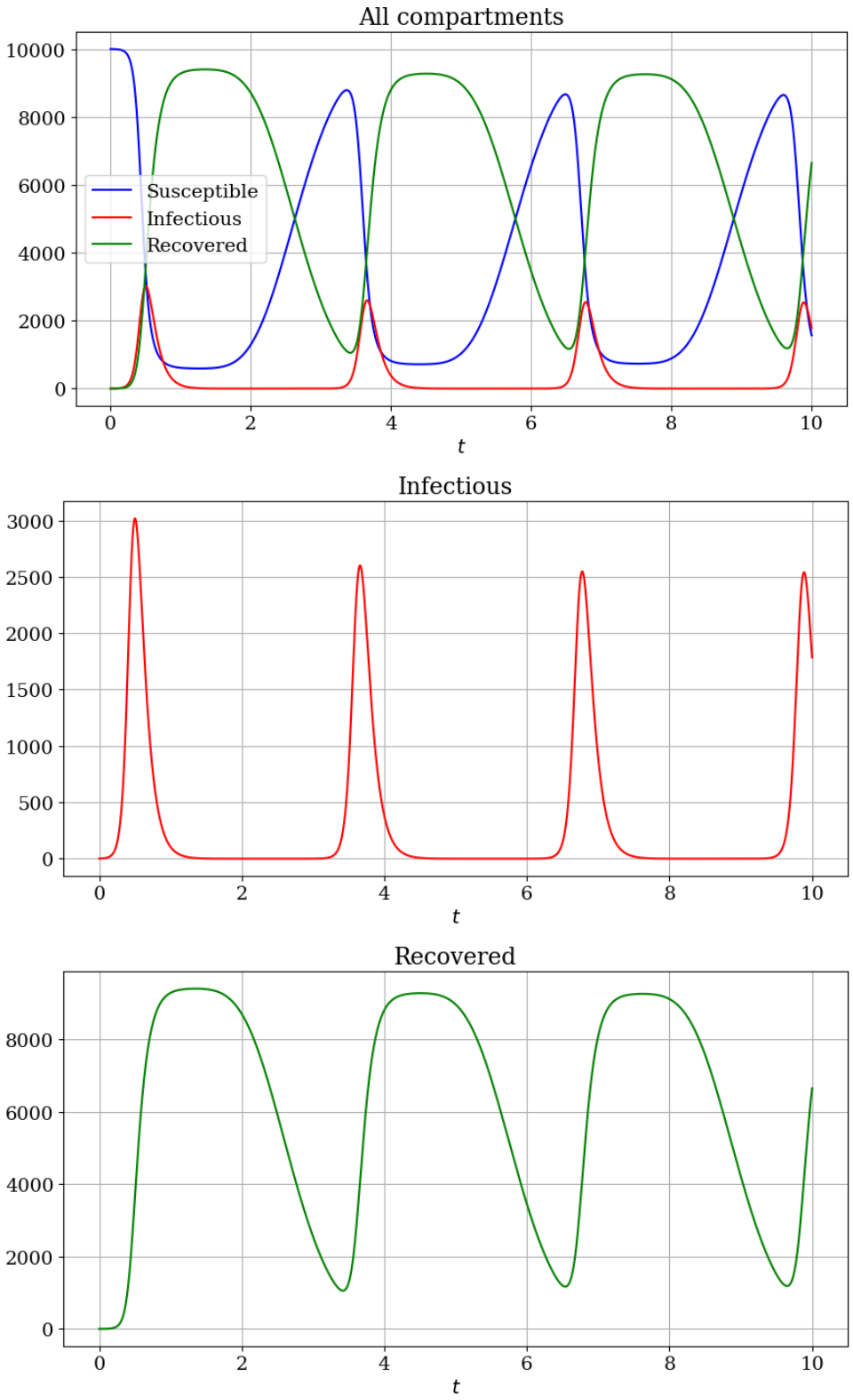

Fig. 4.7: Numerical results of SIRRS model with custom waning profile, scenario 1.

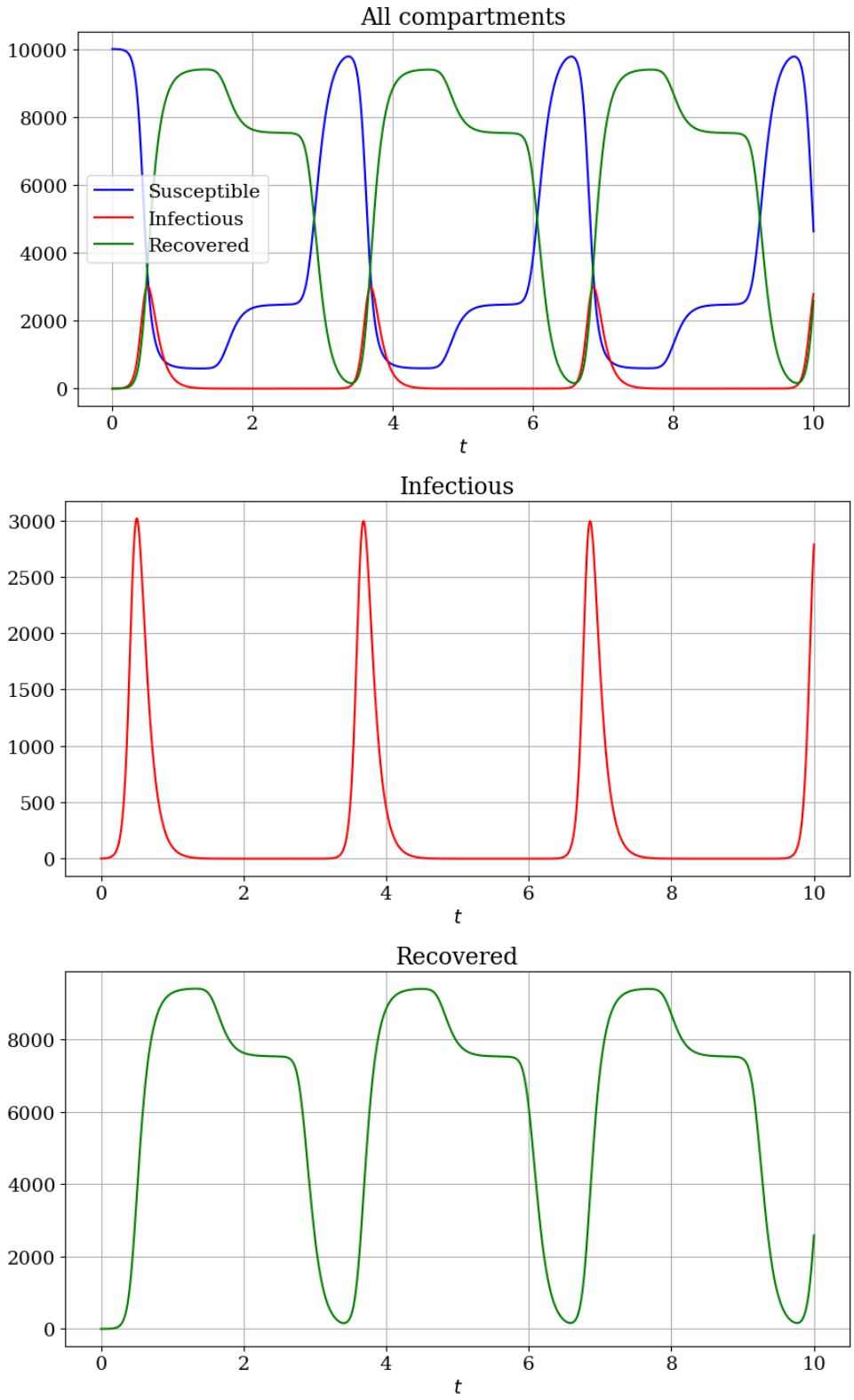

Fig. 4.8: Numerical results of SIRRS model with custom waning profile, scenario 2.

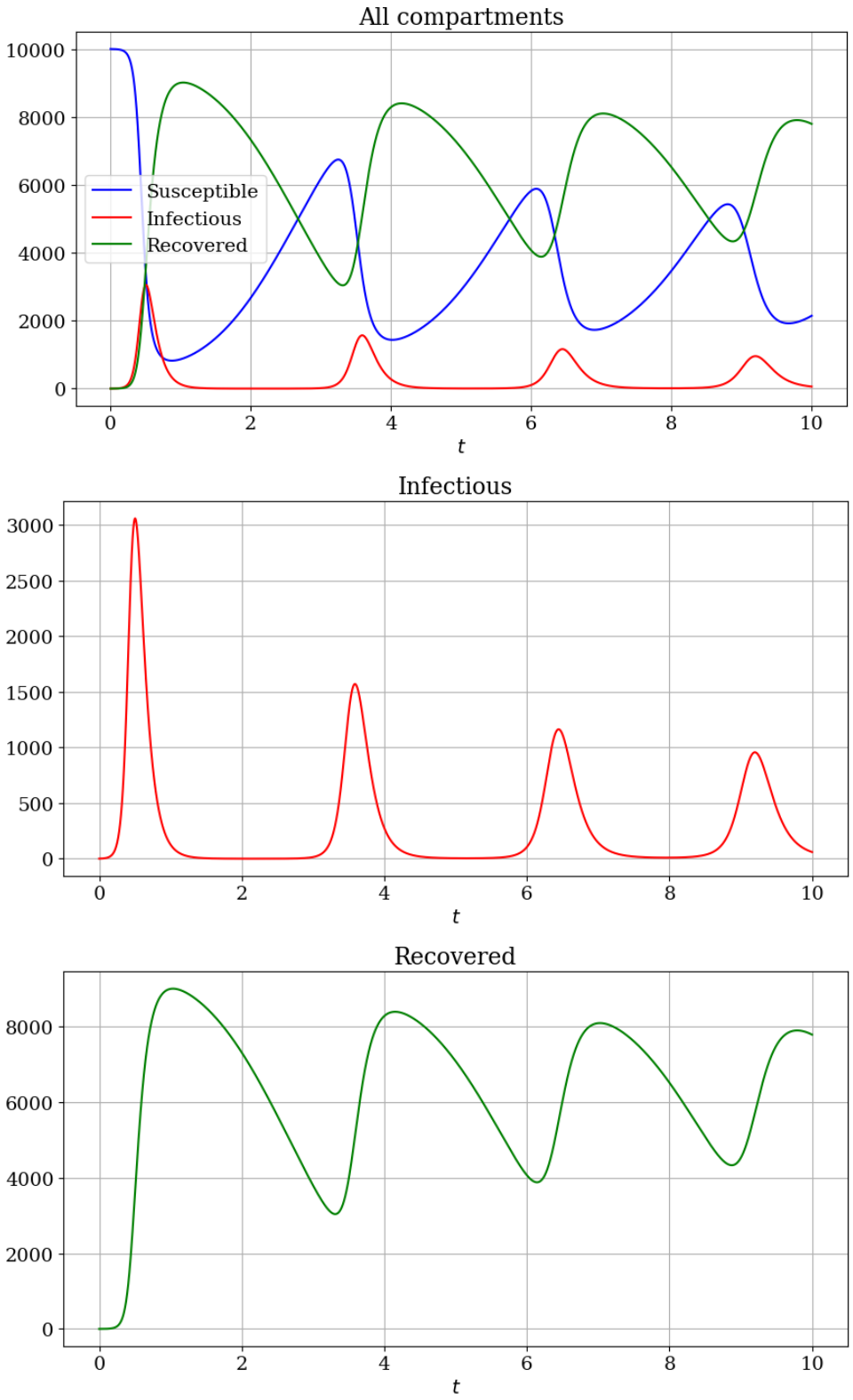

Fig. 4.9: Numerical results of SIRRS model with custom waning profile, scenario 3.

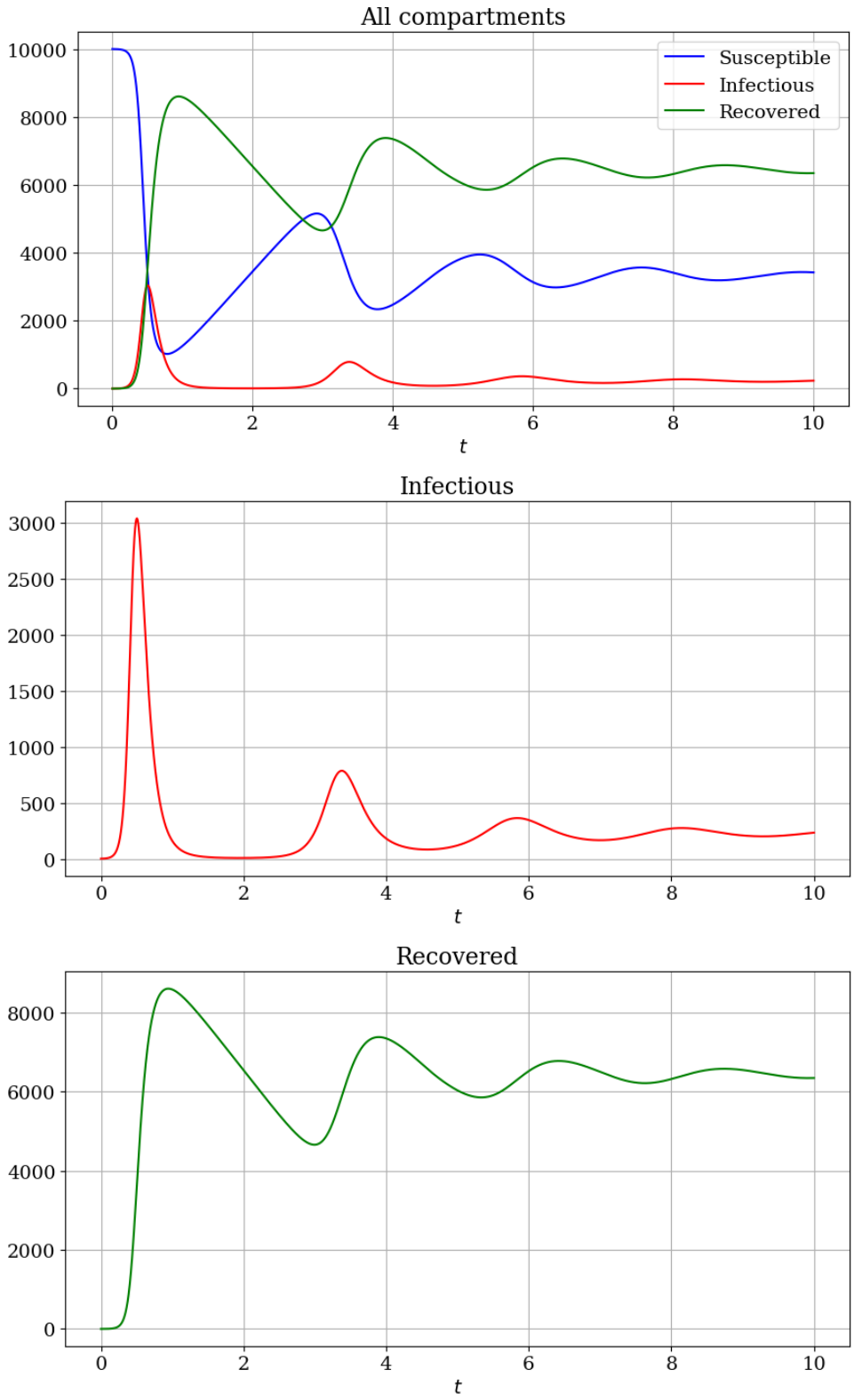

Fig. 4.10: Numerical results of SIRRS model with custom waning profile, scenario 4.

Chapter 5

Spatial models with population diffusion

In this section, a spatial SIR-type model will be introduced. The idea of incorporating spatial information to the model as well as population migration is well-established, see for example [24] or [4]. In this thesis, we introduce a model with a diffusion term with a fractional Laplace operator, which has been adopted as a modeling tool for long-range diffusion [81].

In the same way as in section 2.3.6, we can expressed the SIR model, but exchange the Laplace operator with fractional Laplace operator:

$$\begin{aligned}
\frac{dS(t,x)}{dt} + \kappa(-\Delta)^{\alpha/2} S(t,x) &= -\beta \frac{S(t,x)I(t,x)}{N(t,x)} + \omega R(t,x) \\
\frac{dI(t,x)}{dt} + \kappa(-\Delta)^{\alpha/2} I(t,x) &= \beta \frac{S(t,x)I(t,x)}{N(t,x)} - \gamma I(t,x) \\
\frac{dR(t,x)}{dt} + \kappa(-\Delta)^{\alpha/2} R(t,x) &= \gamma I(t,x) - \omega R(t,x)
\end{aligned} \tag{5.1}$$

for $t \geq 0$ and $x \in [0, L]$, where $-(-\Delta)^{\alpha/2}$ is a fractional Laplace operator.

Initial conditions of the model are:

$$\begin{aligned}
S(t,x)|_{t=0} &= S_0(x), \\
I(t,x)|_{t=0} &= I_0(x), \\
R(t,x)|_{t=0} &= R_0(x), \\
N(t,x)|_{t=0} &= S_0(x) + I_0(x) + R_0(x),
\end{aligned} \tag{5.2}$$

and boundary conditions are of Neumann type:

$$\begin{aligned}\left.\frac{\partial S(t,x)}{\partial x}\right|_{x=0} &= \left.\frac{\partial S(t,x)}{\partial x}\right|_{x=L} = 0\\ \left.\frac{\partial I(t,x)}{\partial x}\right|_{x=0} &= \left.\frac{\partial I(t,x)}{\partial x}\right|_{x=L} = 0\\ \left.\frac{\partial R(t,x)}{\partial x}\right|_{x=0} &= \left.\frac{\partial R(t,x)}{\partial x}\right|_{x=L} = 0\end{aligned} \tag{5.3}$$

for $t \geq 0$, which will be justified later.

5.1 Fractional Laplacian

In this section we introduce the concept of the fractional Laplacian (in one dimension). We present a brief introduction into the topic of modeling of a diffusion process via parabolic and fractional-parabolic partial differential equations. The curious reader is referred to [71] for a more detailed explanation.

5.1.1 Standard diffusion

Let us first consider standard diffusion of population in one dimension. The spatial domain $(-\infty, \infty)$ is discretized into small sections of width dx and population density in section x at time t is denoted $u(t,x)$. The population can migrate either to the section either one to the left or one to the right. This type of diffusion is depicted in fig. 5.1.

Let us suppose that the rate of diffusion depends linearly on the difference in population densities in neighboring sections. Then, rate of change of population density at position x at time t can be expressed as:

$$\begin{aligned}\frac{d}{dt}u(t,x) &= C_{dx}\underbrace{\big(u(t,x-dx)-u(t,x)\big)}_{\text{diffusion to the left}} + C_{dx}\underbrace{\big(u(t,x+dx)-u(t,x)\big)}_{\text{diffusion to the right}}\\ &= C_{dx}\big(u(t,x-dx)-2u(t,x)+u(t,x+dx)\big),\end{aligned}$$

where C_{dx} is a constant ensuring consistent results with varying section size dx. Choosing C_{dx} equal to $\frac{\kappa}{dx^2}$ and taking limit as $dx \to 0^+$, we get parabolic partial differential equation:

$$\frac{\partial}{\partial t}u(t,x) = \kappa\frac{\partial^2}{\partial x^2}u(t,x) = \kappa\Delta u(t,x).$$

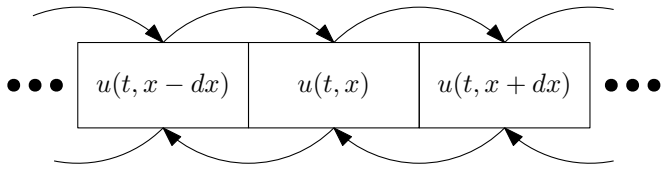

Fig. 5.1: Diagram of ordinary diffusion. Each section can exchange population only with its neighbors.

This equation can be solved in elegant way, when initial condition $u(t,x)|_{t=0} = A\cos(\omega)$. One can easily verify that $u(t,x) = A\exp\left(-\kappa t\omega^2\right)\cos\left(\omega x\right)$ is a solution to this equation. Also note that if initial condition is in form of cosine series: $u(t,x)|_{t=0} = \sum_{n=0}^{N} A_n\cos(\omega_n)$, then solution to diffusion equation has form:

$$u(t,x) = \sum_{n=0}^{N} A_n \exp\left(-\kappa t\omega^2\right)\cos\left(\omega x\right). \tag{5.4}$$

5.1.2 Fractional diffusion

In the same manner as above, let us consider a discretized spatial dimension with the traveling population. This time, the population can travel to whichever section on the real line. Let us say that rate of diffusion from section at position x to section at $x + n\cdot dx$ is linearly proportional to difference of population densities and to $(n\cdot dx)^{-1-\alpha}$ for some parameter $\alpha \in (0,1]$.[1]

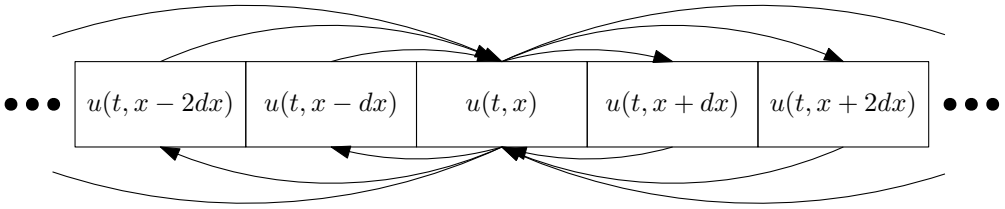

Fig. 5.2: Diagram of anomalous diffusion. Each section can exchange population with any other section.

The rate of change of population density at position x at time t then is:

$$\frac{d}{dt}u(t,x) = C_{dx,\alpha}\sum_{s\neq 0}\frac{u(t,x+s\cdot dx)-u(t,x)}{|s\cdot dx|^{1+\alpha}},$$

where $C_{dx,\alpha}$ is again a correction factor to account for varying section size dx and parameter α. Again, by taking the limit of section size $dx \to 0^+$, the sum on the

[1] This means that travel distance is governed by power law with an infinite variance.

right-hand side changes to principal-value integral:

$$c_\alpha \text{p.v.} \int_{-\infty}^{\infty} \frac{u(t, x+s) - u(t,x)}{|s|^{1+\alpha}} ds, \tag{5.5}$$

where c_α is a factor whose value will be determined below.[2] The right-hand side of the equation is *fractional Laplacian* and is denoted by: $-(-\Delta^{\alpha/2})u(t,x)$.

Value of c_α is determined by solving fractional diffusion problem

$$\frac{\partial}{\partial t} u(t,x) = -\kappa(-\Delta)^{\alpha/2} u(t,x) \tag{5.6}$$

with initial condition $u(t,x)|_{t=0} = A\cos(\omega x)$. We seek the solution in separable form as a damped cosine wave: $u(t,x) = a(t)\cos(\omega x)$. Substituting this back to equation (5.6) we get:

$$\frac{d}{dt} a(t) \cdot \cos(\omega x) = \kappa c_\alpha \text{ p.v.} \int_{-\infty}^{\infty} \frac{a(t)\cos(\omega(x+s)) - a(t)\cos(\omega x)}{|s|^{1+\alpha}} ds,$$

where p.v.$\int ds$ is *Cauchy principal value integral*.

We continue solving by manipulating the right-hand side:

$$\begin{aligned}
&\kappa c_\alpha a(t) \text{ p.v.} \int_{-\infty}^{\infty} \frac{\cos(\omega x + \omega s) - \cos(\omega x)}{|s|^{1+\alpha}} ds. \\
=&\kappa c_\alpha a(t) \lim_{\varepsilon \to 0} \left(\int_{-\infty}^{-\varepsilon} \frac{\cos(\omega x + \omega s) - \cos(\omega x)}{|s|^{1+\alpha}} ds \right. \\
&\qquad \left. + \int_{\varepsilon}^{\infty} \frac{a(t)\cos(\omega x + \omega s) - a(t)\cos(\omega x)}{|s|^{1+\alpha}} ds \right) \\
=&\kappa c_\alpha a(t) \lim_{\varepsilon \to 0} \int_{\varepsilon}^{\infty} \frac{\cos(\omega x - \omega s) - 2\cos(\omega x) + \cos(\omega x + \omega s)}{|s|^{1+\alpha}} ds \\
=&\kappa c_\alpha a(t) \int_{0}^{\infty} \frac{\cos(\omega x - \omega s) - 2\cos(\omega x) + \cos(\omega x + \omega s)}{|s|^{1+\alpha}} ds \\
=&\kappa c_\alpha a(t) \int_{0}^{\infty} \frac{2\cos(\omega x)(\cos(\omega x) - 1)}{|s|^{1+\alpha}} ds \\
=&\kappa c_\alpha a(t) \cos(\omega x) \int_{0}^{\infty} \frac{2(\cos(\omega x) - 1)}{|s|^{1+\alpha}} ds.
\end{aligned}$$

[2] In literature, this factor in one dimension is usually denoted by $c_{1,\alpha}$.

$$= \kappa c_\alpha a(t) \cos(\omega x) \cdot \left(|\omega|^\alpha \cos\left(\frac{\alpha\pi}{2}\right) \Gamma(-\alpha) \right)$$

Choosing $c_\alpha = \left(-\cos\left(\frac{\alpha\pi}{2}\right) \Gamma(-\alpha) \right)^{-1}$ seems to simplify further calculations, that lead to ordinary differential equation for $a(t)$:[3]

$$\begin{aligned} \frac{d}{dt} a(t) \cdot \cos(\omega x) &= \kappa c_\alpha \cos(\omega x) \cdot \left(|\omega|^\alpha \cos\left(\frac{\alpha\pi}{2}\right) \Gamma(-\alpha) \right) \\ \frac{d}{dt} a(t) \cdot \cos(\omega x) &= -\kappa a(t) \cos(\omega x) |\omega|^\alpha \\ \frac{d}{dt} a(t) &= -\kappa a(t) |\omega|^\alpha, \end{aligned}$$

which has solution satisfying boundary condition $a(0) = A$:

$$a(t) = A \exp\left(-\kappa \omega^\alpha t\right),$$

so that solution to the original fractional diffusion equation is:

$$u(t, x) = A \exp\left(-\kappa \omega^\alpha t\right) \cos(\omega x).$$

Similarly, if the initial condition is expressed as a sum of cosines:

$$u(t, x)|_{t=0} = \sum_{n=0}^{N} A_n \cos(\omega_n x),$$

then the solution to the fractional diffusion problem has the form:

$$u(t, x) = \sum_{n=0}^{N} A_n \exp\left(-\kappa \omega_n^\alpha t\right) \cos(\omega_n x). \tag{5.7}$$

Overall, this example shows us three important things. First, the Fourier series can be a powerful tool to solve not only ordinary diffusion problems but also fractional diffusion problems, because fractional Laplacian of can be calculated as:

$$-\left(-\Delta\right)^{\alpha/2} \sum_{n=0}^{N} A_n \cos(\omega_n x) = \sum_{n=0}^{N} A_n \omega_n^\alpha \cos(\omega_n x). \tag{5.8}$$

Second, that by comparing (5.4) to (5.7) we can see that ordinary diffusion is a special case of fractional diffusion, for $\alpha \to 2$. [4] And third, while the Laplacian of a function can be evaluated at point x from its arbitrary small neighborhood of $(x - \varepsilon, x + \varepsilon)$, for evaluating fractional Laplacian, the function on the entire real line must be known.[5]

[3] One might wonder about the negative sign of c_α. But since $\Gamma(-\alpha) \geq 0$ and $\cos\left(\frac{\alpha\pi}{2}\right) \leq 0$ for $\alpha \in [1, 2)$, the negative sign in fact ensures that c_α remains positive.

[4] The connection between Fourier transform and fractional Laplacian has been also used in various applications in signal processing [83].

[5] In the literature, this property is referred to as *non-locality* of fractional Laplacian operator.

5.2 Boundary conditions

Recall that the model (5.1) is valid for $x \in [0, L]$, and not $x \in (-\infty, \infty)$. In this subsection, a choice of Neumann boundary conditions is justified. We present three views on the interpretation of boundary conditions. The reader is referred to section 1.5.4 of [19] for further discussion on boundary conditions and their interpretation.

5.2.1 Ordinary diffusion and population balance

Let us consider an ordinary diffusion problem on finite interval $x \in [0, L]$:

$$\frac{\partial}{\partial t}u(t,x) = \kappa \frac{\partial^2}{\partial x^2}u(t,x), \tag{5.9}$$

with condition that total population is fixed:

$$\int_0^L u(t,x)dx \equiv const.$$

Differentiating both sides with respect to time, we get:

$$\frac{d}{dt}\int_0^L u(t,x)dx = 0.$$

Under conditions of Leibnitz integral rule, we can exchange the order of differentiation and integration:

$$\begin{aligned}
\int_0^L \frac{\partial}{\partial t}u(t,x)dx &= 0 \\
\int_0^L \kappa \frac{\partial^2}{\partial^2 x}u(t,x)dx &= 0 \\
\left[\frac{\partial}{\partial x}u(t,x)\right]_{x=0}^{L} &= 0 \\
\frac{\partial}{\partial x}u(t,x)|_{x=L} - \frac{\partial}{\partial x}u(t,x)|_{x=0} &= 0
\end{aligned}$$

The terms on the left-hand side of above equation can be interpreted as: $\frac{\partial}{\partial x}u(t,x)|_{x=L}$ represents the population inflow from the point $x = L$ into interval $[0, L]$ and term $\frac{\partial}{\partial x}u(t,x)|_{x=0}$ represents population outflow from point $x = 0$ from the interval $[0, L]$.

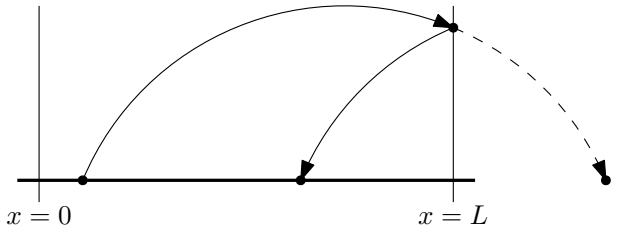

Fig. 5.3: Schematic depiction of reflection boundary. Individual that tries to travel outside the interval $[0, L]$ is "reflected" back by the boundary.

In order to study closed population, we require both of these terms to be equal to zero, which translates into Neumann boundary conditions $0 = \frac{\partial}{\partial x}u(t,x)|_{x=L} - \frac{\partial}{\partial x}u(t,x)|_{x=0}$.

However, this approach would not work for fractional diffusion because of the non-locality of fractional Laplace operator. Only with additional assumptions on u, such as periodicity, a similar argument would be valid.

5.2.2 Reflection boundary

Since fractional Laplacian can be evaluated only if the function on the entire real line is known, the solution to the fractional diffusion problem on finite interval $[0, L]$ can be calculated only if the function is extended beyond this domain. One option of such extension is to make boundaries "reflect" escaping individuals back to the interval $[0, L]$, which is depicted in fig. 5.3. Reflection at point $x = 0$ means that for $0 < \varepsilon < L$ population going to $x = -\varepsilon$ would end up at $x = \varepsilon$. Similarly, reflection at point $x = L$ means that the population going to $x = L + \varepsilon$ would end up at $x = L - \varepsilon$. Multiple reflections are possible, with point x mapping to $\frac{L}{\pi}\arccos\left(\pi\frac{x}{L}\right)$ after all reflections.

These reflections correspond to an even extension (in spatial dimension) of the function defined on $[0, L]$ and then periodical extension of the function period $2L$, so that $u(t,-x) = u(t,x) = u(t,x+2L)$. This type of function extension is depicted in fig. 5.4. In the literature, this approach of extending the studied domain to achieve desired behavior at the boundary is known as *method of (mirror) images* [53].

If we additionally require the function u to be smooth,then by using Taylor expansion around $x = 0$ we get:

$$u(t,\varepsilon) - u(t,-\varepsilon) = u(t,0) + \varepsilon\frac{\partial}{\partial x}u(t,x)|_{x=0} - \left(u(t,0) - \varepsilon\frac{\partial}{\partial x}u(t,x)|_{x=0}\right) + \mathcal{O}(\varepsilon^2)$$

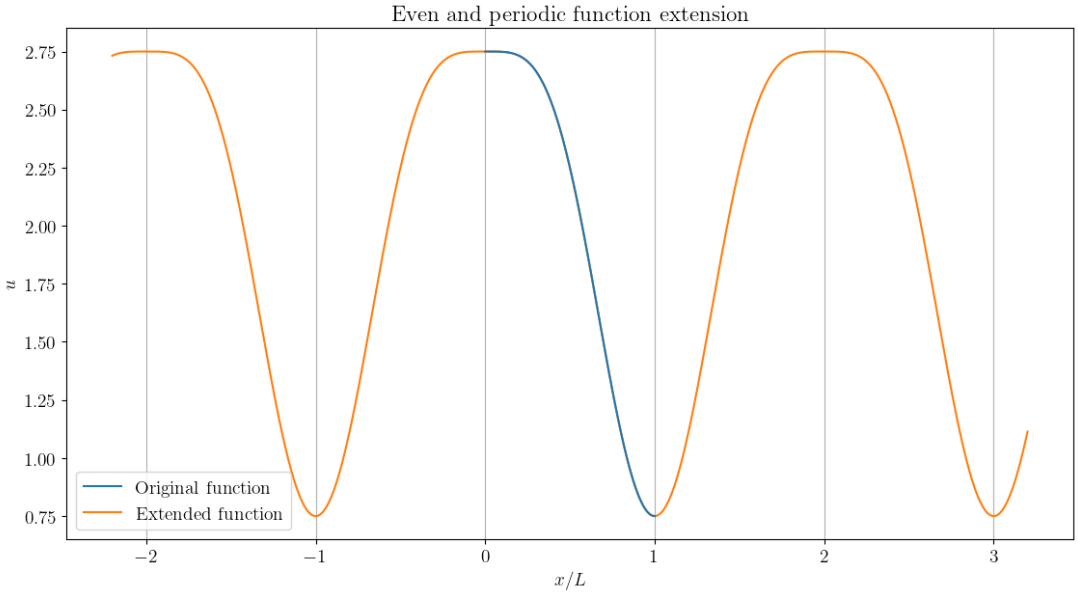

Fig. 5.4: Even and periodic extension of a function defined on $[0, L]$. Note that the horizontal axis is non-dimensionalized to x/L.

$$0 = 2\varepsilon \frac{\partial}{\partial x} u(t,x)|_{x=0} + \mathcal{O}(\varepsilon^2),$$

where the left-hand side is equal to zero, because u is an even function. Finally, by dividing both sides by 2ε and taking limit $\varepsilon \to 0$, we get homogeneous Neumann boundary condition:

$$0 = \frac{\partial}{\partial x} u(t,x)|_{x=0}$$

Similar argument can be made at point $x = L$ to show the boundary condition at $x = L$:

$$0 = \frac{\partial}{\partial x} u(t,x)|_{x=L}.$$

5.2.3 Cosine series

The third presented point of view on Neumann boundary condition is cosine series expansion. Let us consider a (fractional) diffusion problem

$$\frac{\partial}{\partial t} u(t,x) = -\kappa(-\Delta)^{\alpha/2} u(t,x)$$

on a finite interval $x \in [0, L]$ with parameter $\alpha \in (1, 2]$. As was stated in (5.7), if the problem's initial condition could be expressed as the sum of cosines, then the solution could be also expressed as the sum of cosines.

Let us express the initial condition in terms of cosine series:

$$u(t,x)|_{t=0} = \sum_{n=0}^{\infty} A_n \cos(n\pi x/L)$$

Note that this solution satisfies boundary conditions $0 = \frac{\partial}{\partial x}u(t,x)|_{x=0} = \frac{\partial}{\partial x}u(t,x)|_{x=L}$ and also has property of being even and periodic function.[6]

Then, the solution to the diffusion problem is:

$$u(t,x) = \sum_{n=0}^{\infty} A_n \exp(-\kappa n^{\alpha}\pi^{\alpha}L^{-\alpha}t)\cos(n\pi x/L),$$

which also satisfies the same boundary conditions. Furthermore, the total population at time t is

$$\int_0^L u(t,x)dx = \int_0^L \sum_{n=0}^{\infty} A_n \exp(-\kappa n^{\alpha}\pi^{\alpha}L^{-\alpha}t)\cos(n\pi x/L)dx.$$

If the order of summation and integration can be exchanged, we can follow:

$$\begin{aligned}
&= \sum_{n=0}^{\infty}\left(A_n \exp(-\kappa n^{\alpha}\pi^{\alpha}L^{-\alpha}t)\int_0^L \cos(n\pi x/L)dx\right)\\
&= \sum_{n=0}^{\infty}\left(A_n \exp(-\kappa n^{\alpha}\pi^{\alpha}L^{-\alpha}t)\cdot L\delta_n\right)\\
&= A_0 \exp(-\kappa\cdot 0^{\alpha}\pi^{\alpha}L^{-\alpha}t)L\\
&= A_0\cdot L,
\end{aligned}$$

where δ_n is a sequence defined as:[7]

$$\delta_n = \begin{cases} 1 & \text{if } n = 0\\ 0 & \text{otherwise.}\end{cases}$$

[6]There are other kinds of trigonometric series in which an initial condition could be expressed. For example if boundary conditions were $\frac{\partial}{\partial x}u(t,x)|_{x=0} = \frac{\partial}{\partial x}u(t,x)|_{x=L}$ and $u(t,x)|_{x=0} = u(t,x)|_{x=L}$ then we would choose series $u(t,x)|_{t=0} = u_0/L + \sum_{n=1}^{\infty} A_n \sin(2n\pi x/L)$, where u_0 is total population. This would represent a population living along a circle, where the population at one boundary meets the population at the other boundary.

[7]This function is also widely used in signal processing and is a discrete equivalent of Dirac delta function. The use of δ sequence allowed us to state that $\int_0^L \cos(n\pi x/L)dx$ is equal to zero if $n > 0$ and equal to L if $n = 0$, and thus continue the computation with only zero-th summand.

5.3 Numerical methods

In this section, an overview of methods that can be used to solve the model with fractional diffusion is presented. We present a method of lines for the transformation of fractional parabolic partial differential equation into a system of coupled ordinary differential equations, discrete cosine transform for efficient evaluation of the fractional Laplacian and a method based on Fourier series.

5.3.1 Method of lines

To obtain numerical results for the spatial SIR model with diffusion (5.1), we used the method of lines. The spatial dimension was discretized into k sub-intervals $[0, \frac{L}{k}]$, $[\frac{L}{k}, \frac{2L}{k}]$, $\ldots$, $[\frac{(k-1)L}{k}, L]$, and from each sub-interval a midpoint representative was chosen and partial differential equation was transformed into $3k$ ordinary differential equations:

$$\begin{aligned}
\frac{d}{dt}S(t, \tfrac{L}{2k}) &= -\beta\frac{S(t, \frac{L}{2k})I(t, \frac{L}{2k})}{N(t, \frac{L}{2k})} + \omega R(t, \tfrac{L}{2k}) - \kappa(-\Delta)^{\alpha/2}S(t, \tfrac{L}{2k}) \\
\frac{d}{dt}S(t, \tfrac{3L}{2k}) &= -\beta\frac{S(t, \frac{3L}{2k})I(t, \frac{3L}{2k})}{N(t, \frac{3L}{2k})} + \omega R(t, \tfrac{3L}{2k}) - \kappa(-\Delta)^{\alpha/2}S(t, \tfrac{3L}{2k}) \\
&\vdots \\
\frac{d}{dt}S(t, \tfrac{(2k-1)L}{2k}) &= -\beta\frac{S(t, \frac{(2k-1)L}{2k})I(t, \frac{(2k-1)L}{2k})}{N(t, \frac{(2k-1)L}{2k})} + \omega R(t, \tfrac{(2k-1)L}{2k}) \\
&\quad - \kappa(-\Delta)^{\alpha/2}S(t, \tfrac{(2k-1)L}{2k})
\end{aligned}$$

$$\begin{aligned}
\frac{d}{dt}I(t, \tfrac{L}{2k}) &= \beta\frac{S(t, \frac{L}{2k})I(t, \frac{L}{2k})}{N(t, \frac{L}{2k})} - \gamma I(t, \tfrac{L}{2k}) \kappa(-\Delta)^{\alpha/2}I(t, \tfrac{L}{2k}) \\
\frac{d}{dt}I(t, \tfrac{3L}{2k}) &= \beta\frac{S(t, \frac{3L}{2k})I(t, \frac{3L}{2k})}{N(t, \frac{3L}{2k})} - \gamma I(t, \tfrac{3L}{2k}) \kappa(-\Delta)^{\alpha/2}I(t, \tfrac{3L}{2k}) \\
&\vdots \\
\frac{d}{dt}I(t, \tfrac{(2k-1)L}{2k}) &= \beta\frac{S(t, \frac{(2k-1)L}{2k})I(t, \frac{(2k-1)L}{2k})}{N(t, \frac{(2k-1)L}{2k})} - \gamma I(t, \tfrac{(2k-1)L}{2k}) \\
&\quad - \kappa(-\Delta)^{\alpha/2}I(t, \tfrac{(2k-1)L}{2k})
\end{aligned}$$

$$\frac{d}{dt}R(t, \tfrac{L}{2k}) = \gamma I(t, \tfrac{L}{2k}) - \omega R(t, \tfrac{L}{2k}) - \kappa(-\Delta)^{\alpha/2}I(t, \tfrac{L}{2k})$$

$$\frac{d}{dt}R(t,\tfrac{3L}{2k}) = \gamma I(t,\tfrac{3L}{2k}) - \omega R(t,\tfrac{3L}{2k}) - \kappa(-\Delta)^{\alpha/2} I(t,\tfrac{3L}{2k})$$
$$\vdots$$
$$\frac{d}{dt}R(t,\tfrac{(2k-1)L}{2k}) = \gamma I(t,\tfrac{(2k-1)L}{2k}) - \omega R(t,\tfrac{(2k-1)L}{2k}) - \kappa(-\Delta)^{\alpha/2} I(t,\tfrac{(2k-1)L}{2k}).$$

This set of ordinary differential equations can be solved by the numerical method of choice. In the case of this thesis, the Bogacki-Shampine method of order 3 was used [13].[8]

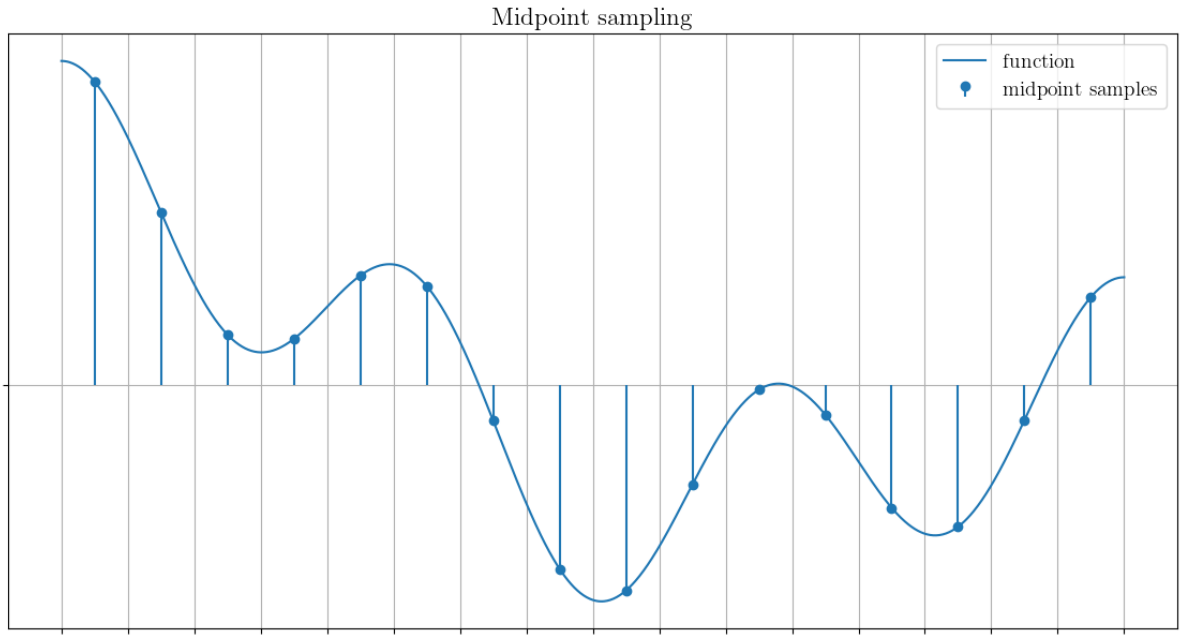

Fig. 5.5: Example of midpoint sampling. Domain $[0, L]$ is subdivided uniformly into $k = 16$ sub-intervals (borders of which are indicated by vertical gray lines), and a function is evaluated in the middle of each sub-interval.

5.3.2 Discrete cosine transformation

When solving the model numerically via the method of lines, a fractional Laplacian must be calculated. As we saw earlier, expressing the function in terms of cosine series is a straightforward approach. For mid-point representatives, a discrete cosine transform

[8] Also other methods were in consideration, such as a numerical method for solving ODEs with quadratic dynamics [58], but these proved to be inefficient.

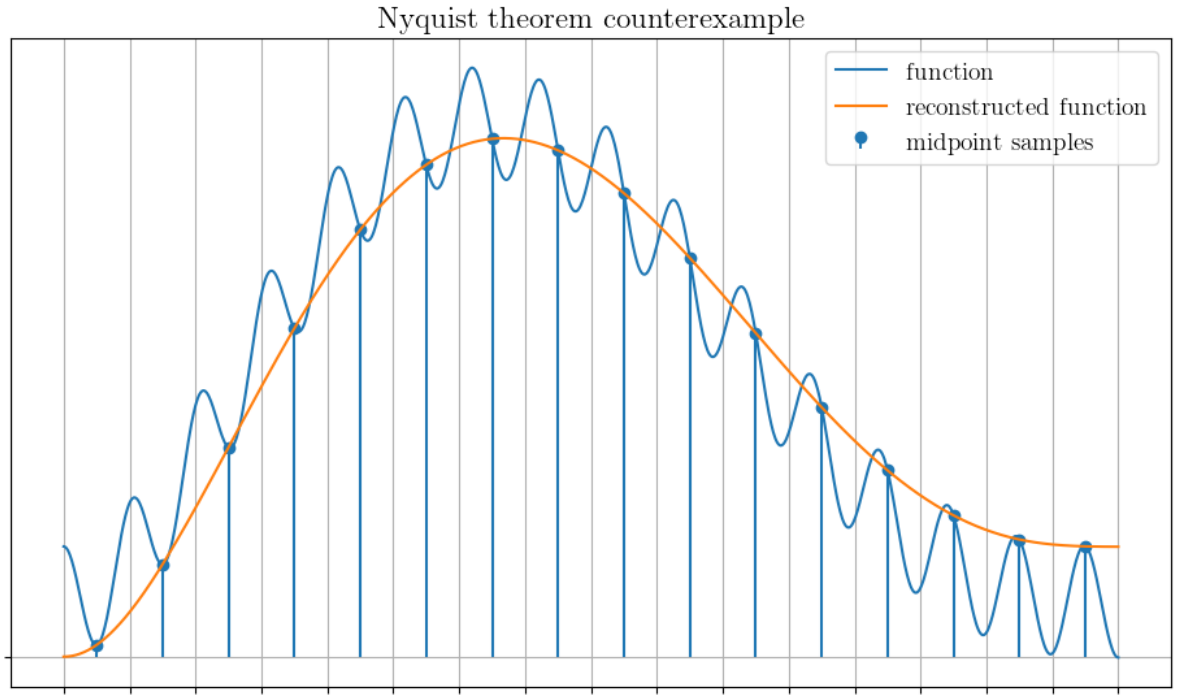

Fig. 5.6: A function that contains higher frequencies than $k/(2L)$ leads to *aliasing* phenomenon and incorrect calculation. The reconstructed function depicted in orange is calculated using equation (5.10).

of type II is used. [9] This type is best suited for mid-point representatives with zero derivatives at the boundary.

A fast algorithm for calculating discrete cosine transform (DCT) is presented in [62]. The algorithm is similar to the fast Fourier transform algorithm, but avoids using complex numbers. By this algorithm, a sequence of length k can be transformed in $\mathcal{O}(k \log k)$ multiplications. This algorithm is implemented in standard packages for numerical computation such as `Scipy` for `Python` or `FFTW` for `Julia`.

DCT-II is a linear transformation of sequence $x_0, x_1, \ldots, x_{k-1}$ into basis formed by

[9] Discrete cosine transform of type II is usually abbreviated to *DCT-II* or simply *the DCT*.

cosines: [10] [11]

$$y_N = 2\sum_{n=0}^{k-1} x_n \cos\left(\frac{\pi N(2n+1)}{2k}\right)$$

If sequence $x_0, x_1, \dots x_{k-1}$ corresponds to $u\left(t, \frac{L}{2k}\right), u\left(t, \frac{3L}{2k}\right), \dots, u\left(t, \frac{(2k-1)L}{2k}\right)$, then coefficients y represent coefficients of cosine series that match the the function u at sampling points: [12]

$$u\left(t, \frac{(2N+1)L}{2k}\right) = \frac{y_0}{2k} + \frac{1}{k}\sum_{n=1}^{k-1} y_n \cos\left(\frac{n\pi x}{L}\right). \tag{5.10}$$

Once coefficients y are calculated, a fractional Laplacian can be evaluated by (5.8):

$$-(-\Delta)^{\alpha/2} u\left(t, \frac{(2N+1)L}{2k}\right) = \frac{1}{k}\sum_{n=1}^{k-1} y_n \left(\frac{n\pi}{L}\right)^{\alpha} \cos\left(\frac{n\pi x}{L}\right)$$

This operation is the inverse of DCT, but with coefficients $y_n(n\pi/L)^\alpha$ instead of y_n, which can also be done in $k \log k$ operations. This way a fractional Laplacian at k sample points can be evaluated using only $\mathcal{O}(k \log k)$ operations. The entire process is depicted in fig. 5.7.

When using the discrete cosine transform, the number of sample points k must be chosen following the Nyquist-Shannon sampling theorem. The theorem says that the sampled function must not "oscillate too fast" in comparison with sampling intervals. An illustration of why this theorem is important is depicted in fig. 5.6. This theorem also implies that the functions that we can work with are all continuous.

If the samples are too apart, even if the original function is non-negative, the reconstructed function can become negative. [13] This is known as *Gibbs phenomenon* in the context of Fourier analysis or *ringing artifacts* in the context of signal processing. This phenomenon is depicted in fig. 5.8. Therefore a non-negativity check is required before

[10] There are other types of DCT, suitable for other choices of representative points, for example DCT-I would work if points $0, L/k, 2L/k, \dots (k-1)L/k, L$ would be chosen.

[11] Sometimes, term y_0 is multiplied by $1/\sqrt{k}$ and other terms by $\sqrt{2/k}$, so the matrix representing this transformation is orthogonal. However, the scaling is not important for calculating fractional Laplacian, because of inverse cosine transformation later.

[12] The following transformation is the inverse of DCT-II, which is (up to a scaling factor of $1/k$) the same as DCT-III.

[13] Usually functions that are steeply increasing from values near zero (or steeply decreasing towards values near zero) usually need many samples to be non-negative after the Discrete Fourier transform. Examples of such functions would be $f(x) = \exp(-x^2)$ or $f(x) = (x/L)^a \cdot (1 - x/L)^b$ if $a \gg b > 1$.

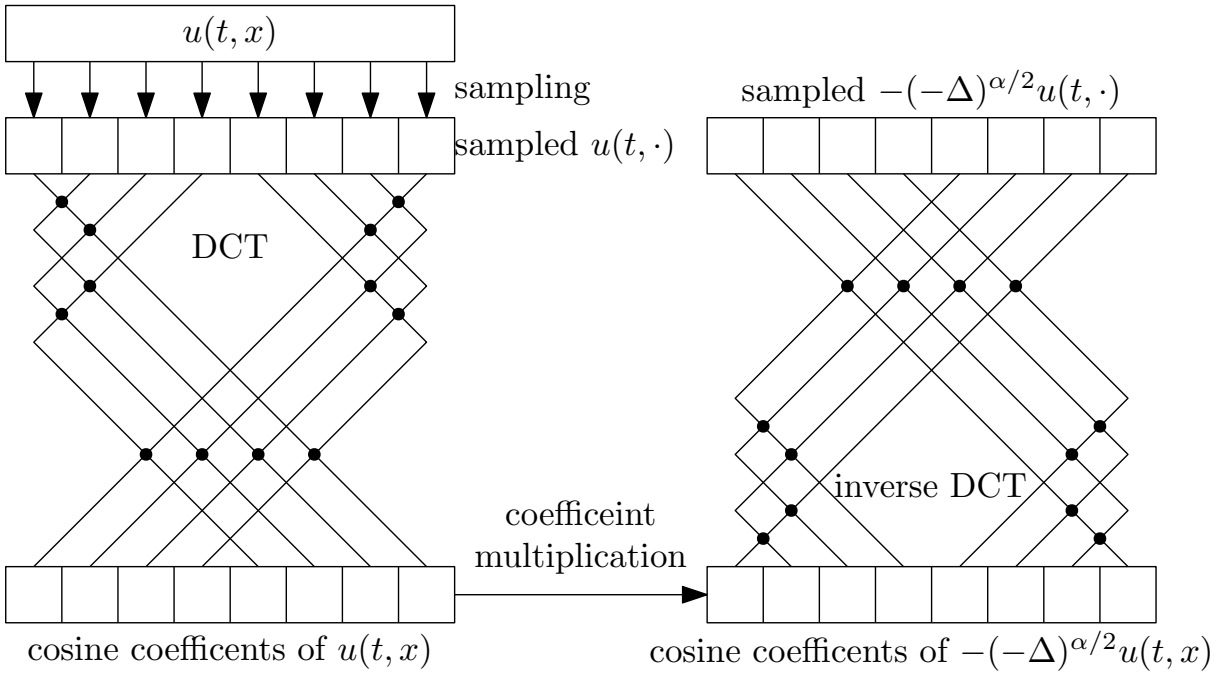

Fig. 5.7: Diagram of calculation of fractional Laplacian at sampled points. First, the function is sampled at k midpoints. Then the cosine coefficients y_n are calculated using DCT. These coefficients are then multiplied by $(n\pi L)^{\alpha/2}$ to obtain fractional Laplacian representation in the cosine domain. Finally, by inverse DCT, values of fractional Laplacian are calculated.

computation. In article [77], a criterion for non-negativity of Fourier series is provided. This criterion can be easily extended for the case of discrete cosine transform.

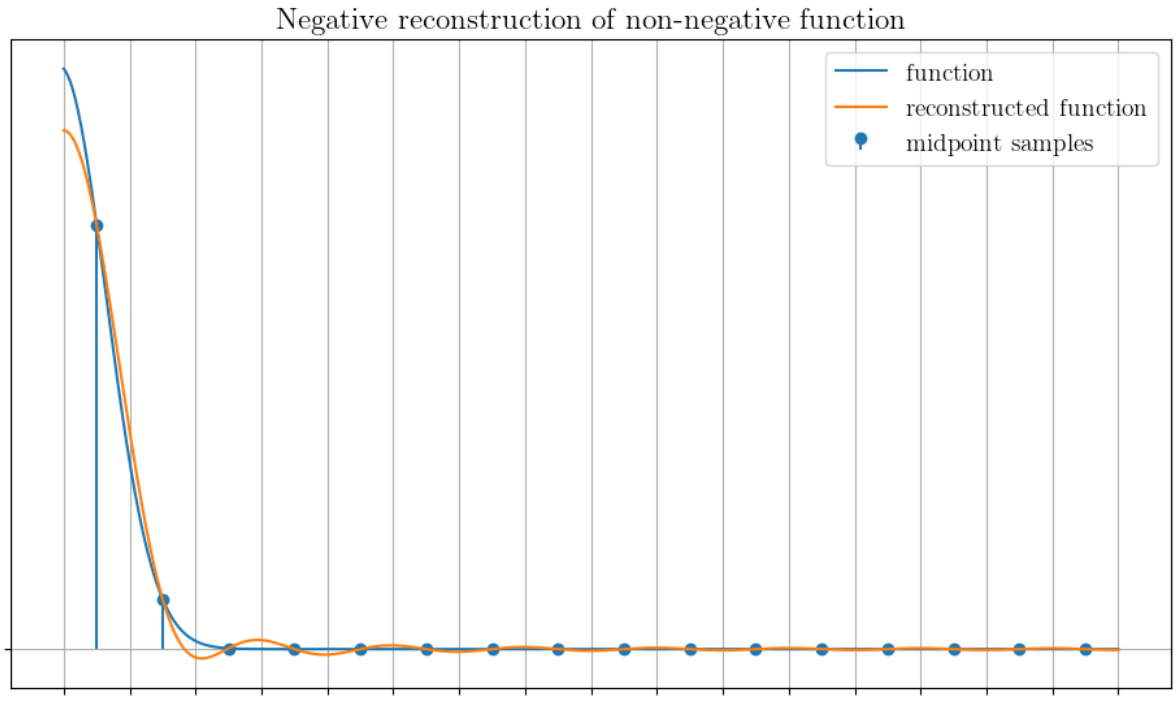

Fig. 5.8: A non-negative function can cross zero after sampling and reconstruction. The function used here is $\exp(-x^2)$.

5.3.3 Transformation into cosine series

For the sake of simplicity let us assume that total population density $N(t,x) = N$ is constant.

We may express compartments S, I, R in terms of cosine series with coefficients s, i, r respectively, that are functions of time:

$$S(t,x) = \sum_{n=0}^{\infty} s_n(t) \cos\left(n\pi x/L\right)$$
$$I(t,x) = \sum_{n=0}^{\infty} s_n(t) \cos\left(n\pi x/L\right)$$
$$R(t,x) = \sum_{n=0}^{\infty} r_n(t) \cos\left(n\pi x/L\right).$$

Then, if we can exchange the order of differentiation and sum:

$$\frac{d}{dt}S(t,x) = \pi/L \sum_{n=0}^{\infty} \frac{d}{dt} s_n(t) n \cos\left(n\pi x/L\right)$$
$$\frac{d}{dt}I(t,x) = \pi/L \sum_{n=0}^{\infty} \frac{d}{dt} i_n(t) n \cos\left(n\pi x/L\right)$$
$$\frac{d}{dt}R(t,x) = \pi/L \sum_{n=0}^{\infty} \frac{d}{dt} r_n(t) n \cos\left(n\pi x/L\right)$$

But also:

$$\begin{aligned}
\frac{d}{dt}S(t) =& -\beta\frac{S(t,x)I(t,x)}{N} + \omega R(t,x) - \kappa(-\Delta)^{\alpha/2}S(t,x) \\
=& -\frac{\beta}{N}\left(\sum_{n=0}^{\infty} s_n(t)\cos\left(n\pi x/L\right)\right)\left(\sum_{n=0}^{\infty} i_n(t)\cos\left(n\pi x/L\right)\right) \\
&+ \omega\sum_{n=0}^{\infty} r_n(t)\cos\left(n\pi x/L\right) \\
&- \kappa\sum_{n=0}^{\infty} s_n(t)(n\pi/L)^{\alpha}\cos\left(n\pi x/L\right)
\end{aligned}$$

From this expression, the first term, representing $S(t,x)\cdot I(t,x)$ can be rewritten by using trigonometric identity $\cos(a)\cdot\cos(b) = \frac{1}{2}\left(\cos(a+b)+\cos(a-b)\right)$:

$$\begin{aligned}
&\left(\sum_{n=0}^{\infty} s_n(t)\cos\left(n\pi x/L\right)\right)\left(\sum_{n=0}^{\infty} i_n(t)\cos\left(n\pi x/L\right)\right) \\
=&\sum_{n=0}^{\infty}\sum_{m=0}^{\infty}\left(s_n(t)\cos\left(n\pi x/L\right)\right)\left(i_m(t)\cos\left(m\pi x/L\right)\right) \\
=&\sum_{n=0}^{\infty}\sum_{m=0}^{\infty} s_n(t)i_m(t)\cos\left(n\pi x/L\right)\cos\left(m\pi x/L\right) \\
=&\sum_{n=0}^{\infty}\sum_{m=0}^{\infty}\frac{1}{2}s_n(t)i_m(t)\left(\cos\left((n+m)\pi x/L\right)+\cos\left((n-m)\pi x/L\right)\right) \\
=&\frac{1}{2}\sum_{n=0}^{\infty}\sum_{m=0}^{\infty} s_n(t)i_m(t)\cos\left((n+m)\pi x/L\right) \\
&+\frac{1}{2}\sum_{n=0}^{\infty}\sum_{m=0}^{\infty} s_n(t)i_m(t)\cos\left((n-m)\pi x/L\right).
\end{aligned}$$

The first term can be expressed as:

$$\frac{1}{2}\sum_{n=0}^{\infty}\sum_{m=0}^{\infty} s_n(t)i_m(t)\cos\left((n+m)\pi x/L\right)$$

$$
\begin{aligned}
&= \frac{1}{2}\sum_{n=0}^{\infty}\sum_{k=0}^{n} s_k(t) i_{k-n}(t) \cos\left(n\pi x/L\right) \\
&= \frac{1}{2}\sum_{n=0}^{\infty} \cos\left(n\pi x/L\right) \sum_{k=0}^{n} s_k(t) i_{k-n}(t),
\end{aligned}
$$

and the second term can be expressed as:

$$
\begin{aligned}
&\frac{1}{2}\sum_{n=0}^{\infty}\sum_{m=0}^{\infty} s_n(t) i_m(t) \cos\left((n-m)\pi x/L\right) \\
=&\frac{1}{2}\sum_{n=0}^{\infty}\sum_{k=n}^{\infty} (s_{k-n}(t) i_k(t) + s_k(t) i_{n+k}(t)) \cos(n\pi x/L) \\
=&\frac{1}{2}\sum_{n=0}^{\infty} \cos(n\pi x/L) \sum_{k=n}^{\infty} (s_{k-n}(t) i_k(t) + s_k(t) i_{n+k}(t))
\end{aligned}
$$

Finally, the equation for susceptible reads:

$$
\begin{aligned}
\pi/L \sum_{n=0}^{\infty} \frac{d}{dt} s_n(t) n \cos(n\pi x/L) = &-\frac{\beta}{2N} \sum_{n=0}^{\infty} \cos\left(n\pi x/L\right) \sum_{k=0}^{n} s_k(t) i_{k-n}(t) \\
&- \frac{\beta}{2N} \sum_{n=0}^{\infty} \cos(n\pi x/L) \sum_{k=n}^{\infty} (s_{k-n}(t) i_k(t) + s_k(t) i_{n+k}(t)) \\
&+ \omega \sum_{n=0}^{\infty} r_n(t) \cos\left(n\pi x/L\right) \\
&- \kappa\pi^{\alpha}/L^{\alpha} \sum_{n=0}^{\infty} s_n(t) \cos(n\pi x/L).
\end{aligned}
$$

By comparison of the terms with the same frequency $\cos(n\pi x/L)$ we get an ordinary differential equation for $s_n(t)$:

$$
\begin{aligned}
\frac{d}{dt} s_n(t) = \frac{L}{\pi}\Big(&-\frac{\beta}{2N} \sum_{k=0}^{\infty} s_k(t) i_{k-n}(t) - \frac{\beta}{2N} \sum_{k=n}^{\infty} (s_{k-n}(t) i_k(t) + s_k(t) i_{n+k}(t)) \\
&+ \omega r_n(t) - \kappa\pi^{\alpha}/L^{\alpha} s_n(t)\Big)
\end{aligned}
\tag{5.11}
$$

In the same manner, an equation for infectious can be derived as:

$$
\begin{aligned}
\frac{d}{dt} i_n(t) = \frac{L}{\pi}\Big(&\frac{\beta}{2N} \sum_{k=0}^{\infty} s_k(t) i_{k-n}(t) + \frac{\beta}{2N} \sum_{k=n}^{\infty} (s_{k-n}(t) i_k(t) + s_k(t) i_{n+k}(t)) \\
&- \gamma i_n(t) - \kappa\pi^{\alpha}/L^{\alpha} i_n(t)\Big).
\end{aligned}
\tag{5.12}
$$

Equation for recovered then reads:

$$
\frac{d}{dt} r_n(t) = \frac{L}{\pi}\Big(\gamma i_n(t) - \omega r_n(t) - \kappa\pi^{\alpha}/L^{\alpha} r_n(t)\Big) \tag{5.13}
$$

The assumption $N(t,x) = N$ can be used to further simplify the model:

$$R(t,x) = N - S(t,x) - I(t,x)$$
$$\sum_{n=0}^{\infty} r_n(t)\cos(n\pi x/L) = N - \sum_{n=0}^{\infty} s_n(t)\cos(n\pi x/L) - \sum_{n=0}^{\infty} i_n(t)\cos(n\pi x/L)$$
$$r_n(t) = \begin{cases} N - s_0(t) - i_0(t) & \text{for } n = 0 \\ -s_n(t) - i_n(t) & \text{for } n > 0, \end{cases}$$

so functions $r_n(t)$ can be obtained without solving corresponding differential equations. This simplification is also beneficial, because to solve the system (5.11) – (5.13) numerically, we have to truncate the infinite sums. However, the "diagonal" terms $s_{k-n}(t)i_k(t)$ and $s_k(t)i_{k+n}(t)$ would be calculated incorrectly. The simplified calculation r_n holds these difficulties back.

5.4 Numerical results

In this section, we present some numerical results of the model (5.1) with a focus on the novel features of the model. The results were obtained by the method of lines, as discussed in 5.3.1 with $k = 256$ lines.

5.4.1 Initial condition

For crafting a suitable initial condition, we proceeded as follows:

First, we selected the total population $N = 100\,000$ and length $L = 10$, so that population density $N_0(x) = N/L$. We chose $R_0(x)$ to be zero, because this is an equilibrium of the model.

Then we chose the initial density of infectious as

$$I_0(x) = \frac{1}{L} + \frac{1}{L}\cos\left(\frac{\pi x}{L}\right) + \frac{\sqrt{3}}{2L}\cos\left(\frac{2\pi x}{L}\right) + \frac{2}{3L}\cos\left(\frac{3\pi x}{L}\right) + \frac{\sqrt{3}}{4L}\cos\left(\frac{4\pi x}{L}\right) + \frac{1}{5L}\cos\left(\frac{5\pi x}{L}\right), \tag{5.14}$$

which is depicted in fig. 5.9. Note that this initial condition is already in the form of a cosine series satisfying the Neumann boundary condition and is non-negative.

Finally, we chose the density of recovered as $R_0(x) = N_0(x) - I_0(x)$.

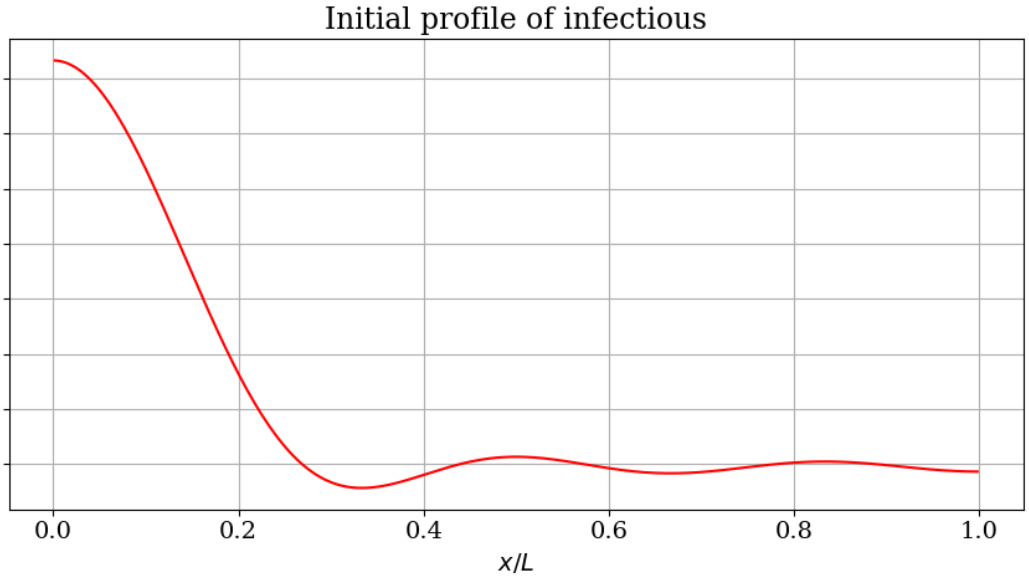

Fig. 5.9: Initial condition $I_0(x)$ described by equation (5.14). Note that the horizontal axis is non-dimensionalized to x/L and hence the vertical axis is unlabelled. The bottom of the graph is at $x = 0$.

5.4.2 Long-term behavior

The model's long-term behavior is to tend towards equilibrium. The quality of equilibrium – disease-free or endemic – depends on the ratio $\frac{\beta}{\gamma}$.

Because of diffusion, all compartments tend to constant function in x as $t \to \infty$: $S(t,x) \to S(t), I(t,x) \to I(t), R(t,x) \to R(t)$ and hence diffusion terms of model (5.1), $-\kappa(-\Delta^{\alpha/2})$, tend to zero. In the limit, the model simplifies into

$$\begin{aligned} 0 = \frac{\partial S}{\partial t} &= -\beta \frac{SI}{N} + \omega R \\ 0 = \frac{\partial I}{\partial t} &= \beta \frac{SI}{N} - \gamma I \\ 0 = \frac{\partial R}{\partial t} &= \gamma I - \omega R. \end{aligned}$$

From the second equation, we have either $I = 0$ or $S = \frac{\gamma}{\beta} N$. Similar to the SIRS model, the stability of these equilibria is determined by reproduction number: if $\beta < \gamma$, disease-free equilibrium is stable; else if $\beta > \gamma$, endemic equilibrium is stable.

This can be seen in fig. 5.10. The parameter values for the two scenarios are listed in table 5.1.

Parameter	β	γ	ω	k	κ	α
Disease-free equilibrium	30	36	8	256	0,1	1
Endemic equilibrium	50	36	8	256	0.1	1

Tab. 5.1: Parameter values for disease-free equilibrium

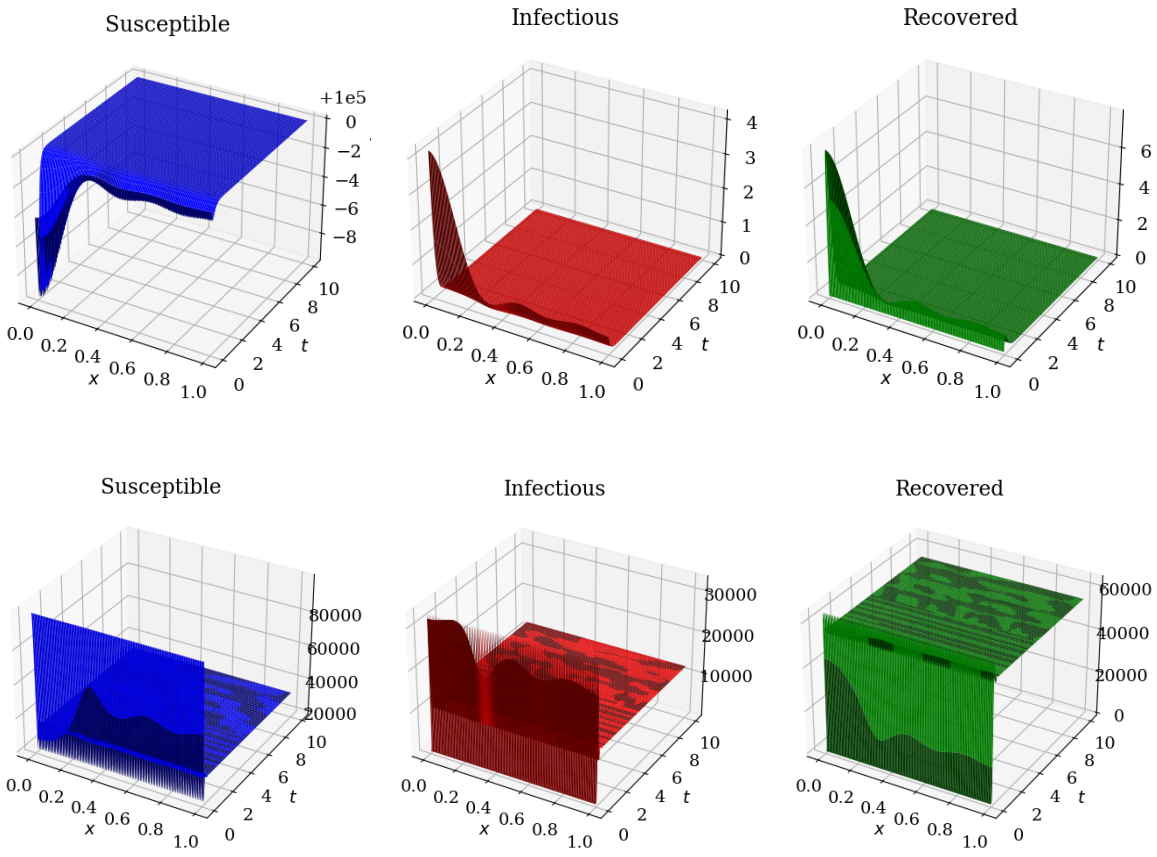

Fig. 5.10: Long-term behavior of the model (5.1). The fast phase in the beginning is followed by a steady phase. Top row: disease-free equilibrium. Bottom row: endemic equilibrium. Note that the vertical axis for susceptible in the disease-free scenario is shifted by 10^5.

5.4.3 Effect of α and κ on initial disease spread

As we saw earlier, the long-term behavior depends only on the ratio β/γ. However, the initial disease spread depends on other parameters. To demonstrate the novel features of this model, we focus on α and κ in this section. The time range is shortened to $t \in [0, 1/2]$. We present four different scenarios with parameter values listed in table 5.2. The figures for each scenario also contain slices of $I(t, x)$ for values $t \in \{0.05, 0.25, 0.5\}$ to better see details that may not be visible on other graphs. Figures include total number

of infectious individuals, i.e.

$$I_{total}(t) = \int_0^x I(t,x)dx$$

Parameter	β	γ	ω	k	α	κ	L
Scenario 1	50	36	8	256	1	0.001	1
Scenario 2	50	36	8	256	2	0.001	1
Scenario 3	50	36	8	256	1	1	1
Scenario 4	50	36	8	256	2	1	1

Tab. 5.2: Parameter values of SIRS model with diffusion for scenarios 1 – 4.

As we can see, the results of scenarios 1 and 2 are almost identical. This is due to diffusion rate κ being almost zero.[14] The difference between the number of infectious people in these two scenarios is at order 10^{-3} with scenario 2 having more total infectious. In the case of very weak diffusion, the profiles of infectious are very similar to initial condition (5.14) with the majority of infectious individuals is located near point $x = 0$.[15]

In scenarios 3 and 4, the results show a more uniform distribution of individuals in each compartment than that in scenarios 1 and 2; this is due to the diffusion coefficient κ being $1\,000$-times larger. The homogeneity seems to increase with the order of fractional Laplacian α. The concentration of infectious individuals is still higher at $x = 0$, but the spatial profiles are flatter. The total number of infectious individuals also seems to increase with the order of fractional Laplacian, α, with the difference at the order of 1.

5.4.4 Effect of spatial dimension

The parameter L represents the length of the spatial interval. The model is not independent of this parameter. This is due to the nature of fractional Laplacian. To demonstrate this effect, we chose to present numerical results with varying L, namely $L = 1$, $L = 100$ and $L = 10\,000$. Other parameters remain unchanged. The full list of parameters can

[14]Note that if we would set $\kappa = 0$, the model would be independent of α and would be equivalent to infinite many ordinary SIRS models with initials conditions $S(0,x), I(0,x)$ and $R(0,x)$.

[15]In fact, the asymptotic behavior of $I(t,x)$ as $t \to 0^+$ can be described as $I(t,x) \sim \exp(atI_0(x))$ for suitable constant a.

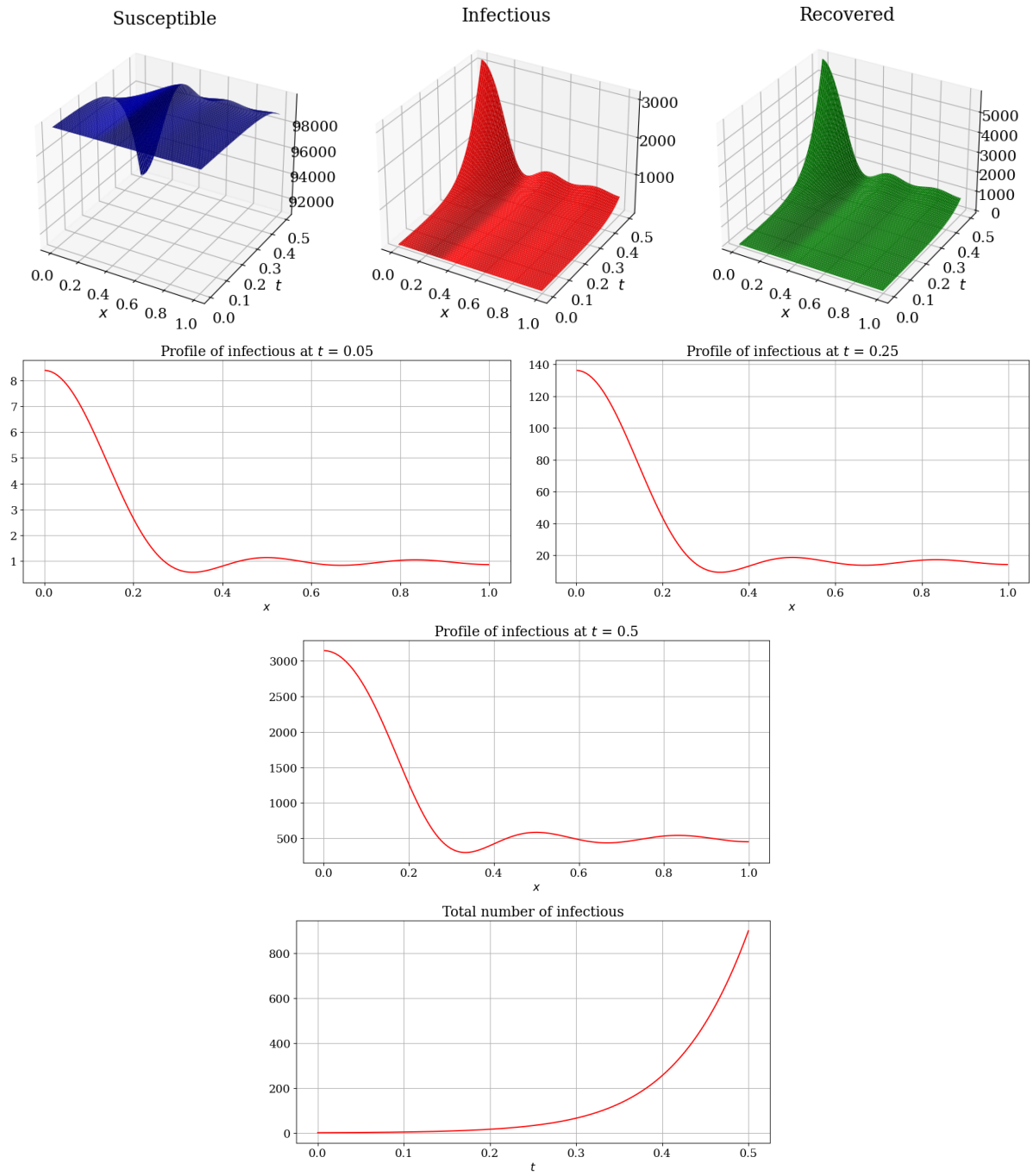

Fig. 5.11: Numerical results of scenario 1

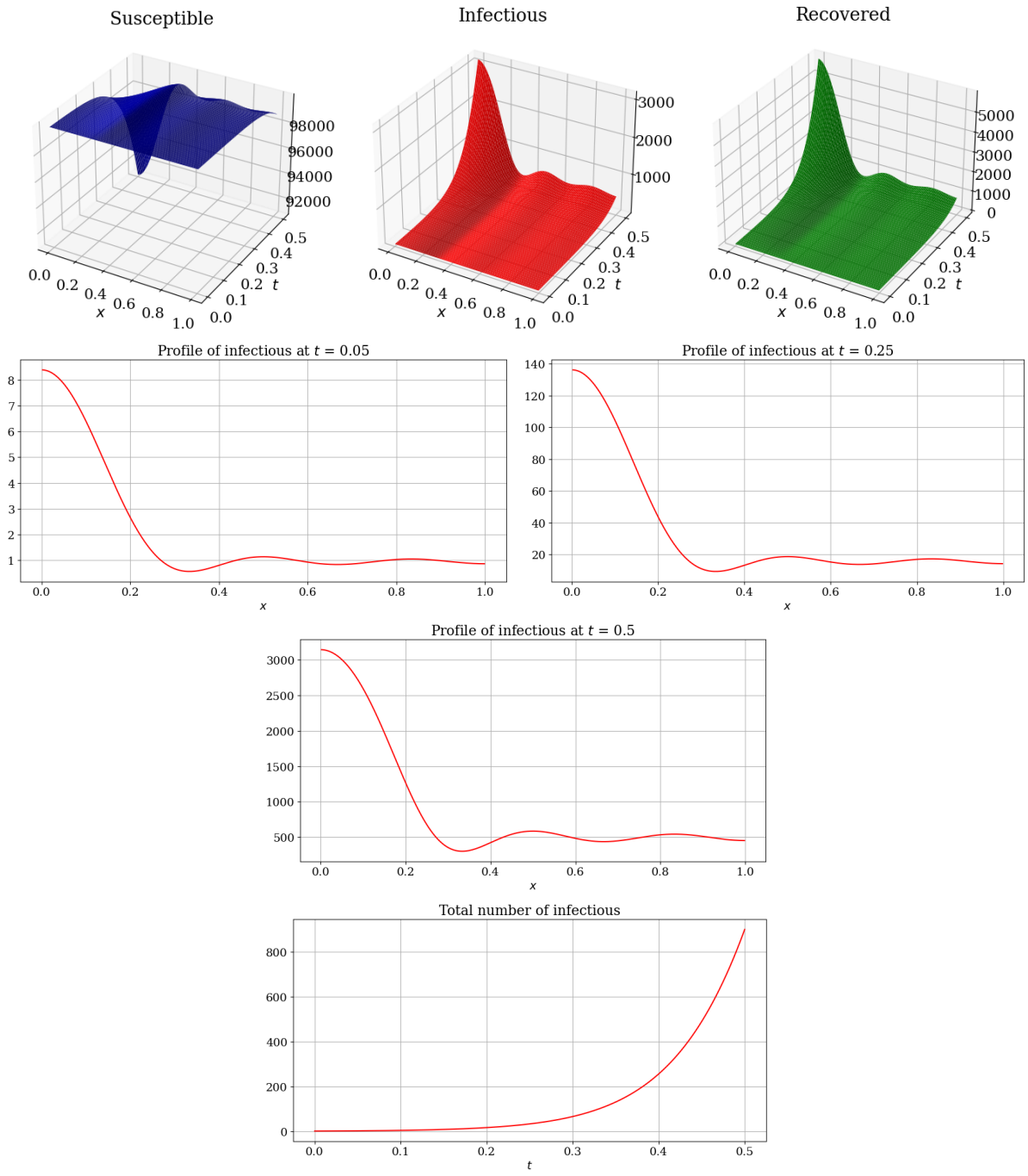

Fig. 5.12: Numerical results of scenario 2

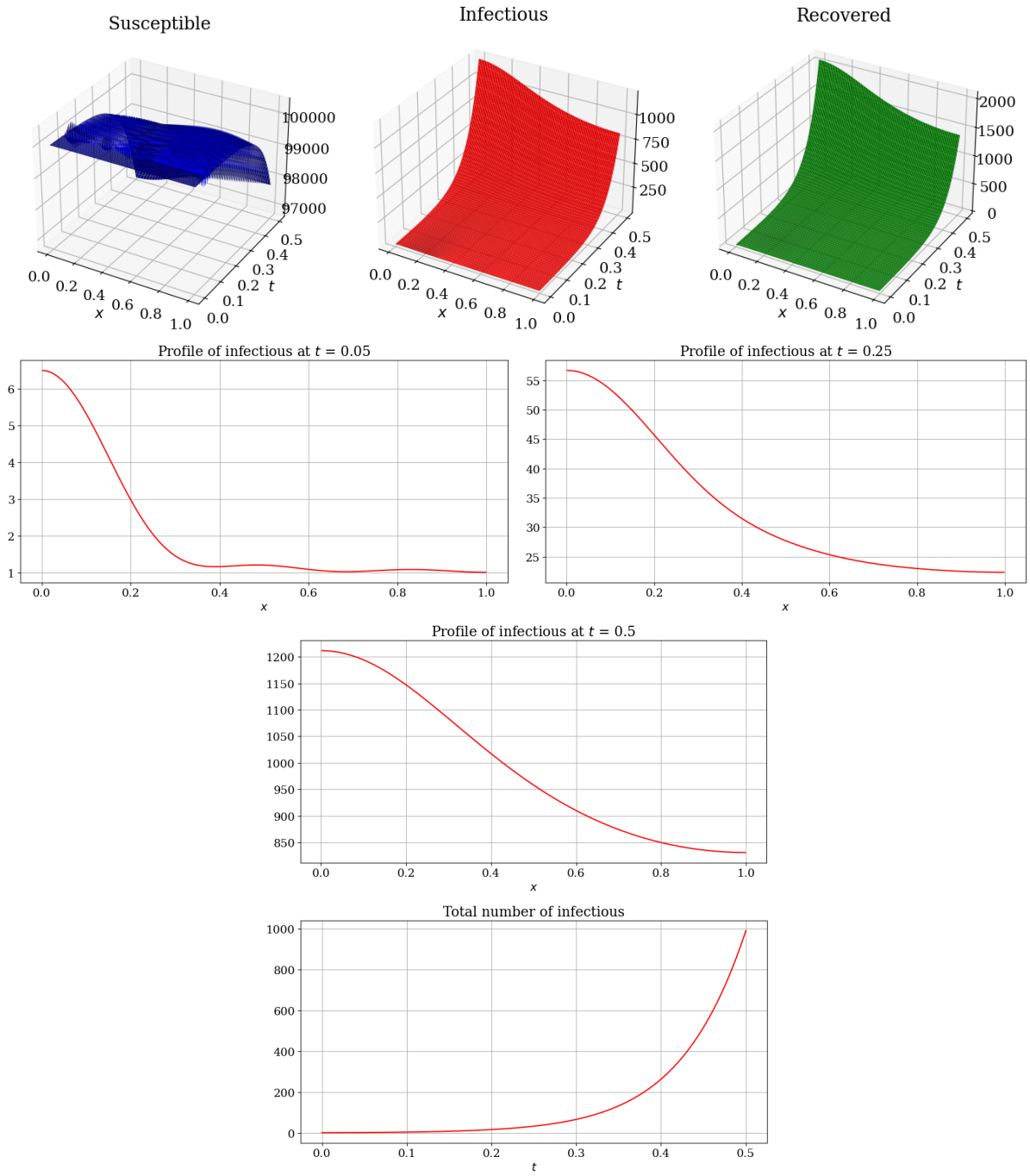

Fig. 5.13: Numerical results of scenario 3

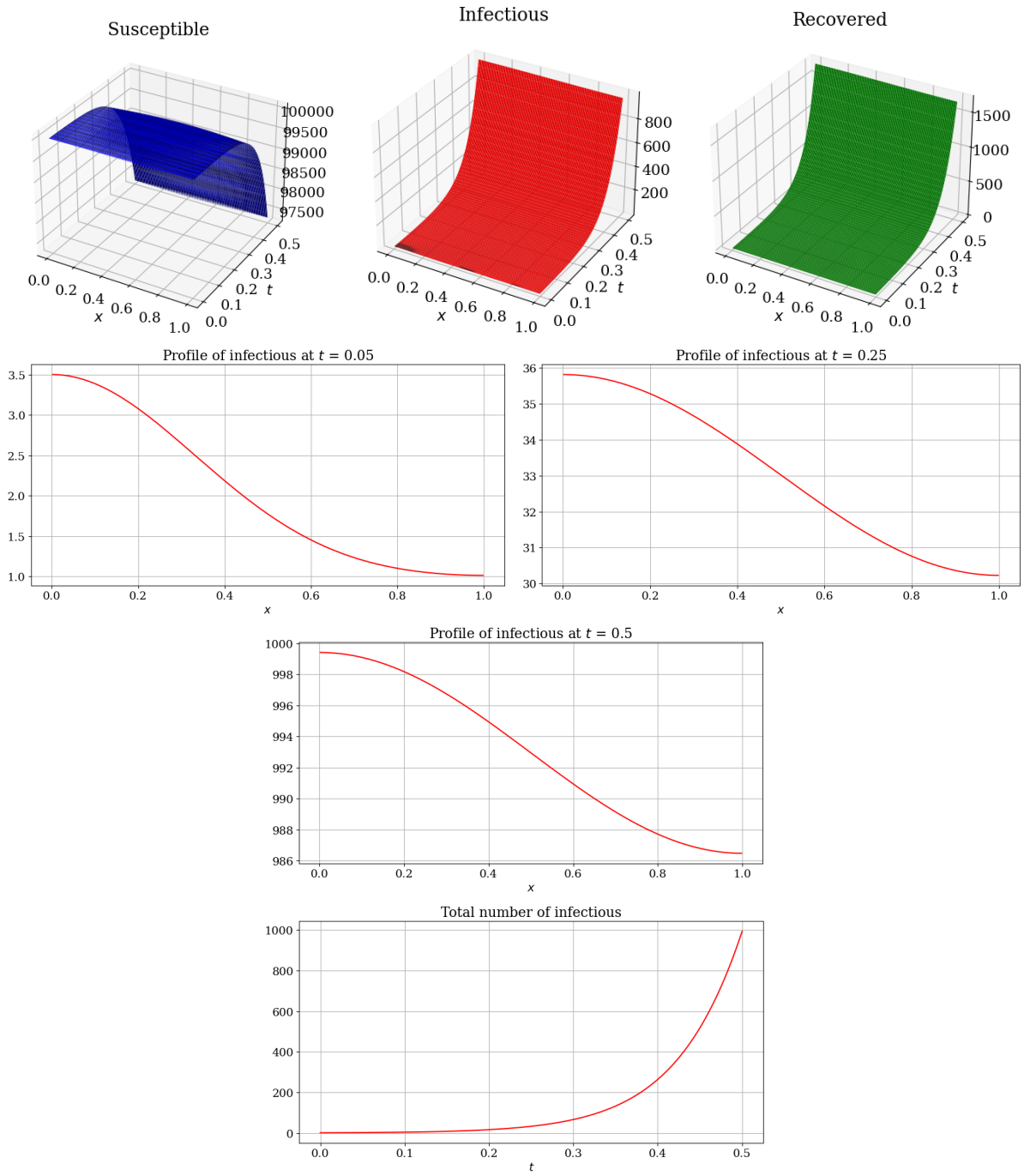

Fig. 5.14: Numerical results of scenario 4

be found in table 5.3. Note that compartments S, I, R represent the population density, so that the results show the overall proportionality to $1/L$. The numerical results for the three scenarios are presented in figures 5.15, 5.16 and 5.17. [16] The spatial profile of infectious at $t = 0.5$ as well as a graph of the total number of infectious individuals is provided for each scenario.

As we can see, the shape of the model solutions is different, even though the initial conditions have the same shape. We can observe that larger L results in delaying the peak of infection and a smaller total number of infectious. This observation has a physical interpretation: when the distances between individuals are higher, the effect of diffusion is smaller and the infection spreads slower.

Contrary to graphs in section 5.4.3, the profile of infectious at time $t = 0.5$ shows that there are more infected individuals near $x = L$ than there are near $x = 0$. This is because the initial density of infected individuals was larger near $x = 0$, the epidemic peak arrived sooner, and at time $t = 0.5$, the number of infected individuals has been decreasing for a longer time. The difference between the number of infected individuals at time $t = 0.5$ between scenarios 1 and 3 is on the order of 10^2.

Parameter	β	γ	ω	k	α	κ	L
Scenario 1	50	36	8	256	1.5	1	1
Scenario 2	50	36	8	256	1.5	1	100
Scenario 3	50	36	8	256	1.5	1	10 000

Tab. 5.3: Parameter values of SIRS model with diffusion, scenarios 1 – 3.

[16] The profile of infectious at time $t = 0.5$ with $L = 1$ shows some wiggles: this is due to numerical problems with explicit Runge-Kutta methods. However, in the `DifferentialEquations` environment of `Julia` language it is difficult to use implicit methods, because DCT operations in the numerical schema are not auto-differentiable and would require large computational overhead.

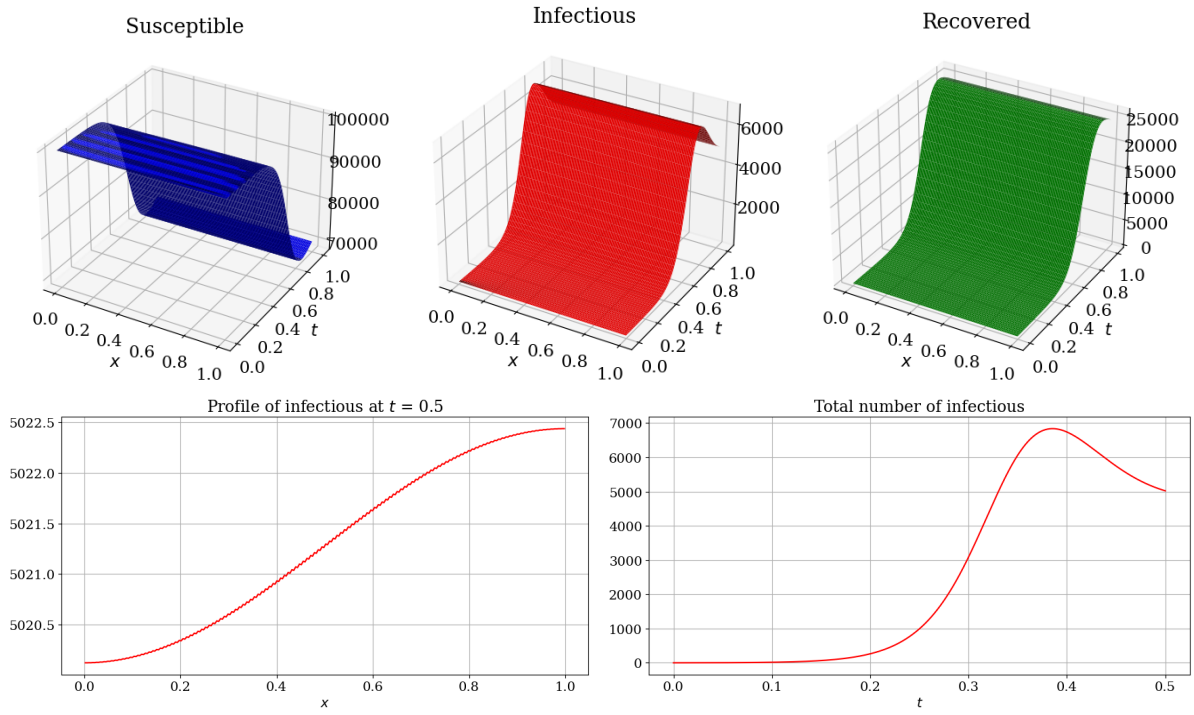

Fig. 5.15: Numerical results of scenario 1

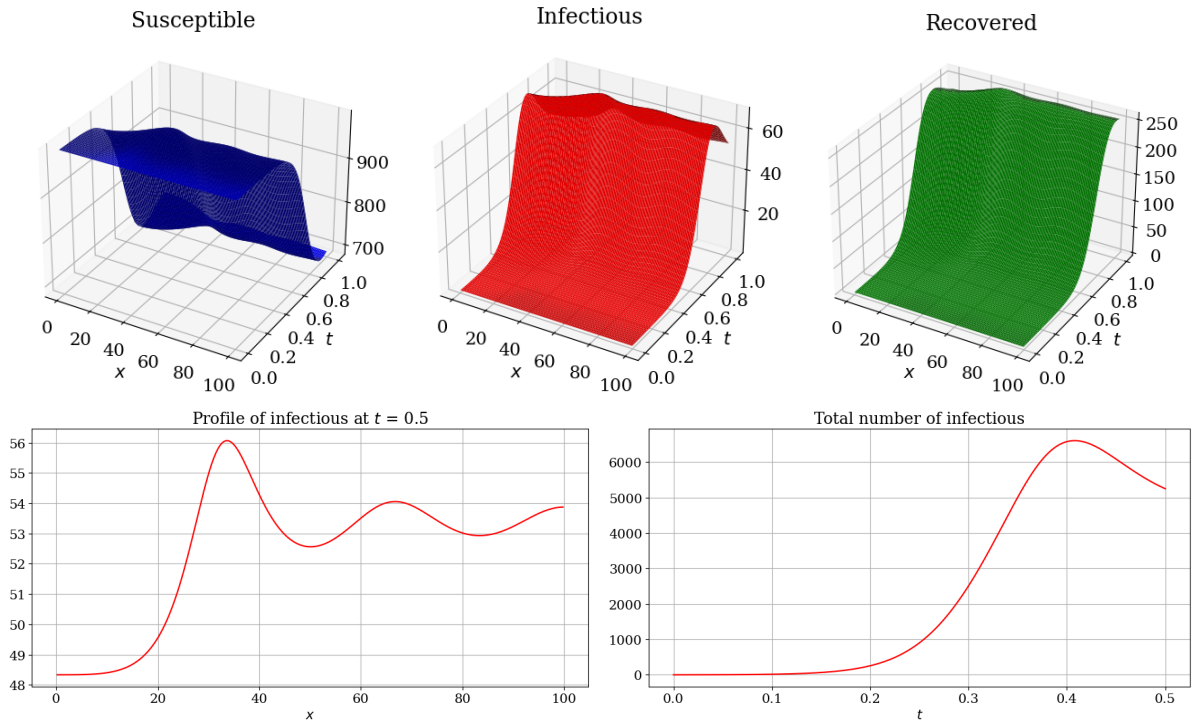

Fig. 5.16: Numerical results of scenario 2

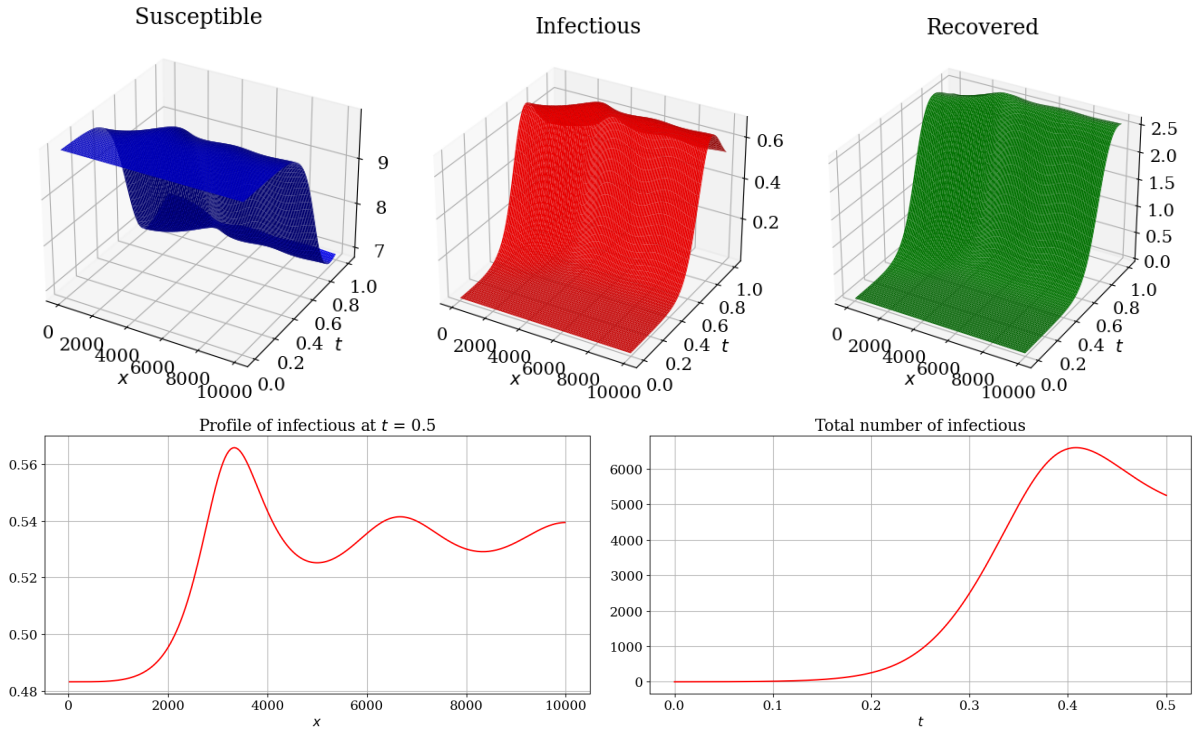

Fig. 5.17: Numerical results of scenario 3

5.5 Conclusion

In this chapter, we provided a gentle introduction to the topic of fractional Laplacian. We formulated a SIRS-type model with population diffusion, where the diffusion was modeled by a fractional Laplace operator. We used Fourier series approach to the diffusion problem and showed that Laplace operator is a special case of fractional Laplace operator with $\alpha = 2$.

We discussed even and period extension of a function and respective behavior at the boundary of the studied domain: we showed that the zero derivative at the boundary of the studied domain represents a reflecting boundary and ensures the conservation of the population.

We elaborated on numerical methods that were used to solve the proposed model. We utilized the method of lines as a tool to transform a partial differential equation into a system of ordinary differential equations. We showed that the discrete cosine transformation is an efficient tool to evaluate fractional Laplacian in the context of periodic functions. We showed an alternative approach based on the cosine series.

Finally, we showed some numerical results of the new model. We showed that

long-term behavior is similar to the standard SIRS model. We investigated the effect of diffusion rate κ and order of fractional Laplacian α on the results. We demonstrated the effect of spatial domain size on numerical results.

Chapter 6

Appendix: Code snippets

In this section, we present selected snippets of code that were used in this thesis to numerically solve various models. The code was written in either Python or Julia.

6.1 SIRRS model

6.1.1 Python implementation

```
import numpy as np
from scipy.integrate import solve_ivp

def SIRRS(t, y, beta, gamma, omega, beta_=0):
    S = y[0]
    I = y[1]
    R = y[2:]
    N = y.sum()

    dS = -beta*S*I/N + omega*R[-1]
    dI = beta*S*I/N - gamma*I

    boosting = beta_ * R*I/N
    dR = stage_progression - boosting
    dR[0] += boosting.sum() + gamma*I

    return dS, dI, *dR


initial_state = (9999, 1, *[0]*16)
tspan = (0, 10)
t_eval = np.linspace(*tspan, 1001)
params = (110, 36, 8, 110)
```

```
sol = solve_ivp(SIRRS, tspan, initial_state,
                t_eval=t_eval, args=params)

S = sol.y[0]
I = sol.y[1]
R = sol.y[2:].sum(axis=0)
```

6.1.2 Julia implementation

```
using DifferentialEquations
using StaticArrays

function SIRRS(state, params, t)
    beta, gamma, omega, beta_ = params

    S = state[1]
    I = state[2]
    R = state[3:end]
    N = sum(state)

    dS = -beta*I/N*S + omega * R[end]
    dI = beta*I/N*S - gamma*I

    dR = similar(R)
    dR[1] = gamma*I - omega*R[1]
    for i in 2:length(R)
        dR[i] = omega*R[i-1] - omega*R[i] - beta_*R[i]/N*I
        dR[1] += beta_*R[i]/N*I
    end

    return [dS, dI, dR...]
end;

initial_state = [9999., 1, zeros(16)...]
tspan = (0., 10.)
t_eval = LinRange(tspan..., 1001)
params = (110, 36, 8, 110)
prob = ODEProblem(SIRRS, initial_state, tspan, params;
                  saveat=t_eval)
sol = solve(prob);
```

6.2 Custom waning profiles (Julia implementation)

```
using OffsetArrays
using StaticArrays

dt = 0.001
t_max = 10.
tau_max = 5.

beta = 30.
gamma = 10.
mu = 0
beta_ = 30.

tau = collect(0:dt:tau_max)
n_tau = length(tau)
t = collect(-tau_max:dt:t_max)
n_t = length(t)

t_0 = searchsortedfirst(t, 0.)
offset = 1-t_0:n_t-t_0;
t = OffsetArray(t, offset)

S_0 = 9999.
I_0 = 1.
R_I = zeros(length(tau))

P = max.(1 .- tau./4, 0)

S = zeros(Float64, size(t)...)
I = zeros(Float64, size(t)...)
R = zeros(Float64, size(t)...)
R_B = zeros(Float64, size(t)...)

S = OffsetArray(S, offset)
I = OffsetArray(I, offset)
R = OffsetArray(R, offset)
R_B = OffsetArray(R_B, offset)

I[0] = I_0
S[0] = S_0
R[1-length(tau):0] = R_I
N = S[0] + I[0] + R[0]

P0 = P[1]
P_ = P ./P0
B_n = @MVector zeros(n_tau)
exp_mu = (1 - mu*dt) .^ collect(1:n_tau)
P_mu = SA[(exp_mu .* P_)...]

for i = 0:(n_t - n_tau - 1)
```

```
    I[i+1] = I[i] + (beta * S[i]*I[i]/N -
                     (gamma + mu) * I[i]) * dt
    R_B[i+1] = beta_ * I[i]*R[i]/N + gamma * I[i] * P0
    B_n[1:end] = -I[i:-1:i-n_tau+1]*
                  beta_./N * dt .|> log1p |> cumsum
    R[i+1] = dt * (sum(R_B[i:-1:i-n_tau+1] .* P_mu .*
                   exp.(B_n)) + R_B[i+1])
    S[i+1] = N - I[i+1] - R[i+1]
end;
```

6.3 Model with diffusion (Julia implementation)

```
using DifferentialEquations
using StaticArrays
import FFTW: dct, idct

function SIRS_diffusion(S_0, I_0, R_0, beta, gamma, omega, mu,
                        L, t_max, kappa, alpha, solver=BS3())
    k = length(S_0)

    x = collect(1:2:2*k) .* (L/(2*k))
    tspan = (0., t_max)
    t_eval = LinRange(tspan..., 1001)

    initial_state = [S_0; I_0; R_0]

    freqs = collect(0:(k-1)) .* (pi / L)
    freqs_alpha = freqs .^ alpha
    function fractional_laplacian(f, kappa=kappa,
                                  freqs_alpha=freqs_alpha)
        coef = dct(f)
        return kappa .* idct(-freqs_alpha .* coef)
    end

    function model!(ret, state, params, t)
        beta, gamma, omega, mu = params

        S = state[1     : k  ]
        I = state[k+1   : 2*k]
        R = state[2*k+1 : 3*k]
        N = S + I + R

        ret[1:k] = -beta*(S.*I)./ N + omega*R - mu*S + mu*N
                    kappa*fractional_laplacian(S)
        ret[k+1:2*k] = beta*(S.*I)./N - (gamma+mu)*I +
                       kappa*fractional_laplacian(I)
        ret[2*k+1:end] = gamma*I - (omega+mu)*R +
                         kappa*fractional_laplacian(R)
        return nothing
```

```
    end;

    prob = ODEProblem(model!, initial_state, tspan,
                      (beta, gamma, omega, mu, p),
                      saveat=t_eval);
    sol = solve(prob, solver);

    sol
end

t_max = 10
alpha = 1.
L = 1.
kappa = 0.1
beta = 110
gamma = 36
omega = 8
t_max = 3
mu = 0

x = collect(1:2:2*k) .* (L/(2*k))
N = 100_000
N_0 = fill(N/L, k)
I_0 = (0.5*cos.(x*(pi/L)) + sqrt(3)/4*cos.(2x*(pi/L)) +
       1/3*cos.(3x*(pi/L)) + sqrt(3)/8*cos.(4x*(pi/L)) +
       1/10*cos.(5x*(pi/L)) .+ 0.5) ./ (L/2)
R_0 = zeros(k)
S_0 = N_0 - I_0 - R_0;

sol = SIRS_diffusion(S_0, I_0, R_0, beta, gamma, omega,
                     mu, L, t_max, kappa, alpha);
u = reduce(hcat, sol.u)
S = u[1:k, :];
I = u[k+1: 2k, :]
R = u[2k+1: 3k, :];
```

Bibliography

[1] Abbey, H. (1952). *An examination of the Reed-Frost theory of epidemics*. Human biology, 24(3), 201.

[2] Abioye, A. I., Ibrahim, M. O., Peter, O. J., Amadiegwu, S., Oguntolu, F. A. (2018). *Differential transform method for solving mathematical model of SEIR and SEI spread of malaria*. International Journal of Sciences: Basic and Applied Research 40(1) 197-219

[3] Ahmad, M. Z., Alsarayreh, D., Alsarayreh, A., Qaralleh, I. (2017). *Differential transformation method (DTM) for solving SIS and SI epidemic models*. Sains Malaysiana, 46(10), 2007-2017.

[4] Ammi, M. R. S., Zinihi, A., Raezah, A. A., Sabbar, Y. (2023). *Optimal control of a spatiotemporal SIR model with reaction–diffusion involving p-Laplacian operator*. Results in Physics, 52, 106895.

[5] Anderson, R., May, R. *Population biology of infectious diseases: Part I*. Nature 280, 361–367 (1979).

[6] Anderson, D. F. (2008). *Incorporating postleap checks in tau-leaping*. The Journal of chemical physics, 128(5), 054103.

[7] Atkinson, A. C. (1979). *The computer generation of Poisson random variables*. Journal of the Royal Statistical Society: Series C (Applied Statistics), 28(1), 29-35.

[8] Atkinson, K., Han, W., Stewart, D. E. (2009). *Numerical solution of ordinary differential equations* (Vol. 81). John Wiley & Sons.

[9] Astuti, F., Suryanto, A., Darti, I. (2019). *Multi-step differential transform method for solving the influenza virus model with disease resistance*. IOP Conference Series: Materials Science and Engineering (Vol. 546, No. 5, p. 052013). IOP Publishing.

[10] Becker, A.D., Grenfell, B.T. (2017) *tsiR: An R package for time-series Susceptible-Infected-Recovered models of epidemics*. PLOS ONE 12(9): e0185528. https://doi.org/10.1371/journal.pone.0185528

[11] Berger, D. W., Herkenhoff, K. F., Mongey, S. (2020). *An SEIR infectious disease model with testing and conditional quarantine* (No. w26901). National Bureau of Economic Research.

[12] Biswas, M. H. A., Paiva, L. T., De Pinho, M. D. R. (2014). *A SEIR model for control of infectious diseases with constraints*. Mathematical Biosciences & Engineering, 11(4), 761.

[13] P. Bogacki, P., Shampine, L. F. (1989). *A 3(2) pair of Runge - Kutta formulas* Applied Mathematics Letters, 2(4), 321-325,

[14] Borchers, H. W., Borchers, M. H. W. (2019). *Package 'pracma'. Practical numerical math functions, version, 2.5*.

[15] Borri, A., Carravetta, F., Mavelli, G., Palumbo, P. (2016). *Block-tridiagonal state-space realization of Chemical Master Equations: A tool to compute explicit solutions*. Journal of Computational and Applied Mathematics, 296, 410-426.

[16] Braun, M. (1976). *Differential equations and their applications: an introducion to applied mathematics*. Texts in aaplied mathematics, Springer

[17] Butcher, J. C. (2016). *Numerical methods for ordinary differential equations*. John Wiley & Sons.

[18] Butcher, J. C. (2000). *Numerical methods for ordinary differential equations in the 20th century*. Journal of Computational and Applied Mathematics, 125(1-2), 1-29.

[19] Cantrell, R. S., Cosner, C. (2004). *Spatial ecology via reaction-diffusion equations*. John Wiley & Sons.

[20] Cao, Y., Gillespie, D. T., Petzold, L. R. (2006). *Efficient step size selection for the tau-leaping simulation method*. The Journal of chemical physics, 124(4), 044109.

[21] Cao, Y., Gillespie, D. T., Petzold, L. R. (2005). *Avoiding negative populations in explicit Poisson tau-leaping*. The Journal of chemical physics, 123(5), 054104.

[22] Carlsson, R. M., Childs, L. M., Feng, Z., Glasser, J. W., Heffernan, J. M., Li, J., Röst, G. (2020). *Modeling the waning and boosting of immunity from infection or vaccination*. Journal of theoretical biology, 497, 110265.

[23] Cossette, H., Landriault, D., Marceau, E., Moutanabbir, K. (2016). *Moment-based approximation with mixed Erlang distributions.* Variance, 10(1), 161-182.

[24] Chinviriyasit, S., Chinviriyasit, W. (2010). *Numerical modelling of an SIR epidemic model with diffusion*. Applied Mathematics and Computation, 216(2), 395-409.

[25] d'Onofrio, A. (2002). *Stability properties of pulse vaccination strategy in SEIR epidemic model*. Mathematical biosciences, 179(1), 57-72.

[26] Danon, L., Ford, A. P., House, T., Jewell, C. P., Keeling, M. J., Roberts, G. O., Vernon, M. C. et al. (2011). Networks and the epidemiology of infectious disease. Interdisciplinary perspectives on infectious diseases.

[27] Diekmann, O., Heesterbeek, J. A. P., Metz, J. A. (1990). *On the definition and the computation of the basic reproduction ratio R 0 in models for infectious diseases in heterogeneous populations*. Journal of mathematical biology, 28(4), 365-382.

[28] Debrabant, K. (2010). *Runge-Kutta methods for third order weak approximation of SDEs with multidimensional additive noise.* BIT Numerical Mathematics, 50, 541-558.

[29] Dormand, J. R., Prince, P. J. (1980). *A family of embedded Runge-Kutta formulae*. Journal of computational and applied mathematics, 6(1), 19-26.

[30] Eames, K. T., Keeling, M. J. (2002). *Modeling dynamic and network heterogeneities in the spread of sexually transmitted diseases*. Proceedings of the national academy of sciences, 99(20), 13330-13335.

[31] Ehrhardt, M., Gašper, J., Kilianová, S. (2019). *SIR-based mathematical modeling of infectious diseases with vaccination and waning immunity*. Journal of Computational Science, 37, 101027.

[32] Erban, R., Chapman, J., Maini, P. (2007). *A practical guide to stochastic simulations of reaction-diffusion processes*. arXiv preprint arXiv:0704.1908.

[33] Fehlberg, E. (1970). *Classical fourth-and lower order Runge-Kutta formulas with stepsize control and their application to heat transfer problems*. Computing, 6, 61-71.

[34] Finkenstädt, B.F., Grenfell, B.T. (2000). *Time series modelling of childhood diseases: a dynamical systems approach*. Journal of the Royal Statistical Society: Series C (Applied Statistics), 49: 187-205.

[35] Fourier, Jean Baptiste Joseph. (1878) *Analytical theory of heat. Translated, with notes by Alexander Freeman.* Cambridge University Press.

[36] Getz, W.M., Dougherty, E.R. (2018) *Discrete stochastic analogs of Erlang epidemic models*. J Biol Dyn. 2018 Dec; 12(1) 16-38.

[37] Gibson, M. A., Bruck, J. (2000). *Efficient exact stochastic simulation of chemical systems with many species and many channels*. The journal of physical chemistry A, 104(9), 1876-1889.

[38] Gillespie, D. T. (1976). *A general method for numerically simulating the stochastic time evolution of coupled chemical reactions*. Journal of computational physics, 22(4), 403-434.

[39] Gillespie, D. T. (1977). *Exact stochastic simulation of coupled chemical reactions*. The journal of physical chemistry, 81(25), 2340-2361.

[40] Gillespie, D. T. (2009). *Deterministic limit of stochastic chemical kinetics*. The Journal of Physical Chemistry B, 113(6), 1640-1644.

[41] Gillespie, D. T. (2001). *Approximate accelerated stochastic simulation of chemically reacting systems*. The Journal of chemical physics, 115(4), 1716-1733.

[42] Gillespie, D. T. (2000). *The chemical Langevin equation*. The Journal of Chemical Physics, 113(1), 297-306.

[43] Greenwood, M. (1931). *On the statistical measure of infectiousness*. Epidemiology & Infection, 31(3), 336-351.

[44] Hairer, E., Wanner, G., Nørsett, S. P. (1993). *Solving Ordinary Differential Equations I: Nonstiff Problems*. Springer.

[45] Hairer, E., Wanner, G. (2015). *Runge–Kutta methods, explicit, implicit*. Encyclopedia of Applied and Computational Mathematics, 1282-1285.

[46] Hairer, E., Ch, Lubich (2012). *Numerical solution of ordinary differential equations*. The Princeton companion to applied mathematics, 293-305.

[47] Harris, C.R., Millman, K.J., van der Walt, S.J. et al. (2020) *Array programming with NumPy*. Nature 585, 357–362.

[48] Hassan, I. A. H. (2008). *Application to differential transformation method for solving systems of differential equations*. Applied Mathematical Modelling, 32(12), 2552-2559.

[49] He, S., Peng, Y., Sun, K. (2020). *SEIR modeling of the COVID-19 and its dynamics*. Nonlinear dynamics, 101(3), 1667-1680.

[50] Hudečková, H., Ševčovič, D., et al. (2017). *Biomatematické modelovanie a vyhodnocovanie indikátorov očkovania ochorení preventabilných očkovaním*. IRIS

[51] Hunter, J. D. (2007). *Matplotlib: A 2D graphic evnironment*. Computing in Science & Engineering, 9(3), 90-95

[52] Chladná, Z., Kopfová, J., Rachinskii, D., Rouf, S. C. (2020). *Global dynamics of SIR model with switched transmission rate*. Journal of Mathematical Biology, 80(4), 1209-1233.

[53] Jackson, J. D. (2021). *Classical electrodynamics*. John Wiley & Sons.

[54] Jones, J. H. (2007), *Notes On* R_0. Standford University

[55] Keeling, M., Rohani, P. (2011). *Modeling Infectious Diseases in Humans and Animals*. Princeton: Princeton University Press.

[56] Kermack, W. O. and McKendrick, A. G. (1927) *A Contribution to the Mathematical Theory of Epidemics*. Proc. R. Soc. Lond 115. 700–721.

[57] Knuth, D. E: (1998) Knuth, D. E. (2014). *Art of computer programming, volume 2: Seminumerical algorithms*. Addison-Wesley Professional.

[58] Kovalnogov, V N., Simons, T. E., Tsitouras, C. (2021): *Runge–Kutta pairs suited for SIR-type epidemic models*. Mathematical Methods in the Applied Sciences, 44(6). 5210-5216.

[59] Lei, J. (2021). *Mathematical Preliminary–Stochastic Modeling*. In Systems Biology (pp. 69-97). Springer, Cham.

[60] Leimkuhler, B., Matthews, C., Tretyakov, M. V. (2014). *On the long-time integration of stochastic gradient systems*. Proceedings of the Royal Society A: Mathematical, Physical and Engineering Sciences, 470(2170), 20140120.

[61] Leuridan, E., Hens, N., Hutse, V., Ieven, M., Aerts, M., Van Damme, P. (2010). *Early waning of maternal measles antibodies in era of measles elimination: longitudinal study*. Bmj, 340.

[62] Makhoul, J. (1980). *A fast cosine transform in one and two dimensions*. IEEE Transactions on Acoustics, Speech, and Signal Processing, 28(1), 27-34.

[63] Martcheva, M., Pilyugin, S. S. (2006). *An epidemic model structured by host immunity*. Journal of Biological Systems, 14(02), 185-203.

[64] Masuda, N., Rocha, L. E. (2018). *A Gillespie algorithm for non-Markovian stochastic processes*. Siam Review, 60(1), 95-115.

[65] McCarthy, Z., Xiao, Y., et al. (2020). *Quantifying the shift in social contact patterns in response to non-pharmaceutical interventions*. Journal of Mathematics in Industry, 10(1), 1-25.

[66] McKendrick A. G. (1926). *Application of Mathematics to medical problems*, Proceedings of the Edinburgh Mathematical Society, 98-130

[67] Murray, J. D. (2007). *Mathematical Biology: I. An Introduction* (Vol. 17). Springer Science & Business Media.

[68] Nakata, Y., Enatsu, Y., Inaba, H., Kuniya, T., Muroya, Y., Takeuchi, Y. (2014). *Stability of epidemic models with waning immunity*. SUT J. Math, 50(2), 205-245.

[69] Newman, M. (2018) *Networks, second edition*. Oxford University Press

[70] Odibat, Z. M., Bertelle, C., Aziz-Alaoui, M. A., Duchamp, G. H. (2010). *A multi-step differential transform method and application to non-chaotic or chaotic systems*. Computers & Mathematics with Applications, 59(4), 1462-1472.

[71] Pozrikidis, C. (2016). *The Fractional Laplacian*. Chapman and Hall/CRC

[72] Rackauckas, C., Nie, Q. (2017). *Differentialequations.jl –– a performant and feature-rich ecosystem for solving differential equations in julia*. Journal of open research software, 5(1).

[73] Risken, H. (1996). *Fokker-planck equation* Springer Berlin Heidelberg.

[74] Rößler, A. (2009). *Second order Runge–Kutta methods for Itô stochastic differential equations*. SIAM Journal on Numerical Analysis, 47(3), 1713-1738.

[75] Säkkä, S., & Solin, A. (2014). *Lecture notes on applied stochastic differential equations. Version as of December.*,(4).

[76] Sari, T., Lobry, C. (2015). *Migrations in the Rosenzweig-MacArthur model and the" atto-fox" problem*. Revue Africaine de la Recherche en Informatique et Mathématiques Appliquées, 20.

[77] Ševčovič, D, Trnovská, M (2015). *Solution to the inverse Wulff problem by means of the enhanced semidefinite relaxation method*. Journal of Inverse and Ill-posed Problems 23.3: 263-285.

[78] Trejos, D. Y., Valverde, J. C., Venturino, E. (2021). *Dynamics of infectious diseases: A review of the main biological aspects and their mathematical translation*. Applied Mathematics and Nonlinear Sciences.

[79] Tsitouras, C. (2011). *Runge–Kutta pairs of order 5 (4) satisfying only the first column simplifying assumption*. Computers & Mathematics with Applications, 62(2), 770-775.

[80] Tuckwell, H.C., Williams. R.J. (2007) *Some properties of a simple stochastic epidemic model of SIR type*. Math Biosci. 208(1):76-97.

[81] Vázquez, J. L. (2012). *Nonlinear diffusion with fractional Laplacian operators*. In Nonlinear partial differential equations (pp. 271-298). Springer, Berlin, Heidelberg.

[82] Virtanen, P., Gommers, R. et al (2020). *Scipy 1.0: Fundamental Algorithms for Scientific Computing in Python*. Nature Methods 17. 261-272.

[83] Waheed, W., Deng, G., Liu, B. (2020). *Discrete Laplacian operator and its applications in signal processing*. IEEE Access, 8, 89692-89707.

[84] Weisstein, Eric W. *Kermack-McKendrick Model*. From MathWorld–A Wolfram Web Resource. https://mathworld.wolfram.com/Kermack-McKendrickModel.html

[85] Yang, L., Grenfell, B. T., Mina, M. J. (2020). *Waning immunity and re-emergence of measles and mumps in the vaccine era*. Current opinion in virology, 40, 48-54.

[86] Zhao, Y. L., Han, B. H., et al. (2019). *Immune persistence 17 to 20 years after primary vaccination with recombination hepatitis B vaccine (CHO) and the effect of booster dose vaccination*. BMC infectious diseases, 19(1), 1-7.

[87] Zibolenová, J., Chladná, Z., et al. (2017). *Estimation of the population susceptibility against measles in Slovakia*. Central European Journal of Public Health, 25(1), 46-54.